

ABSTRACT

Title of Document: AN INTEGRATED TRAFFIC CONTROL SYSTEM
FOR FREEWAY CORRIDORS UNDER NON-
RECURRENT CONGESTION

Yue Liu, Doctor of Philosophy, 2009

Directed By: Professor Gang-Len Chang
Department of Civil and Environmental Engineering

This research has focused on developing an advanced dynamic corridor traffic control system that can assist responsible traffic professionals in generating effective control strategies for contending with non-recurrent congestion that often concurrently plagues both the freeway and arterial systems. The developed system features its hierarchical operating structure that consists of an integrated-level control and a local-level module for bottleneck management.

The primary function of the integrated-level control is to maximize the capacity utilization of the entire corridor under incident conditions with concurrently implemented strategies over dynamically computed windows, including diversion control at critical off-ramps, on-ramp metering, and optimal arterial signal timings. The system development process starts with design of a set of innovative network formulations that can accurately and efficiently capture the operational characteristics of traffic flows in the entire corridor optimization process.

Grounded on the proposed formulations for network flows, the second part of the system development process is to construct two integrated control models, where the base model is designed for a single-segment detour operation and the extended model is designated for general network applications. To efficiently explore the control effectiveness under different policy priorities between the target freeway and available detour routes, this study has further proposed a multi-objective control process for best managing the complex traffic conditions during incident operations.

Due to the nonlinear nature of the proposed formulations and the concerns of computing efficiency, this study has also developed a GA-based heuristic along with a successive optimization process that can yield sufficiently reliable solutions for operating the proposed system in a real-time traffic environment.

To evaluate the effectiveness and efficiency of the developed system, this study has conducted extensive numerical experiments with real-world cases. The experimental results have demonstrated that with the information generated from the proposed models, the responsible agency can effectively implement control strategies in a timely manner at all control points to substantially improve the efficiency of the corridor control operations.

In view of potential spillback blockage due to detour operations, this study has further developed a local-level bottleneck management module with enhanced arterial flow formulations that can fully capture the complex interrelations between the overflow in each lane group and its impact on the neighboring lanes. As a supplemental component for corridor control, this module has been integrated with

the optimization model to fine-tune the arterial signal timings and to prevent the queue spillback or blockages at off-ramps and intersections. The results of extensive numerical experiments have shown that the supplemental module is quite effective in producing local control strategies that can prevent the formation of intersection bottlenecks in the local arterial.

AN INTEGRATED TRAFFIC CONTROL SYSTEM FOR FREEWAY
CORRIDORS UNDER NON-RECURRENT CONGESTION

By

Yue Liu

Dissertation submitted to the Faculty of the Graduate School of the
University of Maryland, College Park, in partial fulfillment
of the requirements for the degree of
Doctor of Philosophy
2009

Advisory Committee:
Professor Gang-Len Chang, Chair
Professor Paul Schonfeld
Professor David Lovell
Professor Martin Dresner
Professor Kaustubh Agashe

© Copyright by
Yue Liu
2009

Dedication

To my wife, Jie Yu, my mother, Haiying Wang, and my father, Zhigang Liu

for their love and support...

Acknowledgements

First and foremost, I would like to express my deepest sense of gratitude and indebtedness to my advisor, Dr. Gang-Len Chang, for his enlightening guidance and persistent inspiration throughout my Ph.D. study at the University of Maryland at College Park. My career has been strongly influenced by his dedication to excellent research work.

I would like to express my gratitude to the members of my doctoral examination committee, Dr. Martin Dresner, Dr. Paul Schonfeld, Dr. David Lovell, and Dr. Kaustubh Agashe for their constructive comments and valuable suggestions on my research work.

Very special thanks go to my colleagues in Traffic Safety and Operations Lab, Nan Zou, Zichuan Li, Xiaodong Zhang, Woon Kim, Sung Yoon Park, and Xin Zhang for their technical and moral supports in proceeding my research and projects.

I profoundly thank my beloved wife, Dr. Jie Yu, who always believes in me and provides me with a constant source of love, comfort, and encouragement, without which this dissertation would not have been completed. Finally, I would like to express my deepest appreciation to my loving family for their unlimited encouragement and support. Especially, to my parents, you deserve my deepest gratitude and love for your dedication and the many years of support during my studies.

Table of Contents

Dedication.....	ii
Acknowledgements.....	iii
Table of Contents.....	iv
List of Tables.....	vi
List of Figures.....	vii
Chapter 1: Introduction.....	1
1.1. Background.....	1
1.2. Research Objectives.....	3
1.3. Dissertation Organization.....	4
Chapter 2: Literature Review.....	8
2.1. Introduction.....	8
2.2. Detour Operations and Route Guidance.....	9
2.2.1. Responsive Strategies.....	10
2.2.2. Predictive Strategies.....	12
2.2.3. Iterative Strategies.....	13
2.2.4. Integrated Strategies.....	14
2.3. Freeway Traffic Control Strategies.....	15
2.3.1. Pre-timed Metering Strategies.....	15
2.3.2. Traffic-Responsive Metering Strategies.....	17
2.3.3. Coordinated Metering Strategies.....	19
2.3.4. Other Metering Strategies.....	25
2.4. Arterial Traffic Control Strategies.....	27
2.5. Integrated Corridor Control Strategies.....	30
2.5.1. Nonlinear Optimization Approach.....	30
2.5.2. Dynamic System-Optimal Control Approach.....	33
2.5.3. Store-and-Forward Approach.....	34
2.5.4. Successive Linear Programming Approach.....	35
2.5.5. Model Predictive Approach.....	36
2.6. Expected Research Contribution.....	37
Chapter 3: A Systematic Modeling Framework.....	39
3.1. Introduction.....	39
3.2. Key Research Issues.....	39
3.3. System Functional Requirements and Key Inputs.....	41
3.3.1 System Functional Requirements.....	41
3.3.2 Required System Input.....	43
3.4. Modeling Framework.....	45
3.5. Conclusion.....	50
Chapter 4: Integrated Corridor Control Strategies.....	51
4.1. Introduction.....	51
4.2. Network Flow Formulations.....	54
4.2.1. Arterial Traffic Flow Formulations.....	54
4.2.2. Freeway Traffic Flow Formulations.....	64
4.2.3. Formulations for On-off Ramps.....	67
4.3. Base Model: Integrated Control of a Single Segment Corridor.....	71
4.3.1. Model Scope and Assumptions.....	71

4.3.2. Network Model Enhancement – Projection of Detour Traffic Impact	73
4.3.3. Model Formulations.....	78
4.4. Extended Model: Integrated Control of A Multi-segment Corridor.....	83
4.4.1. Scope of the Extended Model.....	83
4.4.2. Assumptions for the Extended Model.....	86
4.4.3. Model Formulations.....	86
4.5. Solution Algorithms – A Compromised GA	92
4.5.1. Regret Value Computation	93
4.5.2. Decoding of Control Variables	94
4.6. A Successive Optimization Framework for Real-time Model Application.....	97
4.6.1. Real-time Estimation Or Projection of Model Parameters	98
4.6.2. A Variable-Time-Window Rolling Horizon Scheme	101
4.7. Closure	104
Chapter 5: Case Studies for Integrated Control Strategies	106
5.1. Numerical Test of the Base Model	106
5.1.1. Experimental Design.....	106
5.1.2. Geometric and Network Traffic Flow Characteristics.....	107
5.1.3. Traffic Control Parameters	111
5.1.4. Optimization Model Settings	112
5.1.5. Numerical Results and Analyses	112
5.1.6. Summary	129
5.2. Numerical Test of the Extended Model.....	130
5.2.1. Experimental Design.....	130
5.2.2. Numerical Analyses and Findings	133
5.3. Sensitivity Analyses.....	146
5.4. Closure	148
Chapter 6: Enhanced Control Strategies for Local Bottlenecks	149
6.1. Introduction.....	149
6.2. The Enhanced Network Formulations for Local Bottlenecks.....	149
6.2.1. Model Formulations.....	150
6.2.2. Model Validation	156
6.3. Signal Optimization with the Enhanced Network Formulations	165
6.3.1. The Signal Optimization Model and Solution	166
6.3.2. Numerical Test of the Enhanced Signal Optimization Model	168
6.4. Closure	178
Chapter 7: Conclusions and Future Research	179
7.1. Research Summary and Contributions.....	179
7.2. Future Research	184
Bibliography	187

List of Tables

Table 5.1 Volume Levels for the Case Study of Base Model	107
Table 5.2 Lane Channelization at Intersection Approaches of the Detour Route.....	109
Table 5.3 Phase Diagram of Intersections along the Detour Route.....	111
Table 5.4 Performance of the Proposed Model under Different Scenarios with Various Decision Preferences.....	114
Table 5.5 Model Performance with Various Decision Preferences.....	138
Table 5.6 Distribution of Diversion Flows at Off-ramps and On-ramps.....	141
Table 5.7 Comparison Results between Models 1 and 2.....	145
Table 5.8 Sensitivity Analysis With Respect To The Variation of Diversion Compliance Rates.....	147
Table 6.1 Signal Settings for the Target Intersection.....	157
Table 6.2 Parameter Fitting Results for All Intersection Links.....	160
Table 6.3 Comparison between the Base Model and the Enhanced Model In 5-min Departure Flows (in # of vehicles)	164
Table 6.4 Experimental Scenarios for Model Evaluation.....	169
Table 6.5 Signal Timings from the Enhanced Model and TRANSYT-7F.....	172
Table 6.6 Comparison of CORSIM Simulation Results.....	173

List of Figures

Figure 1.1 Dissertation Organization	4
Figure 3.1 A Modeling Framework of the Proposed System	47
Figure 4.1 Relations between Different Sections in Chapter 4	53
Figure 4.2 Dynamic Traffic Flow Evolutions along an Arterial Link	59
Figure 4.3 Traffic Dynamics in Freeway Sections	66
Figure 4.4 Traffic Dynamics in the On-ramp and Off-ramp	70
Figure 4.5 Scope of the Base Model	72
Figure 4.6 Dynamic Traffic Flow Evolutions Considering the Detour Traffic Impact	74
Figure 4.7 A Signal Controller with a Set of Phases	82
Figure 4.8 Scope of the Extended Model for Integrated Corridor Control	85
Figure 4.9 Illustration of the Pareto Frontier	92
Figure 4.10 Flowchart of the GA-based Compromised Heuristic	97
Figure 4.11 Real-time Estimation of Diversion Compliance Rates.....	100
Figure 4.12 Illustration of the Variable-Time-Window Rolling Horizon Scheme.....	102
Figure 5.1 Layout of the Corridor Segment for Case Study of The Base Model.....	108
Figure 5.2 MOE Changes under Different Weight Assignment (Scenario I).....	115
Figure 5.3 MOE Changes under Different Weight Assignment (Scenario II)...	116
Figure 5.4 MOE Changes under Different Weight Assignment (Scenario III)...	117
Figure 5.5 MOE Changes under Different Weight Assignment (Scenario IV)...	117
Figure 5.6 Time-varying Detour Travel Time over Freeway Travel Time Ratio (Scenario II).....	120
Figure 5.7 Time-varying Detour Travel Time over Freeway Travel Time Ratio (Scenario III).....	121
Figure 5.8 Time-varying Detour Travel Time over Freeway Travel Time Ratio (Scenario IV).....	122
Figure 5.9 Time-varying Total Time Savings (Scenario I).....	125
Figure 5.10 Time-varying Total Throughput Increases (Scenario I).....	125
Figure 5.11 Time-varying Total Time Savings (Scenario II).....	126
Figure 5.12 Time-varying Total Throughput Increases (Scenario II).....	126
Figure 5.13 Time-varying Total Time Savings (Scenario III).....	127
Figure 5.14 Time-varying Total Throughput Increases (Scenario III).....	127
Figure 5.15 Time-varying Total Time Savings (Scenario IV).....	128
Figure 5.16 Time-varying Total Throughput Increases (Scenario IV).....	128
Figure 5.17 A Hypothetical Corridor Network for Case Study.....	132
Figure 5.18 The Control Area ($w_1/w_2 = 10/0$ and $9/1$).....	134
Figure 5.19 The Control Area ($w_1/w_2 = 8/2, 7/3$ and $6/4$).....	134

Figure 5.20 The Control Area ($w_1/w_2 = 5/5, 4/6, \text{ and } 3/7$).....	135
Figure 5.21 The Control Area ($w_1/w_2 = 2/8 \text{ and } 1/9$).....	135
Figure 5.22 The Control Area ($w_1/w_2 = 0/10, \text{ no detour}$).....	136
Figure 5.23 The Impact of Weight Assignment on Corridor Throughput.....	138
Figure 5.24 The Impact of Weight Assignment on Total Diversion Rates.....	139
Figure 5.25 The Impact of Weight Assignment on Total Time by Detour Traffic.....	139
Figure 5.26 Distribution of Diversion Flows ($w_1/w_2 = 10/0 \text{ and } 9/1$).....	142
Figure 5.27 Distribution of Diversion Flows ($w_1/w_2 = 8/2, 7/3 \text{ and } 6/4$).....	142
Figure 5.28 Distribution of Diversion Flows ($w_1/w_2 = 5/5, 4/6, \text{ and } 3/7$).....	143
Figure 5.29 Distribution of Diversion Flows ($w_1/w_2 = 2/8 \text{ and } 1/9$).....	143
Figure 5.30 Control Areas Represented by the Model 1 and 2.....	144
Figure 6.1 Blockages between Lane Groups	152
Figure 6.2 Enhanced Traffic Flow Dynamics along an Arterial Link Considering Lane Group Queue Interactions.....	153
Figure 6.3 A Graphical Illustration of the Target Intersection for Model Validation (MD212@Adelphi Rd.)	157
Figure 6.4 Comparison of 5-minute Movement Departure Flows (VISSIM v.s. The Enhanced Formulation).....	163
Figure 6.5 Flowchart of the Solution Algorithm for Signal Optimization.....	167
Figure 6.6 Experimental Arterial Layout and Phase Settings.....	168
Figure 6.7 Queue Times of Approaches under the Low-demand Scenario.....	175
Figure 6.8 Queue Times of Approaches under the Medium-demand Scenario..	176
Figure 6.9 Queue Times of Approaches under the High-demand Scenario.....	176

Chapter 1: Introduction

1.1. Background

Traffic delays on urban freeways due to congestion have significantly undermined the efficiency and mobility of the highway systems in the United States. Up to 60 percent of those delays are due to non-recurrent traffic congestion caused by reduced capacity on a freeway section coupled with long incident durations. However, if proper routing and control strategies can be implemented in time, motorists can circumvent the congested segments by detouring through parallel arterials. To properly guide such operations, the responsible agency needs to implement effective strategies in a timely manner at all control points, including off-ramps, arterial intersections, and on-ramps.

To contend with this vital operational issue, various types of optimal control models, focused on each individual component of the traffic corridor (freeway control, ramp metering, route guidance, and diversion control), have been proposed in the literature over the past several decades (Ramp Metering: Wattleworth, 1967; Payne and Thompson, 1974; Yagar, 1989; Papageorgiou, 1990a, 1990b; Stephanedes and Chang, 1993; Zhang et al., 1996; Lovell, 1997; Zhang, 1997; Zhang and Recker, 1999; Lovell and Daganzo, 2000; Chang and Li, 2002; Zhang and Levinson, 2004; Freeway Control: Payne, 1971; Papageorgiou, 1990c; Kotsialos et al., 2002; Diversion Control: Messmer and Papageorgiou, 1995; Iftar, 1995; Wu and Chang, 1999a). Certainly,

those research efforts have made an invaluable contribution to the development of control strategies and operational guidelines for freeway system management. However, much remains to be advanced on the development of integrated control, which includes diversion, ramp metering, and signal timings to contend with non-recurrent congestion such as major incidents.

Over the past two decades, only a limited number of studies (Cremer and Schoof et al., 1989; Papageorgiou, 1995; Wu and Chang, 1999b; Van den Berg et al., 2001) have attempted to address this issue of an integrated control for a traffic corridor comprising both freeways and arterials. Hence, prior to the potential implementation of an effective integrated control, many critical theoretical and operational issues await further exploration. Some of those issues include:

- How to choose proper control boundaries (a set of critical on/off ramps and connecting arterials), based on the incident nature, available corridor capacity, and limited resources;
- How to determine the control objectives and criteria for selection of the most effective network control strategy;
- How to implement the most appropriate diversion control strategy in a timely manner in response to time-varying traffic conditions after an incident;
- How to assess the impact of detour traffic on the arterial system;

- How to manage traffic at the local bottlenecks (e.g., update arterial signal timings and ramp metering rates to avoid blockage and spillback) due to the detour operation; and
- How to ensure the real-time application of the control strategy in the presence of time-varying traffic conditions and potential system disturbance.

1.2. Research Objectives

The primary focus of this dissertation is to develop an integrated corridor control system that can assist responsible agencies in generating effective network control strategies under various incident scenarios. More specifically, the system shall have the capability to:

- Determine control boundaries, based on the incident nature and the available corridor capacity to minimize incident impact and maximize total operational efficiency;
- Design dynamic diversion control plans at the selected critical off-ramps within the control boundaries, i.e., temporarily guide part of the freeway traffic to parallel arterials so as to relieve congestion; and
- Update local control strategies, such as changing the timing of signals and ramp metering rates, to avoid local bottlenecks due to the demand surge from the detour operation.

To accomplish all of the above objectives, the proposed system shall have the following features:

- Realistic representation of the complex temporal and spatial interrelations among freeway, arterial, and ramp traffic with acceptable computational efficiency;
- Integration of various levels of control strategies with pre-specified control objectives to ensure the effectiveness of the integrated operations under various incident scenarios;
- Formulations of real-world operational constraints, such as diversion compliance issues; and
- Development of sufficiently efficient and robust solution algorithms that can solve the proposed optimization formulations and generate target control strategies for various real-world networks.

1.3. Dissertation Organization

Based on the proposed research objectives, this study has organized the primary research tasks into seven chapters. The core of those tasks and their interrelations are illustrated in Figure 1.1.

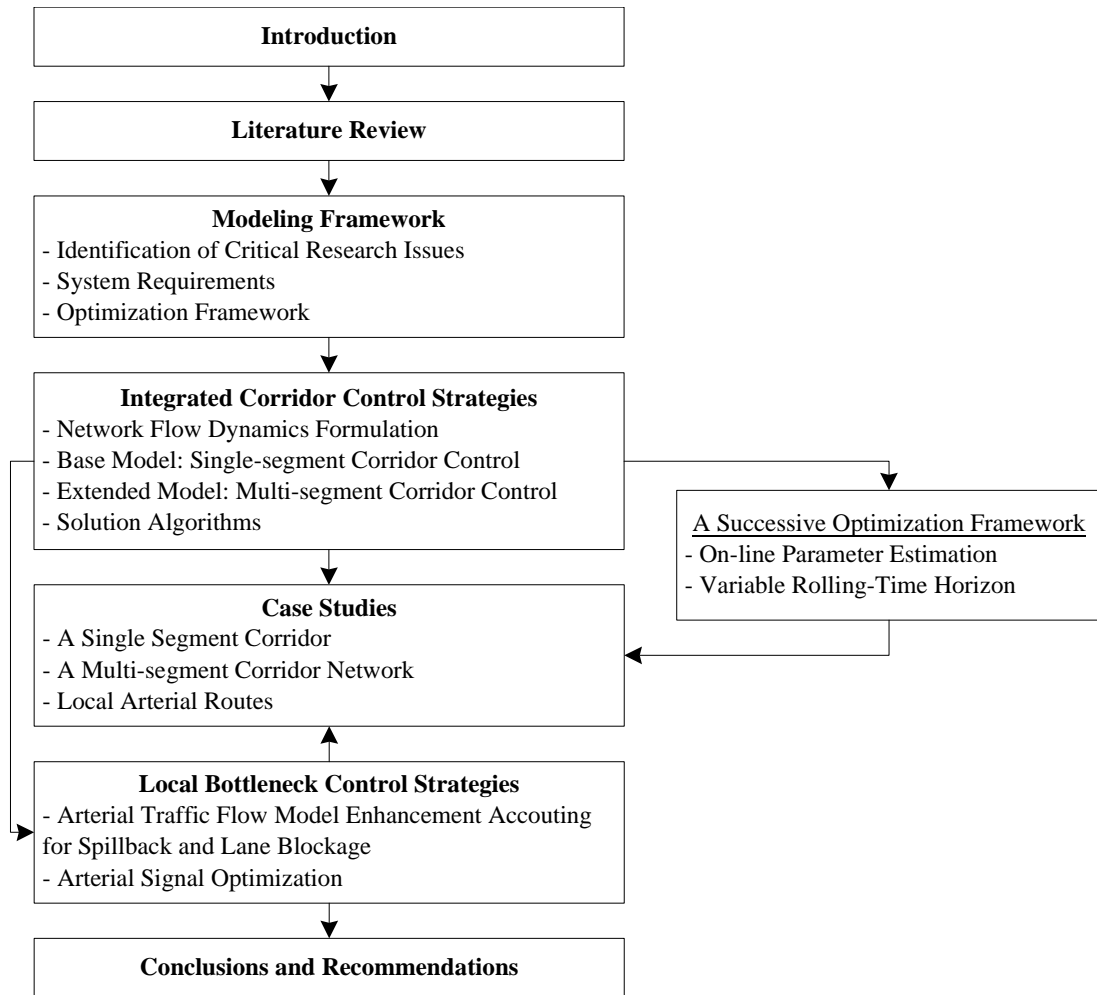


Figure 1.1 Dissertation Organization

The remaining chapters of this dissertation are organized as follows:

- **Chapter 2** presents a comprehensive literature review of existing studies on various control strategies for freeway corridor management, including both model formulations and solution algorithms. The review focuses on identifying the advantages and limitations of those control strategies, along with their potential enhancements.

- **Chapter 3** illustrates the framework of the proposed optimal control system, based on critical issues that need to be taken into account in the design of traffic control strategies. It specifies the required system inputs, the principal system components, their key functional features, and operational interactions, aiming to tackle the operational complexities with concurrent implementation of multiple strategies for real-time large-scale applications.
- **Chapter 4** presents the developed the formulations and solution algorithms for the optimization models to concurrently execute the integrated control strategies, including determining the control boundaries, designing the dynamic diversion control strategies, updating the ramp metering rates, and adjusting the arterial signal timings. Using the lane-group-based concept to model the interactions between link and node (i.e., intersection) flows, a set of innovative formulations is proposed and integrated with the freeway model in a multi-objective control framework that allows the system to efficiently explore the control effectiveness under different policy priorities between the target freeway and available detour routes. Due to the nonlinear nature of the proposed formulations and the concerns of computing efficiency, this study has also developed efficient algorithms that can yield sufficiently reliable strategies for the target corridor control system in real-time operations.
- **Chapter 5** presents numerical analysis results for evaluating the Base Model and the Extended Model proposed in Chapter 4 with a segment

along the I-95 northbound corridor and a hypothetical corridor network. The focus is to demonstrate how to best use the proposed integrated control models for maximizing the operational efficiency under various non-recurrent traffic congestion conditions. The general guidelines derived from the numerical experiment results for implementing those advanced control strategies have also been reported in this chapter.

- **Chapter 6** highlights an enhanced lane-group-based model for arterial network flows proposed in Chapter 4, to capture the complex interrelations between the overflow in each lane group and its impacts on neighboring lanes, such as left-turn lane blockage due to a long through-traffic queue. This critical model feature is essential for realistically accounting for bottlenecks due to the impact of detoured traffic on local intersections. The set of enhanced formulations has been integrated with an optimization model to fine-tune the arterial signal timings during detour operations.
- **Chapter 7** summarizes the contributions of this dissertation and indicates the future research directions, including the development of efficient algorithms for large-scale corridor network applications, interfacing with advanced surveillance systems, and innovative heuristics for solving the proposed model formulations when only partial control inputs are available.

Chapter 2: Literature Review

2.1. Introduction

This chapter summarizes major studies by transportation researchers over the past decades on various aspects of traffic corridor management during non-recurrent traffic congestion. It focuses on both the critical issues and potential research directions identified in the existing literature on this vital subject.

To facilitate the presentation, this chapter will report the review results along the following lines:

- **Detour operations and route guidance:** efficiently utilize more of the available capacity of corridor networks by offering drivers alternative routes;
- **Freeway traffic control strategies:** reduce freeway congestion by manipulating metering flow rates at on-ramps in an orderly and coordinated manner or to implement link controls, such as lane-based controls, variable speed limit controls, etc;
- **Arterial traffic control strategies:** optimize signal timing plans to maximize the traffic corridor capacity and prevent the formation of local bottlenecks; and

- **Integrated corridor control strategies:** integrate all of the aforementioned individual control measures so as to achieve the system-wide optimal state for the traffic corridor.

The remaining sections present a summary of existing methodologies associated with each of the above research lines. Based on the review results, the last section will outline the further research needs for this study.

2.2. Detour Operations and Route Guidance

The mechanism of detour operations or route guidance may be viewed as an optimal load balancing strategy that can best use the real-time measurements from the surveillance module to fully utilize the available capacity of a traffic corridor during non-recurrent congestion. Detour operation and route guidance strategies may prioritize either system-optimal or user-optimal traffic conditions. In the former case, the control goal, in general, is to minimize or maximize a global performance index (e.g., total time spent, total throughput, etc.) even though the cost of taking the detour routes may exceed the regular route. In the latter case, none of the recommended detour routes should be more costly than the regular route. Based on the differences among the reviewed route guidance studies in control logic and model formulations, this section divides them into the following four groups: responsive strategies, predictive strategies, iterative strategies, and integrated strategies.

2.2.1. Responsive Strategies

Responsive route guidance strategies usually provide guiding plans based on current measurements from the surveillance system, without using mathematical models in real time. Most responsive strategies are localized in nature, i.e., they only generate independent plans for each off-ramp or diversion point. Messmer and Papageorgiou (1994) have proposed several types of simple responsive strategies which assign more or less traffic to alternative routes according to the sign and value of the current travel time difference between both directions, thus aiming to reach optimum conditions for users. Operational systems that employ this kind of decentralized responsive strategy have also been developed and evaluated by the city of Aalborg, Denmark, where they have reportedly improved traffic conditions (Mammar et al., 1996; Dörge et al., 1996).

Extending such simple responsive strategies, multivariable responsive strategies, as well as heuristics and advanced feedback control concepts, have been proposed to address the low sensitivity issue with respect to varying demands and driver compliance rates. Hawas and Mahmassani (1995) proposed a procedure for real-time route guidance in congested vehicular traffic networks. Their decentralized approach envisions a set of local controllers scattered or distributed across the network, where every controller can only extract limited "raw" information from network detectors and utilizes this information to guide the within-territory vehicles to their individual destinations. The assignment procedure is driven by informed local search procedure with heuristics. An assessment undertaken to gauge the performance of this local responsive strategy has yielded encouraging results under different

network structures and demand loading patterns. Pavlis and Papageorgiou (1999) developed a feedback-responsive route guidance strategy for complex, meshed traffic networks. Essential components of the strategy are simple, decentralized bang-bang control laws. Their simulation investigation demonstrated the efficiency of the proposed strategy for two example networks under different demand and incident conditions. Wang and Papageorgiou (2000) also examined the performance of multiple feedback routing regulators for freeway networks under different scenarios of disturbances and uncertainties. Some of the factors examined included compliance rate, demand, control interval length, and incidents. Simulation results for such studies also suggest that multivariable feedback routing controllers can efficiently equalize experienced travel times along the alternative routes within the network and perform robustly in many perturbed situations.

Responsive route guidance strategies, though exclusively based on measurable instantaneous travel times (making no predictions and using no demand or origin-destination information), have been shown to achieve equal experienced travel times along the chosen alternative routes in the network and to considerably reduce travel delays compared to the no-control case. However, due to the local nature of their control, responsive route guidance strategies are unlikely to achieve the system-optimal traffic state. Also, these strategies cannot provide information about future traffic conditions under current route guidance settings, which may limit their applications in a large traffic corridor network.

2.2.2. Predictive Strategies

As an extension to responsive strategies, predictive strategies usually employ a dynamic network flow model to predict future traffic conditions under the current route guidance settings, based on the current traffic state, control inputs, and predicted future demands. Compared with responsive strategies alone, these methods are generally more robust and are preferable when the corridor network has long links.

A heuristic expert system with predictive route guidance strategies, OPERA (Morin, 1995), was designed to generate guidance information in cases of non-recurrent congestion in the Scottish interurban motorway network. The system uses an on-line motorway network simulation model for traffic pattern forecast and an on-line expert system module for strategy generation. Messmer et al. (1998) have also presented a control scheme which includes both feedback and feed-forward terms subject to user-optimal constraints and applied it to the Scottish highway network. Such a system employs the feed-forward term to predict travel times and delays along long interurban highway links. Their simulation evaluation results demonstrate the potential for achieving improvements with these kinds of control measures and control strategies. A more advanced predictive feedback routing control scheme was developed by Wang et al. (2002). Their strategy ran a mathematical model only once at each time step and based its routing decisions on the predicted, rather than the currently prevailing, traffic conditions.

Although predictive strategies are more effective than those relying on responsive logic alone, more research and field experience are needed to verify their

applicability under different topological and traffic conditions, especially under non-recurrent traffic congestion.

2.2.3. Iterative Strategies

Iterative strategies run a freeway network model in real time with a route guidance plan dynamically that adjusts at each time interval to ensure the successful achievement of the control goal. Therefore, iterative strategies are predictive in nature and may aim at achieving either the system-optimal or user-optimal condition.

For the system-optimal case, a set of control formulations usually aims at minimizing a specific network performance index under the constraints of splitting rates at diversion points over a preset time horizon. In this regard, Papageorgiou (1990c) developed a macroscopic modeling framework to resolve the dynamic assignment and the route guidance problem for a multi-destination freeway and/or for road networks with time varying demands. A key variable of the model at each network node is the splitting rates of each traffic sub-flow with a specified destination. Charbonnier et al. (1991) have also developed an optimal control approach for route guidance. Their research proposed a decentralized method for estimating state variables and time-varying parameters and used a decentralized heuristic to solve the optimal control problem. The on-line application of nonlinear optimization methods to feedback control of motorway networks was suggested by Messmer and Papageorgiou (1995). Their study considered route diversion via variable message signs (VMS) as the control measure. The control task — formulated as a dynamic, nonlinear, discrete-time optimal control problem with constrained control variables

— was solved by a gradient-based search. Feedback control was realized by solving the optimization problem for each control interval over a sufficiently long future time horizon. Other similar studies focusing on this subject can be found in Lafortune et al. (1993), Wie et al. (1995), and Iftar (1995).

On the other hand, several studies have also focused on establishing user-optimal conditions via iterative route guidance strategies (Mahmassani and Peeta, 1993; Ben-Akiva et al., 1997; Wisten and Smith, 1997; Wang et al., 2001). A key procedure embedded in those strategies modified the path assignment or splitting rates appropriately to reduce travel time differences among all alternative routes, which are evaluated by iteratively running a simulation model over a given time horizon.

2.2.4. Integrated Strategies

In the past two decades, researchers began to realize the benefits of integrating route guidance strategies with other control measures to best the corridor operational condition. Several studies have documented the benefits of ramp metering with diversion over the scenario with no metering controls. Nsour et al. (1992) investigated the impacts of freeway ramp metering, with and without diversion, on traffic flow. The INTRAS model, a microscopic simulation model, was applied to describe traffic flow on both freeway and surface streets. The results suggested that, with proper ramp metering control and coordinated arterial signal timings, the level of service for the entire corridor could be improved. However, their study ignored the interaction of traffic flow between freeway and surface streets.

In the research on integrated optimal control strategies, Moreno-Banos et al. (1993) presented an integrated control strategy addressing both route guidance and ramp metering, based on a simplified traffic flow model. The same problem was also addressed by Elloumi et al. (1996) using a linear programming approach. More advanced integrated control strategies have been developed to generate optimal route guidance schemes concurrently with other control measures (Cremer and Schoof, 1989; Chang et al., 1993; Papageorgiou, 1995; Zhang and Hobeika, 1997; Wu and Chang, 1999b; Van den Berg et al., 2001; Kotsialos et al., 2002). Later sections will review these studies.

2.3. Freeway Traffic Control Strategies

Four decades of research on freeway traffic control has explored some common control measures, including ramp metering strategies, lane-based controls, variable speed limit controls, etc. Since freeway link control is not an area of focus for this study, the following section will emphasize the review of on-ramp metering strategies, categorized into the following four groups: pre-timed metering strategies, traffic-responsive metering strategies, coordinated ramp metering strategies, and other strategies.

2.3.1. Pre-timed Metering Strategies

Pre-timed metering strategies generally aim to determine the metering rates at off-line for different times of day, based on the normal daily demand pattern and freeway capacities. One of the pioneering studies on ramp metering optimization was published by Wattleworth (1963), who developed a ramp metering model using a

linear programming method. The study sought to maximize total entering flow rates within the constraints of freeway mainline capacity and the physical upper- and lower-bounds of metering rates at each ramp. Similar formulations leading to linear or quadratic programming problems have also been investigated with the objective functions of maximizing total travel distance, minimizing total time spent, or balancing ramp queues (Yuan and Kreer, 1971; Tabac, 1972; Wang and May, 1973; Cheng et al., 1974; Schwartz and Tan, 1977).

As an extension of those static models, Papageorgiou (1980) suggested an LP model that could deal with congested situations. Constant travel times for each section were incorporated in formulating the interrelations between ramp flows and mainline flows. A decomposition approach was also proposed to facilitate the process of solving the proposed formulation. Lovell and Daganzo (2000) extended Wattleworth's steady-state model to include time-dependency and developed a computationally-efficient greedy heuristic solution.

Pre-timed ramp metering strategies can yield the optimal set of ramp metering rates if the traffic demand pattern is stable and experiences no disturbances. Hence, such models are obviously not suitable for addressing non-recurrent congestion scenarios, which may lead to either an overload or underutilization of freeway capacity due to the lack of real-time measurements. Also, such models assume that the freeway demand patterns are represented by static or time-dependent OD information, which is usually not available or is difficult to reliably estimate in real-world operations.

2.3.2. Traffic-Responsive Metering Strategies

Traffic responsive strategies are designed to compute suitable ramp metering values, based on real-time traffic measurements — including freeway speed, volume, density and occupancy — in the vicinity of a ramp or a mainline segment. Most existing traffic-responsive strategies can be classified into the following categories: the demand-capacity strategy, the occupancy strategy, and the ALINEA strategy.

The demand-capacity strategy (Masher et al., 1975) attempts to add to the last measured upstream flow ($q_{in}(k-1)$) as much ramp flow ($r(k)$) as necessary to fully utilize the downstream freeway capacity (q_{CAP}). Since the measurement of traffic flow alone is not sufficient to determine whether the freeway is congested, occupancy from downstream detectors ($o_{out}(k)$) is also employed. If the measured downstream occupancy becomes overcritical, the ramp flow is reduced to its minimum, r_{min} , to avoid congestion. Such strategies can be illustrated with the following equation:

$$r(k) = \begin{cases} q_{CAP} - q_{in}(k-1), & \text{if } o_{out}(k) \leq o_{cr} \\ r_{min}, & \text{o.w.} \end{cases} \quad (2.1)$$

where o_{cr} is the critical occupancy at which the freeway flow rate reaches the maximum.

The occupancy strategy is based on the same logic as the demand-capacity strategy. They differ in that the upstream demand ($q_{in}(k-1)$) in the former is estimated using occupancy measurements based on a calibrated curve.

It should be noted that, in the above two traffic-responsive metering strategies, the ramp flow is a control input and downstream occupancy is an output, while the upstream freeway flow is a disturbance. Hence, under such strategies, the control system does not constitute a closed-loop but an open-loop disturbance-rejection policy, which is generally known to be quite sensitive to various traffic disturbances. As an alternative, Papageorgiou et al. (1991) proposed a closed-loop ramp metering strategy (ALINEA), using a well-known classical feedback theory in the following form:

$$r(k) = r(k-1) + K_R[\hat{o} - o_{out}(k)] \quad (2.2)$$

where K_R is a positive regulator parameter; \hat{o} is a desired value set for downstream occupancy (typically set to o_{cr} to have the downstream flow close to q_{CAP}). Compared with the demand-capacity strategy, the ALINEA strategy adjusts the metering rates in response to even slight differences of $\hat{o} - o_{out}(k)$ instead of to a threshold value of o_{cr} ; thus, it may prevent congestion by stabilizing the traffic flow at a high throughput level.

As an enhancement over the local traffic-responsive metering strategies, some researchers have proposed multivariable regulator strategies (Papageorgiou et al., 1990b), which make use of all available mainline measurements on a freeway stretch to calculate metering rates concurrently for all ramps within the stretch. One example of those strategies is METALINE (Diakaki and Papageorgiou, 1994), which is usually viewed as a generalization and extension of ALINEA.

Responsive metering strategies are effective, to some extent, in reducing freeway congestion. However, they need appropriate values or relations to be preset, and the scope of their actions is more or less local. When the queue of vehicles on the ramp becomes so large that it interferes with surface street traffic (a very common phenomenon under non-recurrent congestion situations) or the computed metering rates reach their bounds, an override of the responsive strategies should be implemented to prevent on-ramp queues from spilling back to the surface street. These deficiencies entail the development of coordinated or integrated metering strategies, which will be reviewed in the next section.

2.3.3. Coordinated Metering Strategies

A large body of literature addresses the issue of coordinated metering strategies. Most of such methods employed a sophisticated macroscopic traffic flow model combined with optimal control theory to determine ramp metering rates (Blinkin, 1976; Papageorgiou and Mayr, 1982; Bhourri et al., 1990; Stephanedes and Chang, 1993; Chang et al., 1994; Papageorgiou, 1995; Chen et al., 1997; Zhang and Recker, 1999; Chang and Li, 2002; Kotsialos et al., 2002; Kotsialos and Papageorgiou, 2004). In general, these strategies have the following critical components embedded in the optimal control model:

- A set of dynamic traffic flow models for both freeways and on-ramps to capture the evolution of traffic state variables and to model the physical boundaries or real-world operational constraints, such as the limited

storage capacity of ramps, lower- or upper-bounds of metering rates, freeway capacity, and the impact of incidents;

- An objective criterion to be optimized under the above flow relations and constraints; and
- Numerical solution algorithms for the optimal control model to yield the target metering rates.

Dynamic Traffic Flow Models

A variety of macroscopic traffic flow models on freeways have been developed in the literature. In the late 1970s, Payne (1979) developed the FREFLO model to simulate freeway traffic flow; this model consists of a modified equilibrium speed-density relation, calibration of dynamic interaction parameters, and provision of a discontinuous flow-speed-density relationship. However, such a modeling method cannot replicate traffic flows under high densities, as pointed out by Rathi et al. (1987). To address this issue, Ross (1988) modified Payne's model with a new formulation that postulated the free-flow speed as a constant and an independent parameter of traffic density. Another extension of Payne's model was proposed later by Papageorgiou (1983; 1989; 1990a; 1990b), whose model employed the following set of dynamic traffic state evolution equations:

$$\rho_i(k+1) = \rho_i(k) + T[q_{i-1}(k) - q_i(k) + r_i(k) - s_i(k)] / \Delta_i \quad (2.3)$$

$$v_i(k+1) = v_i(k) + \frac{T}{\tau} \{V[\rho_i(k)] - v_i(k)\} + \frac{T}{\Delta_i} v_i(k)[v_{i-1}(k) - v_i(k)] - \frac{\eta \cdot T[\rho_{i+1}(k)/\lambda_{i+1} - \rho_i(k)/\lambda_i]}{\tau \cdot \Delta_i[\rho_i(k)/\lambda_i + \kappa]} \quad (2.4)$$

where $q_i(k)$ is the weighted sum of traffic volumes of two adjacent freeway segments with a factor α , as denoted by $q_i(k) = \alpha\rho_i(k)v_i(k) + (1 - \alpha)\rho_{i+1}(k)v_{i+1}(k)$; $s_i(k)$ is the exiting flow rate at the off-ramp within the target segment; $r_i(k)$ is the on-ramp flow rate within the target segment; $V[\rho]$ is the fundamental diagram used to depict the relationship between the speed and density of traffic within the segment under homogenous conditions, denoted by $V[\rho] = v_f \left[1 - (\rho / \rho_{jam})^l\right]^m$, with v_f being the free flow speed, ρ_{jam} the jam density, and l and m the model parameters; and τ , η , κ are constant model parameters. Although Papageorgiou's model is well validated and is capable of describing complex traffic phenomena with acceptable accuracy, Equation 2.4 has been extended to address other factors, such as traffic weaving near an on-ramp, congestion at an off-ramp, traffic disturbance due to lane drop, and the influence of incidents (Cremer and May, 1986; Sanwal et al., 1996).

Control Objectives

In selecting an optimal control objective for coordinated ramp metering, a commonly used criterion is to minimize the total time spent in the system over a pre-specified time horizon K (Papageorgiou, 1983), as denoted by:

$$TTT = T \sum_{k=0}^K \left[\sum_{i=1}^n \rho_i(k) \Delta_i + \sum_{i=1}^m l_i(k) \right] \quad (2.5)$$

An alternative to the above optimal control objective is to maximize the total vehicle miles, denoted by $\sum_{k=0}^K T \left[\sum_{i=1}^n q_i(k) \Delta_i \right]$.

Solution Algorithms

Integrating the optimal control model with the macroscopic traffic flow models may result in large-scale, nonlinear optimization problems. Therefore, researchers have developed a number of solution algorithms to deal with this issue, including algorithms based on automatic control theory, rolling horizon and/or successive optimization approaches, and nonlinear optimization strategies or heuristics.

One of the most commonly studied methods within the automatic control theory, for coordinated ramp metering is the well-known linear-quadratic (LQ) feedback strategy (Yuan and Kreer, 1971; Kaya, 1972; Payne et al., 1985). The LQ feedback strategy linearizes the nonlinear model equations around a certain desirable trajectory and employs a quadratic penalty function in the objective function to represent the state and control deviations from the desired trajectory. Papageorgiou (1990a) enhanced the LQ regulator to an LQI feedback regulator with integral parts which does not require the desired values of speed and density, but uses the desired densities of bottlenecks as an input. It should be noted that both LQ and LQI strategies require that some desired traffic state and trajectories be predicted in advance, which may limit their applicability due to the difficulty in reliably predicting those data for the entire time horizon. Therefore, several researchers (Looze et al,

1978; Goldstein and Kumar, 1982; Papageorgiou, 1984; Payne et al., 1985; Bhourri and Papageorgiou, 1991) have proposed hierarchical control schemes to overcome this deficiency. Such control schemes decompose the large-scale multivariable ramp metering problem into a number of hierarchical sub-problems that can interact with each other conveniently and efficiently. The control system consists of three layers: the optimization layer, the adaptation layer, and the direct control layer. An optimization problem for the overall freeway system is solved in the optimization layer in real time, and the traffic state information is updated periodically in the adaptation layer to keep consistency between the predicted and current traffic conditions. The feedback control laws are performed in the direct control layer using the results from the optimization layer as reference values.

Another way to solve the large scale ramp metering system is to implement a rolling time horizon or successive optimization for an area-wide algorithm with updated information. Chang and Wu (1994) presented an algorithm to capture the dynamic evolution of traffic with a two-segment linear flow-density model. A successive linear programming algorithm was employed in the model to determine optimal metering rates. The critical feature of this model is the linearization of flow-density relationship and feedback control. The model has been integrated with INTRA, a microscopic freeway simulation model, for simulation experiments under non-recurrent congestion conditions. A more advanced model employing the rolling time horizon technique in an integrated optimal control of freeway corridors can be found in Chang et al. (1993).

With advancements in computing technologies, more and more researchers have attempted to use nonlinear optimization techniques and heuristics to solve the optimal control model. For example, Stephanedes and Chang (1991, 1993) converted the optimal control into an unconstrained optimization problem by substituting the density evolution equation into the objective function and employed a conjugate gradient search method to solve it. A heuristic simulated annealing algorithm was later presented by Stephanedes and Liu (1993) to solve the optimal control model, and a neural network model trained with the optimal ramping rates obtained was further employed to perform real-time ramp metering control. Kotsialos and Papageorgiou (2004) presented a generic model for optimal coordinated ramp metering control in large scale freeway networks, and employed a feasible-direction nonlinear optimization algorithm for its numerical solution with promising efficiency.

Though covering all essential factors in the freeway traffic system, most coordinated metering strategies share the same deficiency — being too complex or computationally demanding for real-world applications. In addition, control strategies developed along this line encounter the difficulty of getting reliable OD information in real-time operations (especially when non-recurrent congestion occurs), which may prevent these strategies from being implemented widely. Therefore, some simplified but operational ramp metering formulations and algorithms have been developed in practice; these will be outlined in the next section.

2.3.4. Other Metering Strategies

Recognizing the complexity of formulation and the difficulty in obtaining real-time OD information for the aforementioned nonlinear, optimal ramp metering control models, Zhang and Levinson (2004) formulated an optimal ramp control as a linear program whose input variables are all directly measurable by detectors in real time. The solution was tested on a real-world freeway section in a microscopic traffic simulator for demonstration. Time-dependent origin-destination tables and off-ramp exit percentages were compared as two alternative ways to represent the actual real-time demand patterns. However, their approach was based on the assumption that off-ramp exit percentages are stable and predictable, which may not hold true under non-recurrent congestion conditions.

Fuzzy logic theory offers another school of approaches for ramp metering optimization. Chen et al. (1990) presented a fuzzy logic controller for freeway ramp metering under incident conditions. The results of simulation tests with the fuzzy controller in most cases resulted in a reduction of total passenger hours, except that it tended to increase the travel times of the vehicles in the ramp queue. In summary, fuzzy logic controllers are capable of regulating nonlinear and stochastic systems while retaining robustness and computational simplicity. Similar studies on the application of fuzzy control strategies can also be found in Sasaki and Akiyama (1986) and Taylor et al. (1998).

Other types of metering systems follow a predetermined set of relationships between metering rates and traffic variable measurements. Examples of such systems

include rule-based expert systems and artificial neural networks (Gray et al., 1990; Stephanedes et al., 1992; Zhang et al., 1994; Zhang and Ritchie, 1995; Papageorgiou et al., 1995; Zhang, 1997).

Many algorithms based on extensive engineering judgment instead of optimization models have also been proposed by traffic agencies for ramp metering optimization (e.g., the ORINCON incident-specific control strategy: Koble et al., 1980; EPT and ELT control strategy: Kahng et al., 1984; and the Seattle Bottleneck Algorithm: Jacobson et al., 1989, Nihan and Berg, 1991). An extensive summary of those strategies can be found in Bogenberger and May (1999). Although these strategies are limited in many aspects, some field experiments and many simulation studies have found that they successfully reduce delay (Kwon, 2000; Levinson et al., 2002; Hourdakis and Michalopoulos, 2003).

In summary, ramp metering is one of the most direct and efficient measures to mitigate freeway congestion; if appropriately implemented, it can achieve various positive effects on corridor operations, including an increase in the freeway mainline throughput and the effective utilization of excess capacity on parallel arterials. However, under incident conditions, implementing ramp metering alone may achieve higher speeds and throughput on the freeway at the cost of excessive queues at the on-ramp, which may spill back and block neighboring urban arterials and off-ramps. This shift of congestion between urban arterials and freeways, and vice versa, is certainly not optimal. To achieve a better performance for the overall corridor

network, optimal ramp metering strategies should be implemented jointly with other strategies, such as diversion control and arterial signal timing optimization.

2.4. Arterial Traffic Control Strategies

Signal control has been widely accepted as an effective strategy to increase arterial capacity and to mitigate congestion during daily traffic scenarios. Despite the large body of literature related to signal control (Boillot, 1992 and Papageorgiou et al., 2003), most such studies have not focused on contending with non-recurrent congestion in urban networks. Usually, researchers have employed coordinated signal optimization practices to address non-recurrent congestion situations for normal traffic conditions at high demand levels. Thus, this section will review only key models for coordinated arterial signal optimization along the following two lines: analytical approach and network flow-based approach.

In the analytical approach, a set of mixed integer linear programming (MILP) formulations have been proposed in the literature (Gartner et al. 1975a, b; Little et al., 1981; Cohen et al., 1986; Gartner et al., 1991; Chaudhary et al., 1993) aiming to maximize the bandwidth or to minimize the intersection delays. The drawback of this approach is that most of such models have not addressed the issue of having heavy or unbalanced turning movements that may disrupt the progression bandwidth for arterial through traffic. Also, most existing models for bandwidth maximization do not account for traffic flow propagation and queue interactions explicitly thus limit their applicability during oversaturated traffic conditions.

To overcome the limitations of the analytical models, researchers have proposed the use of network flow-based approach, in which mathematical models are developed to represent the complex interactions between traffic state evolution on the surface streets and key control parameters so that signal timings can be optimized accordingly to meet certain performance indices generated from the underlying traffic flow model (e.g. minimizing delays and stops, maximizing throughput, etc.). Various versions of TRANSYT (Robertson, 1969) and TRANSYT-7F (Wallace et al., 1988) are perhaps the most widely used signal timing optimization packages within this category due to its accurate representation of traffic flow. Those programs generate the optimal cycle time, green splits, and offsets aiming to minimize a performance index with a gradient search technique that only guarantees a local optimal signal plan. Other network flow-based approaches include store-and-forward models (D'Ans and Gazis, 1976; Papageorgetiou, 1995), queue-and-dispersion models (Kashani and Saridis, 1983; Wu and Chang, 1999b; Van den Berg et al., 2003), stochastic models (Yu and Recker, 2006), and discrete-time kinematic models (Lo, 2001). Despite the effectiveness of the above models in capturing the interrelation between traffic dynamics and control variables, it remains a challenging task to generate reliable signal control schemes under oversaturated traffic conditions considering the complex and frequently incurring interactions of spillback queues among different lanes and adjacent intersections.

To this regard, TRANSYT-7F was improved in Release 8 with the capability to model oversaturated networks by Li and Gan (1999). Abu-Lebdeh et al. (2007) recently presented models that capture traffic output of intersections in congested

interrupted flow conditions with explicit consideration of interactions between traffic streams at successive signals. However, the improved traffic models have not been implemented in signal optimization programs. The most recent version 13 of TRANSYT by TRL (Binning et al., 2008) employs the cell transmission model in signal optimization as an alternative to the existing platoon dispersion model, which allows accurate modeling of blocking back effects and time-varying flow analysis.

Despite the promising results from those enhanced macroscopic models, some critical issues remain to be addressed. First, most studies model the dynamic queue evolution either at a link-based level or at an individual movement-based level, which could result in either difficulty in integrating with multiple signal phases or in modeling the queue discharging rates when there exist shared lanes in the target intersection approach. Second, the queue interaction among neighboring lane groups in a link due to spillback has not been explicitly and dynamically modeled, which are very common during congested conditions. For example, left turn traffic with insufficient left-turn pocket capacity could block the through traffic, and vice versa. Although some researchers have attempted to address this issue by developing mesoscopic or microscopic traffic-simulation-based signal optimizer (Park et al., 1999; Yun and Park, 2006; Stevanovic et al., 2007), however, without using traffic density as a state variable, it would be difficult for such models to accommodate initial traffic states and explicitly model their evolution. Besides, concerns are often raised regarding the computing efficiency and efforts needed to calibrate various behavioral parameters for such microscopic-simulation methods.

2.5. Integrated Corridor Control Strategies

The aforementioned research efforts on various aspects of traffic control have made an invaluable contribution to the development of control strategies and operational guidelines for congestion management of freeway systems. However, when incidents occur on freeway segments, diversion strategies, ramp metering, and arterial signal timing optimization should be implemented jointly, rather than independently. In reviewing the literature, it is noticeable that early studies in these areas focused mainly on modeling and simulation analyses (Reiss et al., 1981; Van Aerde and Yagar, 1988). Few analytical studies attempt to deal with integrated controls for mixed freeway and urban corridor networks. Some of those studies are reviewed below.

2.5.1. Nonlinear Optimization Approach

Cremer and Schoof (1989) first formulated an integrated control model in which four types of traffic control measures, including off-ramp traffic diversion, on-ramp metering, mainline speed limit, and signal timings at the surface street were optimized in an integrated manner. Two types of dynamic traffic flow models were introduced for modeling the freeway system and surface streets. For the freeway system, a set of difference equations identical to Equations 2.3 and 2.4 was employed, with two modifications. To incorporate the mainline speed control variable ($u_2 \in [0.5,1]$) into the traffic flow model, the speed-density relation was extended as follows:

$$V[\rho, u] = v_f \cdot u_2 \cdot \left[1 - \left(\rho / \rho_{jam} \right)^{(3-2u_2)} \right]^m \quad (2.6)$$

For off-ramp flows, a normal portion and an additional diversion portion were considered:

$$s_i(k) = \theta_i(k)q_i(k) + [1 - \theta_i(k)] \cdot u_3 \cdot \varepsilon_i \cdot q_i(k) \quad (2.7)$$

where u_3 is the binary diversion control variable, which takes only the values of 0 and 1; ε_i is the diversion fraction; and $\theta_i(k)$ is the normal exiting fraction.

For the on-ramp, the entering flow rates were set to be constrained by congestion on the freeway, the metering rate, and the number of waiting and arriving vehicles.

On the surface street, the platoon dispersion model for TRANSYT was employed to capture the traffic flow evolution along the arterial link. Assuming known turning fractions at each intersection, a sequence of green times at each intersection was selected as the control variables.

Based on the aforementioned dynamic traffic flow formulations, a mixed integer nonlinear optimal control model incorporating all four types of control variables was formulated with the control objective of minimizing the total delay time within the entire corridor system. A heuristic decomposition approach using a two-layer structure was proposed to solve the proposed model. On the upper level, a decision was made for route diversion optimization, while on the lower level, ramp metering, mainline traffic speed, and surface street signal timings were optimized

independently. A special branch-and-bound algorithm was designed to achieve the optimal sequence of binary route decision variables. To optimize the freeway subsystem, the steepest descend search method was employed. A heuristic random search method was applied to green time optimization.

The case study results showed some congestion alleviation benefits in the corridor with respect to the reduced performance index. However, this approach has the following deficiencies:

- Control variables are not optimized concurrently with the proposed two-layer optimization framework;
- Coordination of signals on the surface streets is neglected;
- Optimization of the sequence of green times is performed over the entire time horizon, which results in intensive computation loads (a huge number of TRANSYT-7F runs) and inaccuracy of prediction; and
- The impacts of detour traffic on the surface streets during non-recurrent congestion (e.g., dynamic variations of intersection turning movements and queue spillbacks) are overlooked.

Another study, done by Zhang and Hobeika (1997), proposed a nonlinear programming model to determine diversion routes and rates, ramp metering rates, and arterial signal timings for a freeway corridor under incident conditions. The major feature of their approach was the application of multiple parallel diversion routes, which involved multiple upstream off-ramps and downstream on-ramps, to mitigate the incident impact. Their optimization model was capable of preventing congestion

by limiting queue lengths with constraints and penalizing long queues in the objective function. A gradient projection method was employed to solve the diversion and signal control measures simultaneously. Model performance, evaluated by simulation runs of TRANSYT-7F and INTEGRATION, showed improved traffic conditions over the entire corridor. However, this approach had the following disadvantages:

- Arrivals and departures of traffic flows were modeled over a large time interval, which may pose problems for modeling the blocking effect that often occurs during the incident conditions; and
- Delays at on-ramps and off-ramps were neglected, and only stop delays on the freeway and arterial intersections were considered;

2.5.2. Dynamic System-Optimal Control Approach

Chang et al. (1993) presented a dynamic system-optimal control model for a commuting corridor, including a freeway and parallel arterial. The major feature of this approach was that ramp metering and intersection signal timing variables were incorporated into a single optimization model and solved simultaneously in a system-optimal fashion. Traffic diversion and route choice of all traffic demands were treated as predictable, with travel times and queue lengths assumed to be known. Therefore, traffic flows over the network could be formulated as linear functions of control variables. The objective function of the control problem was formulated as the total travel times over the corridor network, a linearization algorithm was designed to solve the model, and a rolling-time-horizon technique was employed to reduce the

computation burden. However, to assume that travel times and queue lengths are known seems unrealistic under incident conditions.

2.5.3. Store-and-Forward Approach

Store-and-forward modeling of traffic networks, first suggested by Gazis and Potts (1963) and D'Ans and Gazis (1976), has since been used in various investigations, notably for road traffic control. The main idea when using store-and-forward models for road traffic control is to introduce a model simplification that enables the mathematical description of the traffic flow process without the use of discrete variables. Therefore, it opens the way to applying a number of highly efficient optimization and control methods for coordinated control over large-scale networks in real time, even under saturated traffic conditions.

Papageorgiou (1995) developed a linear optimal control model for the design of integrated control strategies for traffic corridors, including both motorways and signal-controlled urban roads, based on the store-and-forward modeling logic. However, the efficiency of the store-and-forward approach is subject to some unrealistic or impractical assumptions — such as constant travel times on links, fixed turning movements at intersections without considering the impact of diversion, and controllable discharging flow rates — which would limit its suitability to particular network topologies and specific traffic conditions.

2.5.4. Successive Linear Programming Approach

Wu and Chang (1999b) have presented a linear programming model and a heuristic algorithm for optimal integrated control of commuting corridors under non-recurrent congestion situations, including ramp metering, off-ramp diversion, and arterial signal timings. Flow interactions at the surface streets were modeled with three sets of formulations: flow conservation within sections, flow transitions between sections, and flow discharge at intersections. They also applied a similar concept to model all freeway and ramp links. A major feature of the proposed approach was the simplification of the speed-density relation with a two-segment linear function that facilitated the use of a successive linear programming algorithm to achieve global optimality. The proposed approach also featured the adaptive estimation of time-dependent model parameters using real-time traffic measurements, instead of assuming these as predetermined. Case studies based on INTRAS, a microscopic simulation program developed by the Federal Highway Administration (FHWA), have demonstrated the potential of the proposed model and algorithm for integrated control of commuting corridors. However, this approach has some disadvantages:

- The assumption of a two-phase signal timing for all arterial intersections was oversimplified;
- Model formulations for intersection discharge flows was inadequate, as were the queue interactions for various lane channelization and phase settings; and

- Coordination of arterial signals was not included.

2.5.5. Model Predictive Approach

Van den Berg et al. (2001) proposed a model predictive control (MPC) approach for mixed urban and freeway networks, based on enhanced macroscopic traffic flow models. Their study employed the METANET macroscopic traffic flow model to represent freeway dynamics and proposed a new model, based on Kashani and Saridis (1983), which described urban arterial traffic by using horizontal queues, a shorter time step, and destination-dependent queues. Connections between the two models via on-ramps and off-ramps were modeled explicitly using a concept similar to the arterial model. The overall model aimed to minimize the total time spent by all vehicles in the network, and a model predictive control framework was employed as the solution approach. The model and the control approach were illustrated via a simple case study; the MPC control resulted in an 8 percent reduction in total time compared to the fixed-time control. However, the proposed model has the following deficiencies:

- Although the queue-dependent queues are flexible in order to model the interaction between the arrival and departure of movements and complex phase settings, they do not model the flow interactions at the intersection shared lanes;
- The impact of detour traffic on the surface streets, off-ramps, and on-ramps is neglected; and
- Signal coordination for surface streets is not considered.

2.6. Expected Research Contribution

In summary, this chapter has provided a comprehensive review of existing research efforts in the design of various network control strategies for corridor management under incident conditions, including route guidance, ramp metering, and arterial signal optimization. Limitations of those strategies have also been identified to be used to constitute the basis for subsequent developments of integrated corridor control strategies. Some additional areas which have not been adequately addressed in the literature are summarized below:

- The evolution of diversion traffic along the detour route and its impacts on intersection turning movement patterns have not been modeled explicitly in a dynamic context. Most previous studies address this issue either by projecting the turning proportions at arterial intersections, based on dynamic OD and travel time information, which may not be available in a real-world application, or by applying a fixed additional amount of flow to the impacted movement, which often does not reflect changes in the time-dependent pattern;
- More realistic formulations of discharge flows at intersection approaches are needed, since most studies model dynamic queue evolution either at a link-based level or at an individual-movement-based level, which could result in either difficulty in integrating with multiple signal phases or inaccuracy in modeling the queue discharging rates in a shared lane;

- Existing approaches are incapable of addressing severe congestion due to non-recurrent incidents. For example, they have not adequately captured local bottlenecks on arterials (e.g., turning bay spillback and blocking effects) caused by the demand surges due to diversion;
- The coordination of arterial signal controllers has not been concurrently considered in the control process; and
- The inherently multi-objective nature of the integrated corridor control has not been fully addressed. Most previous studies proposed an optimal control model with one objective — either to minimize total network delay or to maximize its total throughput. However, the single control objective may result in a significant unbalance of travel time between the detour route and the freeway mainline which could cause unacceptable driver compliance rates and degrade the control performance, while a multi-objective approach may have the potential to best capture the trade-offs between the target freeway and available detour routes.

In view of the above limitations in the existing studies and the additional functional requirements for real-world system applications, this study aims to develop a promising integrated corridor control model and algorithm for effectively contending with non-recurrent congestion management.

Chapter 3: A Systematic Modeling Framework

3.1. Introduction

This chapter will illustrate the framework of the proposed integrated corridor control system for managing non-recurrent congestion, and the interrelations between its principle components. Also included are the key research issues and challenges to be addressed in the development of each system component. The rest of this chapter is organized as follows: Section 3.2 presents the major research issues and challenges involved in developing a system that can contend with non-recurrent congestion. Section 3.3 specifies the functional requirements and key inputs of the proposed integrated control system, based on the research scope and intended applications. A modeling framework is then discussed in Section 3.4, including the functions of each principle control component and their operational interrelations. Key research tasks for this study are summarized in Section 3.5.

3.2. Key Research Issues

The proposed integrated control system for non-recurrent congestion management aims to maximize the operational efficiency for managing traffic in the entire corridor via real-time traffic guidance and responsive signal control. To achieve the intended objective, modeling efforts must effectively take into account the dynamic interactions between all critical system components under the incident

conditions. Some major research issues to be addressed in developing such an integrated corridor control system are listed below:

- Detection of an incident, which yields the time, location, severity, and potential duration of an incident occurring on the freeway mainline segment;
- Formulations of the time-varying traffic conditions after incidents occur, to capture the traffic dynamics over the corridor network and to represent the spatial, as well as temporal, interactions between traffic controls and the resulting network flow distributions;
- Identification and prediction of the demands of detoured traffic over time along the corridor network;
- Modeling of local bottlenecks due to detour operations under incident conditions, e.g., queue interactions and spillbacks at off-ramps and arterial intersections;
- Construction of optimal traffic control models, including identification of the proper control objectives based on the incident nature and available corridor capacity so as to effectively exercise different control strategies under an integrated operational framework; and
- Development of solution algorithms which are sufficiently robust to solve the proposed formulations and generate viable controls for a freeway corridor network of a realistic size in the presence of time-varying traffic conditions and potential system disturbance.

It should be noted that all above tasks are interrelated and that each is indispensable for the design/implementation of an effective integrated corridor control system. In view of the large body of literature on incident detection, this study will focus on the development of systematic models and algorithms for addressing the other five critical research issues. The next section will first identify critical functional requirements to be fulfilled by each proposed system component.

3.3. System Functional Requirements and Key Inputs

3.3.1 System Functional Requirements

This study aims to design an integrated control system which can efficiently generate effective traffic control strategies to assist responsible agencies in responding to incidents occurring on the freeway mainline under various traffic conditions. To accomplish this goal, the proposed system should have the following functions:

- **Monitoring and projecting the evolution of traffic states over the corridor network.** Traffic state variables to be monitored include density, speeds, flow rates, and queue lengths which can be estimated from detector data in a surveillance system. This function should also be able to realistically project the time-varying traffic flow propagation along the corridor network, the potential queue formation and dissipation process, and the dynamic impacts of detour traffic. Such a function is critical for the model to generate effective strategies under incident conditions.

- **Pursuing optimal control strategies under the operational constraints.**

The formulations of the control model for non-recurrent congestion need to take into account realistic operational constraints, such as local bottlenecks.

- **Producing viable control decisions with an efficient algorithm.**

The stretch of the corridor network and the type of employed control strategies will affect the size of the formulations, thus determining the required computing efforts. To ensure its applicability for real-time operations, some heuristic techniques will be developed to ensure that the solutions are efficient and deployable within a tolerable time window for large-sized networks.

- **Integrating a feedback mechanism.**

Due to the stochastic nature of traffic conditions and the response of driver behavior during the management of a corridor incident, the control model parameters may vary over time. Hence, the control system should incorporate a feedback mechanism to concurrently identify the difference between actual traffic conditions and the ideal traffic states obtained from the optimal control model and to update control decisions in a timely manner.

- **Providing measurements of effectiveness for evaluating the control strategies.**

This function is proposed in order to provide selected measurements of effectiveness so that the system operators can assess the effectiveness of the implemented plans and take necessary actions.

3.3.2 Required System Input

Incident Information

As stated in Section 3.2, incident detection and impact estimation, though beyond the scope of this research, are critical inputs for implementing the proposed integrated control system. In this regard, one can take advantage of a large body of literature and can generate the following three types of input information:

- Time and location of an incident that has occurred;
- Potential duration of the incident; and
- Freeway mainline capacity reduction due to the occurrence of the incident.

Traffic Demand Patterns

The related input for the proposed system consists of the following two types of information:

- Time-varying traffic demand patterns for the corridor network under non-incident conditions, including freeway and arterial volumes, intersection turning fractions, and off-ramp exiting rates (either assumed to be known or obtainable from historical data); and
- Demand pattern changes for normal traffic due to incident or detour operations (assumed to be obtainable from the online surveillance system).

Diversion Route Development

In this study, multiple diversion routes that involve two or more upstream off-ramps and downstream on-ramps are adopted in the system development. Therefore, when a freeway mainline section is partially or fully blocked by an incident, system operators can dynamically select different off-ramps and on-ramps along with different portions of the parallel arterial to detour traffic so as to relieve freeway congestion. The related input here for the proposed system includes a segment of arterial designated as the diversion route, and a set of upstream off-ramps as well as downstream on-ramps for potential detour operations.

Static System Parameters

The input related to this category includes the following four types of information:

- Fixed phase sequences and constant clearance times at arterial intersections to avoid confusing drivers;
- A common cycle length for all intersections for better synchronization performance;
- Preset minimum and maximum allowable values for the control parameters, e.g., cycle length, diversion rates, and metering rates; and
- Off-line calibrated network flow model parameters, such as the speed-density relationship.

3.4. Modeling Framework

In view of the above functional and input requirements, Figure 3.1 depicts the framework of the proposed integrated control system for non-recurrent congestion management, highlighting interrelations between principal system components. This study will focus only on those modules within the optimization models and algorithms, as highlighted in the figure's dark gray box.

Note that this framework applies a hierarchical model development structure. The focus of the integrated-level control is on maximizing the utilization of the entire corridor capacity under incident conditions, with control strategies concurrently implemented over different time windows, including dynamic diversion rates at critical off-ramps, on-ramp metering rates, and arterial signal timing plans. As a supplemental component, the strategy for local-level bottleneck management centers on enhancing the signal control plans generated from the integrated-level models so as to prevent queue spillback or blockages at local sections of the corridor, such as off-ramps and intersection approaches, due to the demands of detoured traffic.

A brief description of each key system component is presented below:

- **Network flow formulations.** This component employs mathematical equations to represent traffic dynamics over the corridor network. As the foundation for developing all other principal system components, these network formulations should: 1) accommodate time-varying demand patterns and network capacity under incident conditions, 2) realistically

model traffic flow evolution along both the freeway and arterial routes, 3) capture the physical queue formation and dissipation process, and 4) represent the interaction between control parameters and network flow distributions. Section 4.2 will discuss the details of this component, in which a set of innovative formulations based on the lane-group-based concept is proposed to improve modeling accuracy and efficiency at arterials and ramps. This set of formulations is then integrated with the freeway model to form a set of overall corridor formulations to capture the dynamics of the corridor network.

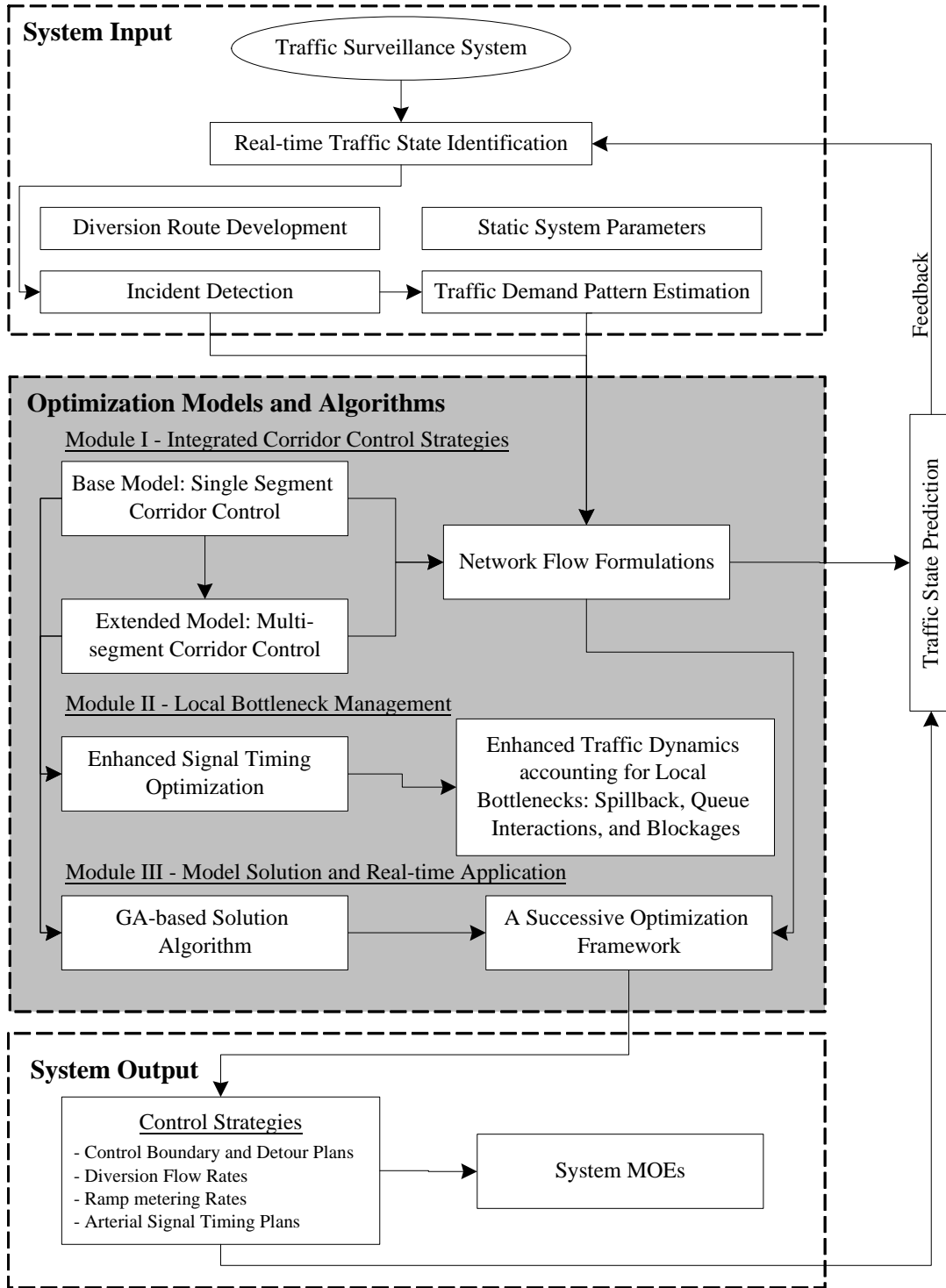


Figure 3.1 A Modeling Framework of the Proposed System

- **Integrated control strategy.** This component integrates the above network formulations into an effective multi-objective control framework to determine the best set of control strategies for efficiently exploring the effectiveness of the control under different priority policies between the target freeway and available detour routes. Two sets of formulations have been developed for this component: one for a single-segment corridor and the other for a multi-segment corridor. Section 4.3 will present the single-segment control model (the “base model”), which involves only one detour route. This set of formulations is based on an enhancement of network formulations that features its ability to project the impact of detoured freeway traffic over the corridor network. The output includes the diversion rates at the off-ramp upstream from the incident, metering rates at the on-ramp downstream from the incident, and intersection signal timing plans for the connecting surface streets. Section 4.4 extends the base model to cover a multi-segment corridor with multiple detour routes, in which critical upstream off-ramps and downstream on-ramps will be selected and dynamically paired via different segments of parallel arterial routes for detour operations. Those formulations are proposed to accommodate various operational complexities and constraints caused by the interactions among different detour routes.
- **Solution algorithms.** Due to the nonlinear nature of the proposed formulations and the concerns about computing efficiency, this component contains an efficient algorithm that can yield sufficiently reliable strategies

for the target corridor control system in real-time operations and that offers multi-objective control. Section 4.5 will present the detailed solution procedure for the integrated control formulation.

- **A successive optimization framework for real-time model application.**

This component functions to improve the computing efficiency and effectiveness of the proposed control model under time-varying traffic conditions and potential system disturbance. Section 4.6 will present a successive optimization framework for real-time application of the proposed integrated control model.

- **Local bottleneck strategy.** This component is designed to enhance the lane-group-based traffic flow formulations to capture the complex interrelations between the queue overflow in each lane group and its impact on neighboring lanes, such as left-turn lane blockage due to a long queue of through traffic. This critical model feature is essential to realistically account for bottlenecks due to the impact of detoured freeway traffic, which often causes a volume surge at off-ramps and arterial intersections. The enhanced formulations are then integrated into an optimization model to fine-tune the signal timings at off-ramps and intersections.

3.5. Conclusion

In view of the key research issues and essential system functional requirements, this chapter has presented a modeling framework for the proposed integrated corridor control system under non-recurrent congestion. The proposed modeling framework incorporates interactions between all principal system components and features a hierarchical control structure, as well as efficient solution strategies for real-time operations. Grounded on the proposed modeling framework, this study will devote the remaining chapters to the following tasks.

- **Task 1:** Propose network flow models to represent traffic dynamics at arterials, freeway, and ramps with accuracy and computational efficiency;
- **Task 2:** Develop a set of formulations for the integrated-level control to perform dynamic diversion control, ramp metering, and arterial signal optimization concurrently;
- **Task 3:** Develop an efficient algorithm that can yield sufficiently reliable strategies for the target corridor control system in real-time operations;
- **Task 4:** Develop a set of formulations to enhance signal control strategies at off-ramps and arterial intersections, based on an extended network flow model to account for queue interactions and blockages at local bottlenecks caused by the volume surge from detour operations; and
- **Task 5:** Design case studies to evaluate the proposed optimal control system under various incident scenarios and traffic conditions, with proposed measurements of effectiveness.

Chapter 4: Integrated Corridor Control Strategies

4.1. Introduction

This chapter presents the model and its formulations for design of integrated corridor control that intends to produce the optimal set of diversion and metering rates at off-ramps and on-ramps during non-recurrent congestion. The proposed control model will also concurrently adjust signal timings at the arterial intersections to best accommodate the demand pattern changes due to detour operations. The remaining sections are organized as follows.

Section 4.2 presents the network formulations that realistically capture the temporal/spatial interactions of traffic over the corridor network, including the freeway segments, arterials, and ramps. An innovative formulation using the lane-group-based concept is proposed for arterial links and ramps, which offers a reliable representation of the relationships between the arriving and departing flows under various types of lane channelization (e.g. shared lanes) at each intersection approach. This unique modeling feature, when properly integrated with the freeway model, can accurately and efficiently capture the operational characteristics of traffic in the overall corridor optimization process. This chapter will present the application of such models for integrated corridor control in response to various types of incident scenarios, including the detour needs for single-segment and multi-segment corridor.

Grounded on the above network formulations, Section 4.3 presents a base control model for single-segment corridor which involves one detour route, including the incident upstream on-ramp and off-ramp, the incident downstream on-ramp, and the connected parallel arterial. This model features a network enhancement that can precisely project the time-varying impacts of detour traffic on the existing demand patterns. An effective multi-objective control framework is introduced to determine the best set of control strategies that can efficiently explore the control effectiveness under different priority policies between the target freeway and available detour routes.

Section 4.4 extends the proposed base model for integrated control of a multi-segment corridor, in which multiple detour routes comprising several on-ramps, off-ramps, and several segments of parallel arterials are employed to coordinately divert traffic under incident conditions. The network formulations are further enhanced to accommodate various operational complexities due to the interactions between multiple diversion routes. The extended model aims to determine a set of critical off-ramps and on-ramps for detour operations (a control area), and to optimize the control actions at those critical ramps as well as intersections on the target route.

Section 4.5 develops efficient algorithms that can yield sufficiently reliable solutions for applying the proposed models in practice with a multi-objective control function. A GA-based heuristic is developed to yield approximate solutions for each control interval during the entire optimization stage. The proposed algorithm features

its capability to identify the solution closest to the “ideally best point” of the multi-objective problem rather than to obtain the entire Pareto solution set.

Section 4.6 presents a successive optimization framework for real-time application of the proposed integrated control model, in which the model input and control strategy are regularly updated to improve the computing efficiency and effectiveness under time-varying traffic conditions and potential system disturbance.

Section 4.7 summarizes research efforts that have been completed in this chapter. Figure 4.1 illustrates the relations between different sections in this Chapter.

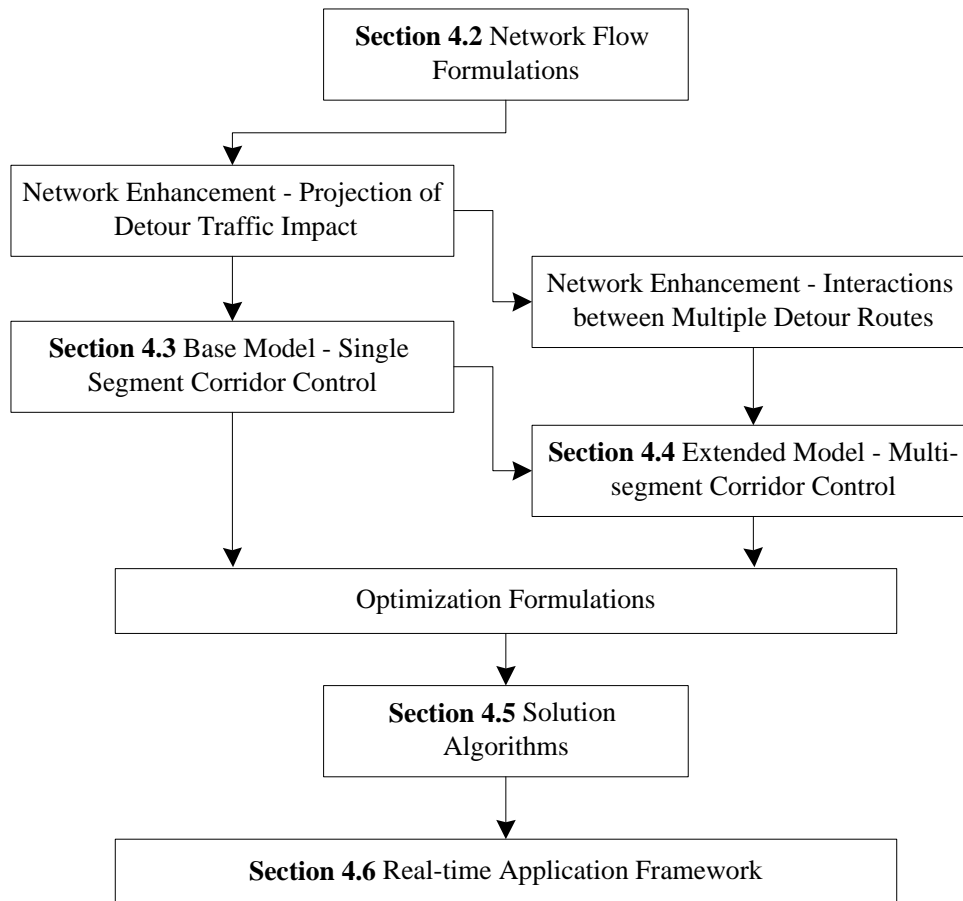


Figure 4.1 Relations between Different Sections in Chapter 4

4.2. Network Flow Formulations

As the foundation for developing the integrated optimization models, this section presents the mathematical formulations that represent traffic flow evolution over the corridor network, including arterials, freeway sections, and ramps.

4.2.1. Arterial Traffic Flow Formulations

To accommodate the complexity associated with large-scale network applications and to improve the computing efficiency, this study presents a macroscopic formulation for use as the underlying arterial traffic flow model.

A variety of approaches have been proposed in the literature on this regard. For instance, Kashani and Saridis (1983) have developed an urban arterial traffic flow model based on horizontal queues and large time steps. The cell transmission models (Daganzo, 1994; Lo et al., 2001) were also proposed and revised to model urban traffic flows. Wu and Chang (1999a; 1999b) formulated a series of dynamic traffic state evolution equations with a flow transition mechanism between adjacent roadway segments and links. Two-phase signals were modeled with G/C ratios instead of green splits, offsets, and cycle lengths. Van den Berg et al. (2003) proposed a modified and extended version of Kashani's model which is able to capture individual movement-based horizontal queues and takes into account the blocking effect due to the downstream spillback. Many existing traffic signal optimization programs, such as SYNCHRO and TRANSYT-7F have also developed their own macroscopic models. However, most existing studies model the dynamic queue evolution either at a link-based level or at an individual movement-based level, which could result in

either difficult integration with multiple signal phases or inaccurate estimation of the queue discharging rate at intersections having shared lanes.

To overcome the above modeling deficiencies as well as to ensure the computing efficiency, this study proposes a lane-group based macroscopic model to capture the evolution process of arterial traffic. To facilitate the model presentation, the notations used hereafter are summarized below:

Notation

Δt	: Time step for updating arterial status (secs);
T_h	: Length of the control time interval h (#. of Δt);
H	: The entire control time horizon;
k	: Time step index of arterial system corresponds to time $t = k\Delta t$;
S_N	: Set of arterial intersections;
$n, n \in S_N$: Index of arterial intersections;
S^U	: Set of arterial links;
S^{OUT}	: Set of outgoing arterial boundary links;
$i, i \in S^U$: Index of links,
S_r	: Set of traffic demand entries;
P_n	: Set of signal phases at intersection n ;
$p, p \in P_n$: Index of signal phase at the intersection n ;
$\Gamma(i), \Gamma^{-1}(i)$: Set of upstream and downstream links of link i ;
l_i	: Length of link i (ft);

- n_i : Num. of lanes in link i ;
 N_i : Storage capacity of link i (vehs);
 Q_i : Discharge capacity of link i (veh/h);
 $\rho^{\min}, v_i^{\text{free}}$: Minimum density (veh/mile/lane) and the free flow speed at link i (mph);
 $\rho^{\text{jam}}, v^{\min}$: Jam density (veh/mile/lane) and the minimum speed (mph);
 α, β : Constant model parameters;
 S_i^M : Set of lane groups at link i ;
 $m, m \in S_i^M$: Index of lane groups at link i ;
 $\delta_m^{ij}, j \in \Gamma^{-1}(i)$: A binary value indicating whether the movement from link i to j uses lane group m ;
 Q_m^i : Discharge capacity of lane group m at link i (veh/h);
 $d_r[k], r \in S_r$: Demand flow rate at entry r at step k (veh/h);
 $q_r[k], r \in S_r$: Flow rate enter the link from entry r at step k (veh/h);
 $w_r[k], r \in S_r$: Queue waiting on the entry r at step k (vehs);
 $q_i^{\text{in}}[k]$: Upstream inflows of link i at step k (vehs);
 $\gamma_{ij}[k], j \in \Gamma^{-1}(i)$: Relative turning proportion of movement from link i to j ;
 $N_i[k]$: Num. of vehicles at link i for at step k (vehs);
 $v_i[k]$: Mean approaching speed of vehicles from upstream to the end of queue at link i at step k (mph);

$\rho_i[k]$: Density of the segment from upstream to the end of queue at link i at step k (veh/mile/lane);

$q_i^{arr}[k]$: Flows arriving at end of queue of link i at step k (vehs);

$s_i[k]$: Available space of link i at step k (vehs);

$x_i[k]$: Total num. of vehicles in queue at link i at step k (vehs);

$q_m^i[k]$: Flows join the queue of lane group m of link i at step k (vehs);

$x_m^i[k]$: Queue length of lane group m at link i at step k (vehs);

$\lambda_m^{ij}[k], j \in \Gamma^{-1}(i)$: Percentage of movement from link i to j in lane group m ;

$Q_m^i[k]$: Flows depart from lane group m at link i at step k (vehs);

$Q_{ij}^{pot}[k]$: Flows potentially depart from link i to link j at step k (vehs);

$Q_{ij}[k]$: Flows actually depart from link i to link j at step k (vehs);

$g_n^p[k]$: Binary value indicating whether signal phase p of intersection n is set to green at step k .

The proposed model consists of the following six sets of equations: demand entries, upstream arrivals, propagation to the end of queue, merging into lane groups, departing process, and flow conservation (see Figure 4.2). It has the following key features:

- Satisfy both computational efficiency and modeling accuracy;
- Capture the dynamic evolution of physical queues with respect to the signal status, arrivals, and departures;

- Model the merging and splitting of vehicle movements at intersections;
and
- Take into account complex traffic interactions at different congestion levels;

Demand Entries

Arterial demand entries are modeled as follows:

$$q_r[k] = \min \left[d_r[k] + \frac{w_r[k]}{\Delta t}, Q_i, \frac{s_i[k]}{\Delta t} \right] \quad (4.1)$$

$$w_r[k + 1] = w_r[k] + \Delta t [d_r[k] - q_r[k]] \quad (4.2)$$

Equation 4.1 indicates that the flow enters downstream link i from demand entry r depends on the existing flows queuing at r , discharge capacity of the link i , and the available space in the link i . Equation 4.2 updates the queue waiting at the demand entry during each time step.

Upstream Arrivals

Upstream arrival equations depict the evolution of flows arriving at the upstream of the link over time. Equations 4.3 and 4.4 define the flow dynamics for different types of links.

For internal links (with both sets of upstream and downstream links), inflows to link i can be formulated as the sum of actual departure flows from all upstream links:

$$q_i^m[k] = \sum_{j \in \Gamma(i)} Q_{ji}[k] \quad (4.3)$$

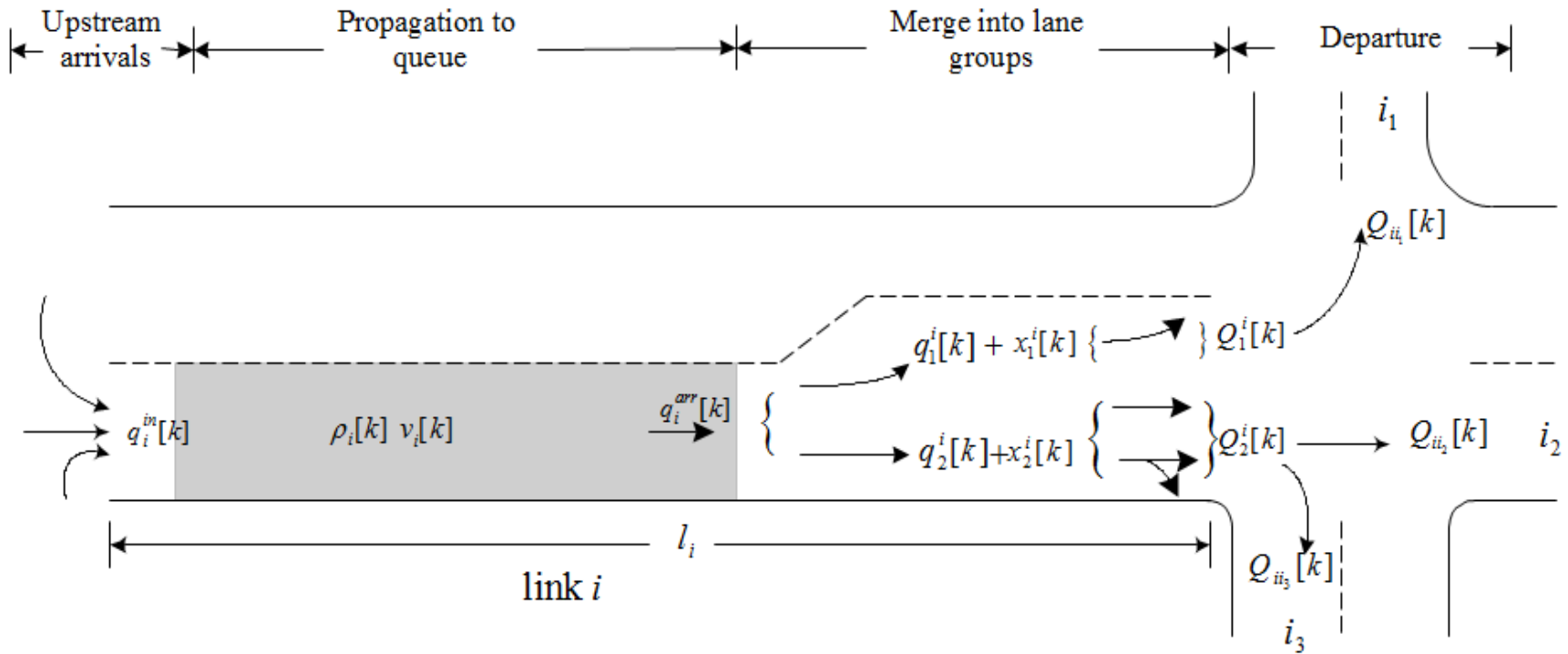


Figure 4.2 Dynamic Traffic Flow Evolutions along an Arterial Link

For source links (connected with demand entry r), inflows can be stated as:

$$q_i^{in}[k] = q_r[k] \cdot \Delta t \quad (4.4)$$

Propagation to the End of Queue

This set of dynamic equations represents the evolution of upstream inflows to the end of queue with the average approaching speed. The mean speed of vehicles, $v_i[k]$, depending on the density of the segment between the link upstream and the end of queue, $\rho_i[k]$, can be described with the following equation (Ben-Akiva, 1996):

$$v_i[k] = \begin{cases} v_i^{free}, & \text{if } \rho_i[k] < \rho^{\min} \\ v^{\min} + (v_i^{free} - v^{\min}) \cdot \left[1 - \left(\frac{\rho_i[k] - \rho^{\min}}{\rho^{jam} - \rho^{\min}} \right)^\alpha \right]^\beta, & \rho_i[k] \in [\rho^{\min}, \rho^{jam}] \\ v^{\min}, & \text{if } \rho_i[k] > \rho^{jam} \end{cases} \quad (4.5)$$

The density of the segment from link upstream to the end of queue is computed with the following equation:

$$\rho_i[k] = \frac{N_i[k] - x_i[k]}{n_i \left(l_i - \frac{x_i[k]}{n_i \rho^{jam}} \right)} \quad (4.6)$$

$N_i[k] - x_i[k]$ represents the number of vehicles moving at the segment between the link upstream and the end of queue, and $l_i - x_i[k]/(n_i \cdot \rho^{jam})$ depicts the length of that segment over time. Then, the number of vehicles arriving at the end of queue at link i can be dynamically updated with:

$$q_i^{arr}[k] = \min\{\rho_i[k] \cdot v_i[k] \cdot n_i \cdot \Delta t, N_i[k] - x_i[k]\} \quad (4.7)$$

$\rho_i[k] \cdot v_i[k] \cdot n_i \cdot \Delta t$ represents the flows potentially arriving at the end of queue at time step k , and $N_i[k] - x_i[k]$ is the maximal number of vehicles that can arrive at the end of queue at time step k .

Merging into Lane Groups

After arriving at the end of queue at a link, vehicles may change lanes and merge into different lane groups based on their destinations. It should be noted that the number of vehicles that may merge into lane group m at time step k , denoted as $q_m^i[k]$, can be approximated as follows:

$$q_m^i[k] = \sum_{j \in \Gamma^{-1}(i)} q_i^{arr}[k] \cdot \gamma_{ij}[k] \cdot \delta_m^{ij} \quad (4.8)$$

$q_i^{arr}[k]$ is the total flow arriving at the end of queue of link i at time step k ; $\gamma_{ij}[k]$ is the turning fraction going from link i to j ; δ_m^{ij} is a binary value indicating whether traffic going from link i to j uses lane group m .

Departing Process

The number of vehicles potentially departing from link i to link j at time step k is given by:

$$Q_{ij}^{pot}[k] = \sum_{m \in S_i^M} \min\{q_m^i[k] + x_m^i[k], Q_m^i \cdot g_n^p[k]\} \cdot \lambda_m^{ij}[k] \quad (4.9)$$

$$\lambda_m^{ij}[k] = \frac{\delta_m^{ij} \cdot \gamma_{ij}[k]}{\sum_{j \in \Gamma^{-1}(i)} \delta_m^{ij} \cdot \gamma_{ij}[k]} \quad (4.10)$$

$\min\{q_m^i[k] + x_m^i[k], Q_m^i \cdot g_n^p[k]\}$ depicts the potential departing flows from lane group m at time step k ; $g_n^p[k]$ is a binary variable to represent the signal status of phase p at intersection n at each time step k . $\lambda_m^{ij}[k]$ is the percentage of traffic in lane group m going from link i to j . Therefore, $\min\{q_m^i[k] + x_m^i[k], Q_m^i \cdot g_n^p[k]\} \cdot \lambda_m^{ij}[k]$ reflects the flows potentially departing from link i to j in lane group m . Then the summation of it over all lane groups in link i can be shown with Equation 4.9. Now assuming that a total of one unit flow is to depart from link i at time step k , $\delta_m^{ij} \cdot \gamma_{ij}[k]$ will be the amount of flows going to link j from lane group m within that one unit, and $\sum_{j \in \Gamma^{-1}(i)} \delta_m^{ij} \cdot \gamma_{ij}[k]$ will be the total amount of flows departing from lane group m . Hence, one can have Equation 4.10 holds.

Note that the actual number of vehicles departing from link i to link j at time step k is also constrained by the available storage space of the destination link j . Since the total flow towards one destination link j may consist of several flows from different upstream links, this study assumes that the free storage space of link j allocated to accommodate upstream departing flow from link i is proportional to link i 's potential departing flow. Therefore, the actual departing flows from link i to link j at time step k is given by the following equation:

$$Q_{ij}[k] = \max \left\{ 0, \min \left\{ Q_{ij}^{pot}[k], \frac{Q_{ij}^{pot}[k]}{\sum_{i \in \Gamma(j)} Q_{ij}^{pot}[k]} \cdot s_j[k] \right\} \right\} \quad (4.11)$$

$s_j[k]$ is the available space in link j at time step k , and $Q_{ij}^{pot}[k]/\sum_{i \in \Gamma(j)} Q_{ij}^{pot}[k]$ is the proportion of the available space in link j allocated to accommodate flows from link i .

Then, the actual flow departing from lane group m at link i can be obtained with:

$$Q_m^i[k] = \sum_{j \in \Gamma^{-1}(i)} Q_{ij}[k] \cdot \delta_m^{ij} \quad (4.12)$$

Flow Conservation

Flow conservation equations depict the evolution of the arterial link status over time. With the lane group based concept, queues at links and lane groups will be updated at every unit time interval k .

The lane group based queues are advanced as follows:

$$x_m^i[k+1] = x_m^i[k] + q_m^i[k] - Q_m^i[k] \quad (4.13)$$

Then, the total number vehicles queued at link i is computed as:

$$x_i[k+1] = \sum_{m \in S_i^M} x_m^i[k+1] \quad (4.14)$$

The evolution of total number of vehicles present at link i can be stated as:

$$N_i[k+1] = N_i[k] + \sum_{j \in \Gamma(i)} Q_{ji}[k] - \sum_{j \in \Gamma^{-1}(i)} Q_{ij}[k] \quad (4.15)$$

Finally, one can compute the available storage space of link i as follows:

$$s_i[k+1] = N_i - N_i[k+1] \quad (4.16)$$

4.2.2. Freeway Traffic Flow Formulations

The macroscopic traffic flow model proposed by Messmer and Papageorgiou (1990) was employed in this study to model traffic evolution for the freeway section. In their model, the freeway link is divided into segments, and assumed to have homogeneous flow, density, and speed within each segment, as shown in Figure 4.3.

The traffic state in segment m of link i at time step t can be described with the variables $\rho_{im}[t]$, $v_{im}[t]$, and $q_{im}[t]$. These variables evolve as follows:

$$\rho_{im}[t+1] = \rho_{im}[t] + \frac{\Delta T}{l_{im} n_{im}} (q_{i,m-1}[t] - q_{im}[t]) \quad (4.17)$$

$$q_{im}[t] = \rho_{im}[t] \cdot v_{im}[t] \cdot n_{im} \quad (4.18)$$

$$V_{im}(\rho_{im}[t]) = v_f^i \exp \left[-\frac{1}{\alpha_f} \left(\frac{\rho_{im}[t]}{\rho_{cr}^i} \right)^{\alpha_f} \right] \quad (4.19)$$

$$v_{im}[t+1] = v_{im}[t] + \frac{\Delta T}{\tau} [V(\rho_{im}[t]) - v_{im}[t]] + \frac{\Delta T}{l_{im}} v_{im}[t] [v_{i,m-1}[t] - v_{im}[t]] - \frac{\eta \cdot \Delta T [\rho_{i,m+1}[t] - \rho_{im}[t]]}{\tau \cdot l_{im} [\rho_{im}[t] + \kappa]} \quad (4.20)$$

In the above equations, ΔT is the time step to update freeway status (usually 5 - 10 s); l_{im} is the length of segment m ; n_{im} is the number of lanes in segment m ; Equation 4.19 is the fundamental diagram used to depict the relation between the speed and density of traffic within the segment; v_f^i is the free flow speed in link i ; ρ_{cr}^i is the critical density of link i ; α_f is a constant driver behavioral related parameter.

Equation 4.20 depicts the evolution of speed in segment m which is affected by the density of the segment, the speed of vehicles from the upstream segment, and

the perception of density difference in the downstream segment. In it, τ is the relaxation time constant, η is the anticipation coefficient, and κ is a positive constant that limits the anticipation term to be within a reasonable range.

For the segments adjacent to the off-ramp ν and on-ramp μ , this study has extended the model with the following equations:

$$q_{i-1,N(i-1)}[t] = \rho_{i-1,N(i-1)}[t] \cdot v_{i-1,N(i-1)}[t] \cdot n_{i-1,N(i-1)} \cdot [1 - \gamma_{\nu}^h - \beta_{\nu}^h \cdot Z_{\nu}^h] + q_{\nu}^{in}[t] \quad (4.21)$$

$$q_{i0}[t] = q_{i-1,N(i-1)}[t] - q_{\nu}^{in}[t] \quad (4.22)$$

$$q_{i+1,0}[t] = q_{i,N(i)}[t] + Q_{\mu}[t] \quad (4.23)$$

In the above equations, as shown in Figure 4.3, $N(i)$ is the number of segments in link i ; $q_{i-1,N(i-1)}[t]$ represents the actual flow rate leaving from the freeway link right before the off-ramp ν at time step t ; γ_{ν}^h is the normal exit rate for off-ramp ν during the control interval h ; Z_{ν}^h is the diversion rate during the control interval h ; β_{ν}^h is the driver compliance rate to the detour operation during the control interval h ; $q_{\nu}^{in}[t]$ is the actual entering flow rate into off-ramp ν at time step t (given by Equation 4.30). $q_{i0}[t]$ depicts the actual entering flow rate into the freeway link right after the off-ramp ν at time step t . $q_{i+1,0}[t]$ represents the flow rate entering the freeway link right after the on-ramp μ at time step t , and $Q_{\mu}[t]$ is the actual merging flow rate into freeway from on-ramp μ at time step t (given by Equation 4.28).

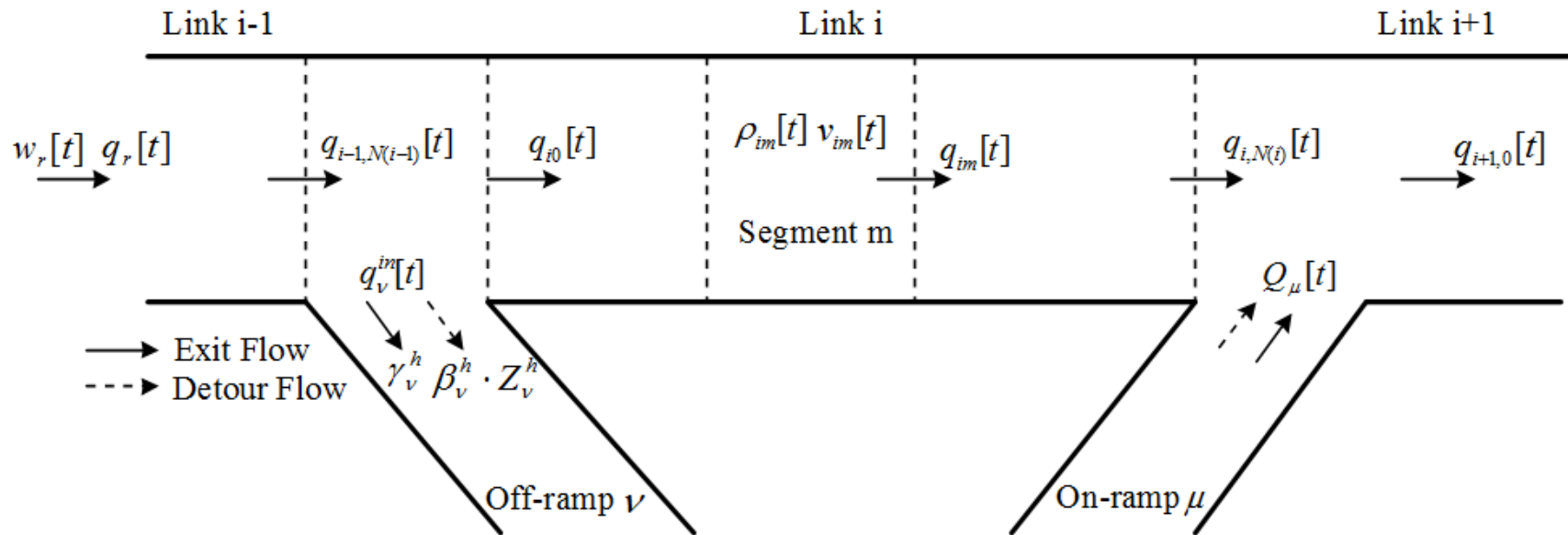


Figure 4.3 Traffic Dynamics in Freeway Sections

Demand origins on freeway are modeled as follows:

$$q_r[t] = \min \left[d_r[t] + \frac{w_r[t]}{\Delta T}, Q_i[t] \cdot \min \left[1, \frac{\rho^{jam} - \rho_i[t]}{\rho^{jam} - \rho_i^{crit}} \right] \right] \quad (4.24)$$

$$w_r[t+1] = w_r[t] + \Delta T [d_r[t] - q_r[t]] \quad (4.25)$$

$q_r[t]$ is the flow rate entering the freeway mainline from the demand origin r at time step t ; $d_r[t]$ is the demand flow rate at origin r at time step t ; $w_r[t]$ is the flow queuing at the origin r at time step t .

4.2.3. Formulations for On-off Ramps

Ramps can be viewed as simplified arterial links in the proposed lane-group based model (see Figure 4.4) as long as the update time interval for traffic propagation equations are consistent with that used for the freeway system. An approach by Van den Berg et al. (2001) to keep consistency between updating steps in freeway and arterial systems is adopted below for modeling traffic dynamics at on-ramps and off-ramps:

On-ramp

The on-ramp can be modeled as a simplified arterial link with only one lane group and one downstream link, as shown in Figure 4.4-(a). Since the update step for freeway (ΔT) is larger than the one for arterial (Δt), the following relation was defined to maintain consistency between these two systems:

$$\Delta T = l \cdot \Delta t \quad (4.26)$$

l is a positive integer. Therefore, corresponding to the time step t for freeway, the time step for the arterial is:

$$k = l \cdot t \quad (4.27)$$

The only difference between an on-ramp and an arterial link is the departing process. The actual flow that is allowed to merge into freeway from on-ramp μ during the interval from t to $t+l$ is given by:

$$Q_\mu[t] = \min \left(\frac{x_\mu[l \cdot t] + \sum_{k=lt}^{l(t+1)-1} q_\mu^{arr}[k]}{\Delta T}, Q_\mu \cdot R_\mu^h, Q_\mu \cdot \min[1, \frac{\rho^{jam} - \rho_{i+1,0}[t]}{\rho^{jam} - \rho_i^{crit}}] \right) \quad (4.28)$$

$x_\mu[l \cdot t] + \sum_{k=lt}^{l(t+1)-1} q_\mu^{arr}[k]$ is the potential number of vehicles to merge into freeway mainline from on-ramp μ at time step t ; Q_μ is the discharge capacity of on-ramp μ ; R_μ^T is the metering rate for on-ramp μ during the control interval h , and other parameters are the same as before. Thus, based on the assumption of equal distribution of $Q_\mu[t]$ over the time interval between t and $t+l$, one can approximate the actual number of vehicles departing from on-ramp μ at each arterial time step k between $l \cdot t$ and $l \cdot (t+1) - 1$ by:

$$Q_\mu[k] = \frac{Q_\mu[t] \cdot \Delta T}{l}, \quad \forall k \in [l \cdot t, l \cdot (t+1) - 1] \quad (4.29)$$

Off-ramp

The off-ramp could also be modeled as an arterial link if the upstream arrival process is modified properly, as shown in Figure 4.4-(b). The actual flow that enters off-ramp ν at time step t is given by:

$$q_{\nu}^{in}[t] = \min\left\{\rho_{i-1,N(i-1)}[t] \cdot v_{i-1,N(i-1)}[t] \cdot n_{i-1,N(i-1)} \cdot (\gamma_{\nu}^h + \beta_{\nu}^h \cdot Z_{\nu}^h), \right. \\ \left. Q_{\nu}, \frac{s_{\nu}[l \cdot t] + \sum_{k=lt}^{l(t+1)-1} \sum_{j \in \Gamma^{-1}(\nu)} Q_{\nu_j}[k]}{\Delta T}\right\} \quad (4.30)$$

Q_{ν} represents the capacity of off-ramp ν , and $s_{\nu}[l \cdot t] + \sum_{k=lt}^{l(t+1)-1} \sum_{j \in \Gamma^{-1}(\nu)} Q_{\nu_j}[k]$ is the available space at off-ramp ν . Other parameters keep the same meanings.

Similarly, one may assume $q_{\nu}^{in}[t]$ to be uniformly distributed during the time interval between t and $t+l$, then the actual number of vehicles arriving at the upstream of off-ramp ν at each arterial time step k between $l \cdot t$ and $l \cdot (t+1) - 1$ is stated as:

$$q_{\nu}^{in}[k] = \frac{q_{\nu}^{in}[t] \cdot \Delta T}{l}, \quad \forall k \in [l \cdot t, l \cdot (t+1) - 1] \quad (4.31)$$

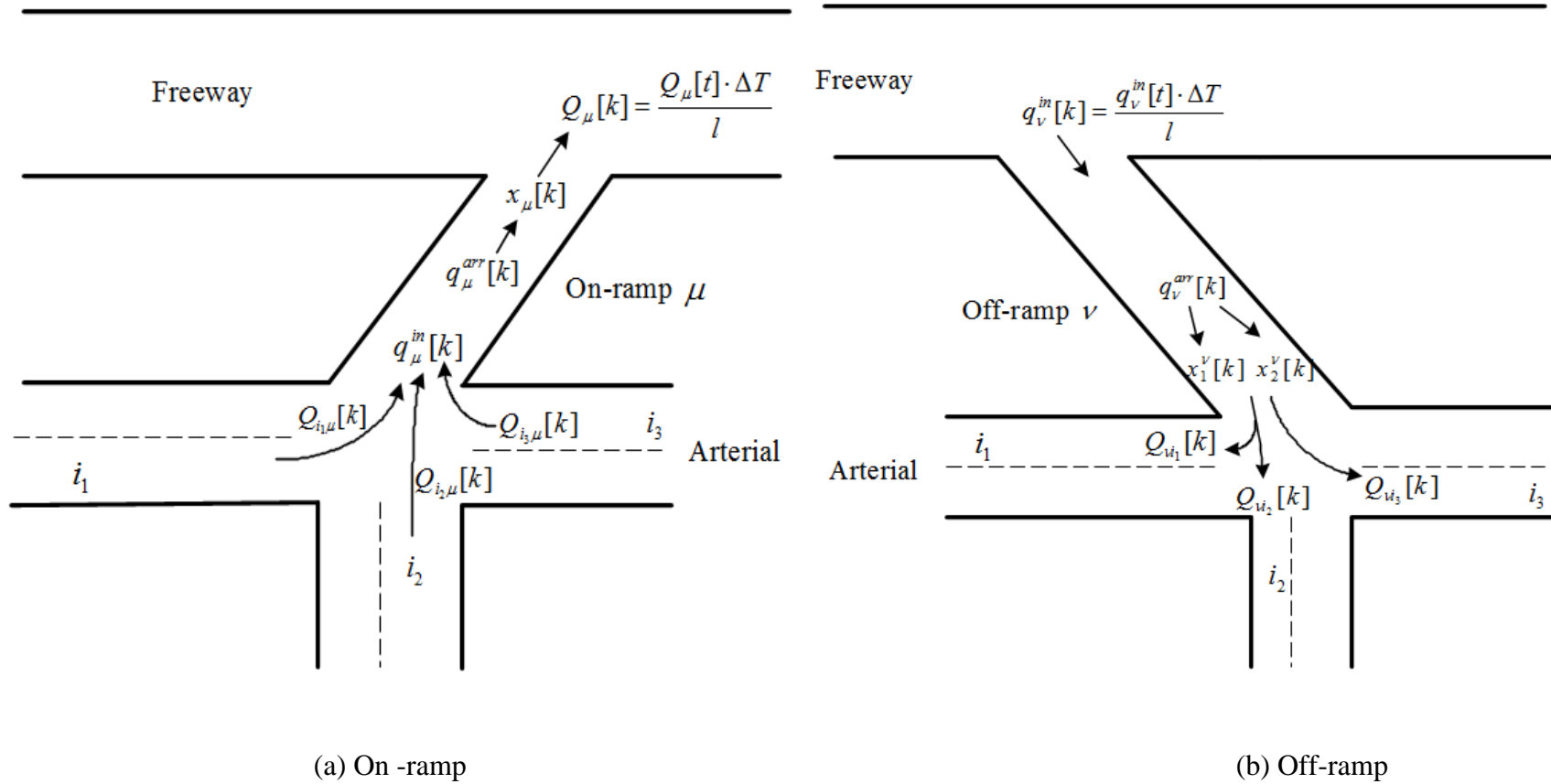


Figure 4.4 Traffic Dynamics in the On-ramp and Off-ramp

4.3. Base Model: Integrated Control of a Single Segment Corridor

4.3.1. Model Scope and Assumptions

This section will illustrate the formulations of the base model for integrated corridor control, which includes a segment of the freeway mainline experiencing an incident, the on-ramp and off-ramp upstream to the incident location, the connecting parallel arterial, and the on-ramp and off-ramp right beyond the incident location (see Figure 4.5). The control decisions mainly include: 1) the percentage of freeway traffic to be diverted to the detour route, 2) the metering rates at the incident upstream on-ramp, and 3) the signal timing plans at arterial intersections.

To ensure that the proposed formulations for the base model are tractable and also realistically reflect the real-world constraints, this section has employed the following assumptions:

- Traffic is diverted to the arterial through the off-ramp just upstream to the incident section, and will be guided back to the on-ramp right after the incident section. The compliance rate for drivers is assumed to be known or obtainable from the on-line surveillance system deployed in the control area;
- For the freeway segment, only the direction plagued by the incident is included in the control process. In contrast, both directions of the arterial will be included in the control boundaries;

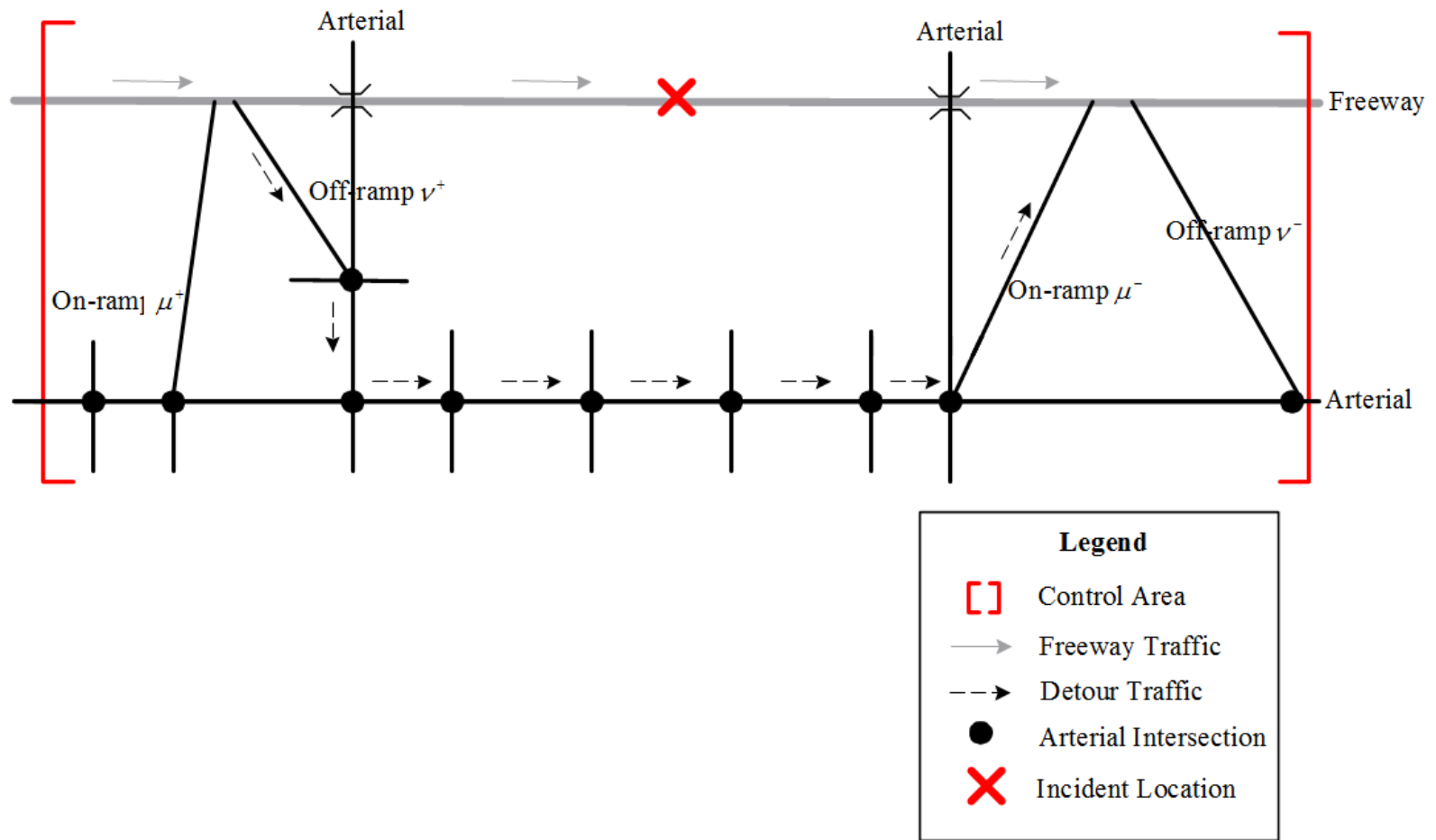


Figure 4.5 Scope of the Base Model

- Normal traffic patterns, including off-ramp exit rates, normal traffic getting into the freeway via the on-ramp, and existing arterial intersection turning proportions, are assumed to be stable and not impacted by the detour traffic, or the impact can be estimated (see Section 4.3.2);
- A common cycle length C^h is assumed for all intersections in the arterial during control interval h , and the phase sequence is pre-set; and
- The entire control time horizon H is decomposed into a series of control time intervals h (i.e. $\sum_h T_h = H$). The length of each control interval, T_h , is an integer multiple of the common cycle length C^h (i.e. $T_h = c \cdot C^h$). Control decisions are optimized over each successive time interval h .

4.3.2. Network Model Enhancement – Projection of Detour Traffic Impact

To ensure the effectiveness of the generated control strategies, one of the critical tasks is to project the impact of detour traffic given the detour route and the dynamic diversion rates. This section illustrates an enhanced network model that can precisely project the time-varying impacts of detour traffic on the existing corridor demand patterns with the aforementioned lane-group-based concept. The key concept is to track the evolution of normal traffic and detour traffic separately over the arterial link, as shown in Figure 4.6. Hereafter lists several additional variables to be incorporated in the enhanced model formulations.

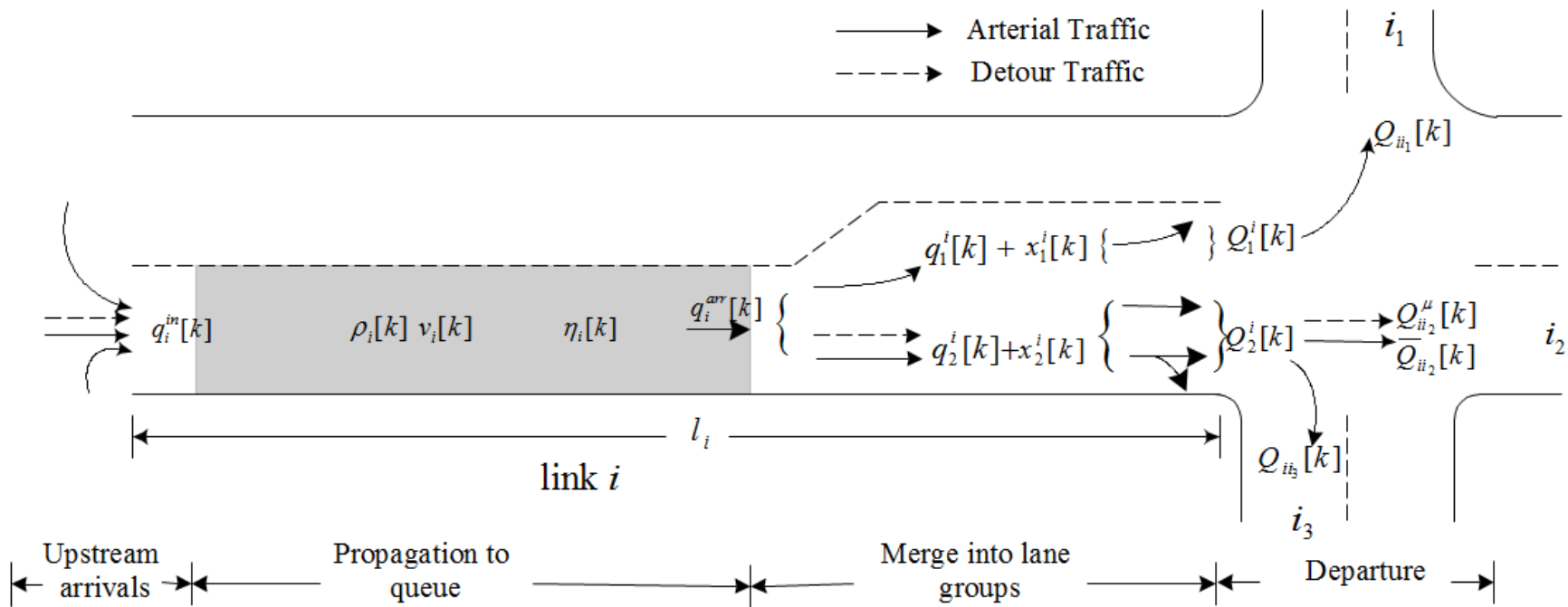


Figure 4.6 Dynamic Traffic Flow Evolutions Considering the Detour Traffic Impact

Additional Variables

μ^+, ν^+	Index of the incident upstream on-ramp and off-ramp, respectively (see Figure 4.5)
μ^-, ν^-	Index of the incident downstream on-ramp and off-ramp, respectively (see Figure 4.5)
$\bar{\gamma}_{ij}[k], j \in \Gamma^{-1}(i)$	Relative turning proportion of <u>normal</u> arterial traffic from link i to j
$\gamma_{ij}^{\mu^-}, j \in \Gamma^{-1}(i)$	A binary value indicating whether <u>detour</u> traffic at link i heading to downstream on-ramp μ^- will use downstream link j or not
$\bar{N}_i[k]$	Num. of vehicles from <u>normal</u> arterial traffic at link i at step k
$N_i^{\mu^-}[k]$	Num. of <u>detour</u> vehicles heading to downstream on-ramp μ^- at link i at step k
$\eta_i[k]$	Fraction of <u>normal</u> arterial traffic in total traffic at link i at step k
$\bar{\lambda}_m^{ij}[k], j \in \Gamma^{-1}(i)$	Percentage of <u>normal</u> arterial traffic in lane group m going from link i to j
$\bar{Q}_{ij}[k]$	<u>Normal</u> arterial traffic flows actually depart from link i to link j at step k
$Q_{ij}^{\mu^-}[k]$	<u>Detour</u> traffic flows heading to downstream on-ramp μ^- actually depart from link i to link j at step k

Enhanced Formulations

In formulating the upstream arrivals, considering both normal arterial traffic and detour traffic, Equation 4.3 could be extended as follows:

$$q_i^{in}[k] = \sum_{j \in \Gamma(i)} \bar{Q}_{ji}[k] + \sum_{j \in \Gamma(i)} Q_{ji}^{\mu^-}[k] \quad (4.32)$$

$\bar{Q}_{ji}[k]$ and $Q_{ji}^{\mu^-}[k]$ represent the actual flows departing from upstream link j to link i for normal arterial traffic and detour traffic, respectively.

In formulating the process of propagation to the end of queue, Equation 4.6 and Equation 4.7 will be extended as:

$$\rho_i[k] = \frac{\bar{N}_i[k] + N_i^{\mu^-}[k] - x_i[k]}{n_i \left(l_i - \frac{x_i[k]}{n_i \cdot \rho^{jam}} \right)} \quad (4.33)$$

$$q_i^{arr}[k] = \min \left\{ \rho_i[k] \cdot v_i[k] \cdot n_i \cdot \Delta t, \bar{N}_i[k] + N_i^{\mu^-}[k] - x_i[k] \right\} \quad (4.34)$$

$\bar{N}_i[k] + N_i^{\mu^-}[k] - x_i[k]$ represents the number of vehicles (both normal arterial traffic and detour traffic) moving at the segment between the link upstream and the end of queue.

In formulating the process of merging into lane groups, Equation 4.8 can be extended as:

$$q_m^i[k] = \sum_{j \in \Gamma^{-1}(i)} q_i^{arr}[k] \cdot [\eta_i[k] \cdot \bar{\gamma}_{ij}[k] + (1 - \eta_i[k]) \cdot \gamma_{ij}^{\mu^-}] \cdot \delta_m^{ij} \quad (4.35)$$

$q_i^{arr}[k] \cdot \eta_i[k] \cdot \bar{\gamma}_{ij}[k]$ represents the normal arterial traffic flow going to link j at time step k , and $q_i^{arr}[k] \cdot (1 - \eta_i[k]) \cdot \gamma_{ij}^{\mu^-}$ denotes the detour traffic flow going to link j at time step k ; δ_m^{ij} is a binary value indicating whether traffic going from link i to j uses lane group m . Hence, one can approximate Equation 4.35 as the potential level of flows that may merge into lane group m at time step k .

In formulating the departure process, Equation 4.10 will be modified as:

$$\lambda_m^{ij}[k] = \frac{\delta_m^{ij} \cdot [\eta_i[k] \bar{\gamma}_{ij}[k] + (1 - \eta_i[k]) \gamma_{ij}^{\mu^-}]}{\sum_{j \in \Gamma^{-1}(i)} \delta_m^{ij} \cdot [\eta_i[k] \bar{\gamma}_{ij}[k] + (1 - \eta_i[k]) \gamma_{ij}^{\mu^-}]} \quad (4.36)$$

$\lambda_m^{ij}[k]$ is the percentage of traffic in lane group m going from link i to j . Assuming that a total of one unit flow is to depart from link i at time step k , $\eta_i[k] \bar{\gamma}_{ij}[k] + (1 - \eta_i[k]) \cdot \gamma_{ij}^{\mu^-}$ will be the amount of flows within that one unit to go to link j , and $\delta_m^{ij} \cdot [\eta_i[k] \bar{\gamma}_{ij}[k] + (1 - \eta_i[k]) \cdot \gamma_{ij}^{\mu^-}]$ will be the amount of flows going to link j by lane group m , and $\sum_{j \in \Gamma^{-1}(i)} \delta_m^{ij} \cdot [\eta_i[k] \bar{\gamma}_{ij}[k] + (1 - \eta_i[k]) \cdot \gamma_{ij}^{\mu^-}]$ will be the total amount of flows departing from lane group m . Hence, $\lambda_m^{ij}[k]$ can be approximated with Equation 4.36. Similarly, the percentage of normal arterial traffic in lane group m going from link i to j , $\bar{\lambda}_m^{ij}[k]$, can be approximated with Equation 4.37:

$$\bar{\lambda}_m^{ij}[k] = \frac{\delta_m^{ij} \cdot \eta_i[k] \cdot \bar{\gamma}_{ij}[k]}{\sum_{j \in \Gamma^{-1}(i)} \delta_m^{ij} \cdot [\eta_i[k] \bar{\gamma}_{ij}[k] + (1 - \eta_i[k]) \gamma_{ij}^{\mu^-}]} \quad (4.37)$$

By substituting Equations 4.36 and 4.37 into Equations 4.9, 4.11, and 4.12, one can obtain the flows actually departing from lane group m at time step k , $Q_m^i[k]$, which includes both normal arterial traffic and detour traffic.

Then, the actual departing flow of normal arterial traffic from link i to link j at time step k is given by:

$$\bar{Q}_{ij}[k] = Q_m^i[k] \cdot \bar{\lambda}_m^{ij}[k] \quad (4.38)$$

Note that, the percentage of detour traffic in lane group m going from link i to j with destination to on-ramp μ^- can be obtained as $(\lambda_m^{ij}[k] - \bar{\lambda}_m^{ij}[k])$.

Therefore, the actual departing flow of detour traffic from link i to link j heading to downstream on-ramp μ^- at time step k is given by:

$$Q_{ij}^{\mu^-}[k] = Q_m^i[k] \cdot (\lambda_m^{ij}[k] - \bar{\lambda}_m^{ij}[k]) \quad (4.39)$$

In formulating the flow conservation, Equations 4.15 and 4.16 will be substituted by the following set of equations:

The evolution of the total number of normal arterial vehicles at link i can be stated as:

$$\bar{N}_i[k+1] = \bar{N}_i[k] + \sum_{j \in \Gamma(i)} \bar{Q}_{ji}[k] - \sum_{j \in \Gamma^{-1}(i)} \bar{Q}_{ij}[k] \quad (4.40)$$

The evolution of the total number of detour vehicles heading to on-ramp μ^- at link i can be stated as:

$$N_i^{\mu^-}[k+1] = N_i^{\mu^-}[k] + \sum_{j \in \Gamma(i)} Q_{ji}^{\mu^-}[k] - \sum_{j \in \Gamma^{-1}(i)} Q_{ij}^{\mu^-}[k] \quad (4.41)$$

One can compute the available storage space of link i as follows:

$$s_i[k+1] = N_i - \bar{N}_i[k+1] - N_i^{\mu^-}[k+1] \quad (4.42)$$

Finally, the fraction of normal arterial traffic at link i is updated as:

$$\eta_i[k+1] = \frac{\bar{N}_i[k+1]}{\bar{N}_i[k+1] + N_i^{\mu^-}[k+1]} \quad (4.43)$$

4.3.3. Model Formulations

Based on the above enhanced network formulations, an effective multi-objective control model is formulated in this section to determine the best set of control strategies that can efficiently explore the control effectiveness under different policy priorities between the target freeway and available detour routes.

Objective Functions

Given the entire time horizon H for control, the first objective of the control model is to maximize the utilization of the parallel arterial so as to relieve congestion on the freeway mainline. This objective can further be stated as maximizing the total throughput of the freeway corridor during the incident management period by using the parallel arterial as the detour route. Since the throughput equals the total number of vehicles entering the freeway link downstream of the on-ramp μ^- plus the total number of vehicles entering the arterial outgoing links, it can be stated as:

$$\max \quad \sum_{t=1}^H q_{i+1,0}[t] \cdot \Delta T + \sum_{k=1}^H \sum_{i \in S^{OUT}} q_i^{in}[k] \quad (4.44)$$

$q_{i+1,0}[t]$ is the flow rate entering the freeway link $(i+1)$ downstream of the on-ramp μ^- ; S^{OUT} is the set of outgoing links in the arterial network.

The second objective function is designed to reflect the perspective of detour travelers, which aims at minimizing their total travel time on the detour route to ensure their compliance to the routing guidance. This objective is given by:

$$\min \quad \sum_{k=1}^H \left[\sum_{i \in S^U} N_i^{\mu^-}[k] + N_{\nu^+}^{\mu^-}[k] + N_{\mu^-}^{\mu^-}[k] \right] \cdot \Delta t \quad (4.45)$$

$N_i^{\mu^-}[k]$, $N_{\nu^+}^{\mu^-}[k]$, and $N_{\mu^-}^{\mu^-}[k]$ represent the number of detour vehicles present at link i , off-ramp ν^+ , and on-ramp μ^- within the control area at time step k , respectively.

Decision Variables

Decision variables need to be solved in the optimization formulation include:

$\{C^h, h \in H\}$	Common cycle length for all intersections in the control interval h
$\{\Delta_n^h, \forall n \in S_N, h \in H\}$	Offset of intersection n for each control interval h
$\{G_{np}^h, \forall n \in S_N, p \in P_n, h \in H\}$	Green time for phase p of intersection n for each control interval h
$\{R_{\mu^+}^h, h \in H\}$	Metering rate at the incident upstream on-ramp μ^+ for each control interval h
$\{Z_{\nu^+}^h, h \in H\}$	Diversion rate at the incident upstream off-ramp ν^+ for each control interval h

Operational Constraints

Representing the traffic state evolution along different parts of the traffic corridor, Equations 4.1, 4.2, 4.4, 4.5, 4.9, 4.11 – 4.14, 4.17 – 4.25, and 4.28 – 4.43 constitute the principal constraints for the control model. Moreover, the following constraints are common restrictions for the control decision variables:

$$C^{\min} \leq C^h \leq C^{\max} \quad (4.46)$$

$$G_{np}^{\min} \leq G_{np}^h < C^h, \forall n \in S_N, p \in P_n, h \in H \quad (4.47)$$

$$\sum_{p \in P_n} G_{np}^h + \sum_{p \in P_n} I_{np} = C^h, \forall n \in S_N, p \in P_n, h \in H \quad (4.48)$$

$$0 \leq \Delta_n^h < C^h, \forall n \in S_N, h \in H \quad (4.49)$$

$$R^{\min} \leq R_{\mu^+}^h \leq R^{\max}, h \in H \quad (4.50)$$

$$\beta_{\nu^+}^h \cdot Z_{\nu^+}^h + \gamma_{\nu^+}^h \leq Z^{\max}, h \in H \quad (4.51)$$

C^{\min} and C^{\max} are the minimum and maximum cycle length, respectively; P_n is the set

of signal phases at intersection n ; G_{np}^{\min} is the minimal green time for phase p of intersection n ; and I_{np} represents the clearance time for phase p of intersection n . R^{\min} and R^{\max} are the minimum and maximum metering rates for on-ramp, and Z^{\max} is the maximum percentage of traffic (including both detour and normal exiting) that can diverge from freeway to arterial.

Equation 4.46 restricts the common cycle length to be between the minimal and maximal values. Equation 4.47 requires that the green time for each phase should at least satisfy the minimal green time, and not exceed the cycle length. The sum of green times and clearance times for all phases at intersection n should be equal to the cycle length (see Equation 4.48). Furthermore, the offset of intersection n shall be constrained by Equation 4.49, and lie between 0 and the cycle length. Equation 4.50 limits the metering rate for on-ramp μ^+ , and the diversion rate is bounded by Equation 4.51.

Note that, the arterial traffic state equations are not explicitly related to the signal control variables C^h , Δ_n^h , and G_{np}^h . To represent the signal status of phase p at each time step k , the binary variable $g_n^p[k]$ is defined before to indicate whether or not the corresponding phase p is in green. For a signal controller with a set of phases P_n shown in Figure 4.7, this study proposes the following equations to model relations between the signal status at time step k and signal control parameters:

$$(\delta_n^p[k] - 0.5) \cdot \text{mod}(k - \Delta_n^h, C^h) \leq (\delta_n^p[k] - 0.5) \cdot \sum_{j=1}^{p-1} (G_{nj}^h + I_{nj}) \quad (4.52)$$

$$p \in P_n, n \in S_N, h \in H, k \in T_h$$

$$(\delta_n^{''p}[k] - 0.5) \cdot \text{mod}(k - \Delta_n^h, C^h) > (\delta_n^{''p}[k] - 0.5) \cdot \left(\sum_{j=1}^{p-1} (G_{nj}^h + I_{nj}) + G_{np}^h \right) \quad (4.53)$$

$$p \in P_n, n \in S_N, h \in H, k \in T_h$$

$$g_n^p[k] = 1 - \delta_n^{'p}[k] - \delta_n^{''p}[k], \quad p \in P_n, n \in S_N, k \in T_h \quad (4.54)$$

$\{\delta_n^{'p}[k], \delta_n^{''p}[k], p \in P_n, n \in S_N, k \in T_h\}$ are a set of auxiliary 0-1 variables.

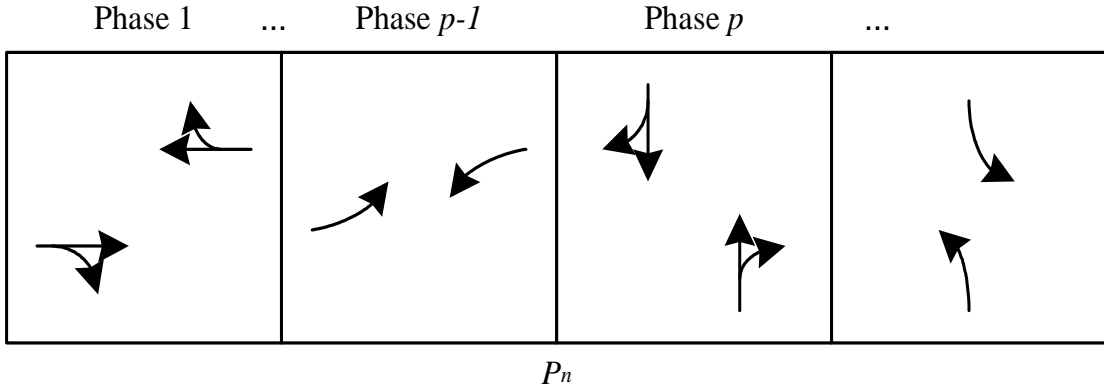


Figure 4.7 A Signal Controller with a Set of Phases P_n

Other constraints include nonnegative constraints and initial values of the link state variables in the corridor network, which can be obtained from the on-line surveillance system to reflect the actual network condition preceding the onset of an incident.

The Overall Model

In summary, the mathematical description of the multi-objective integrated corridor control problem is recapitulated as follows:

$$\begin{aligned}
\min \quad & \Phi(s) = \begin{bmatrix} f_1(s) \\ f_2(s) \end{bmatrix} \\
f_1 : & - \left[\sum_{t=1}^H q_{i+1,0}[t] \cdot \Delta T + \sum_{k=1}^H \sum_{i \in S^{OUT}} q_i^{in}[k] \right] \\
f_2 : & \sum_{k=1}^H \left[\sum_{i \in S^U} N_i^{\mu^-}[k] + N_{v^+}^{\mu^-}[k] + N_{\mu^+}^{\mu^-}[k] \right] \cdot \Delta t \\
s.t. \quad & s : \{C^h, \Delta_n^h, G_{np}^h, R_{\mu^+}^h, Z_{v^+}^h, \forall h \in H\}
\end{aligned} \tag{4.55}$$

s denotes the feasible solution space defined by Equations 4.1, 4.2, 4.4, 4.5, 4.9, 4.11 – 4.14, 4.17 – 4.25, 4.28 – 4.43, and 4.46 – 4.54.

4.4. Extended Model: Integrated Control of A Multi-segment Corridor

4.4.1. Scope of the Extended Model

This section presents the extended model for integrated control of a multi-segment traffic corridor, in which multiple detour routes composed of several on-ramps, off-ramps, and different segments of parallel arterials are operated integrally to divert traffic (as illustrated in Figure 4.8) during the period of incident management.

The extended model includes additional constraints are formulated to accommodate various operational complexities due to the interactions between multiple diversion decisions. The optimized plan mainly yields the following three types of control parameters: 1) a set of critical upstream off-ramps and downstream on-ramps to be covered in the detour operations (i.e. a control area); 2) dynamic

diversion rates and detour destinations for traffic at all critical upstream off-ramps; and 3) the target on-ramp metering rates and arterial signal timings during each control time interval. The proposed model will be able to best demonstrate its effectiveness under the following two scenarios:

- **Under a lane-blockage incident.** When a lane-blockage incident occurs in a freeway mainline segment, its impact may quickly exceed the boundaries of a single-segment corridor and spill back to its upstream ramps.
- **With insufficient ramp capacity.** The effectiveness of detour operations is usually constrained by the available ramp capacity. Implementation of detour operations only for the incident segment may not be effective if the demand surge due to diversion induces a bottleneck at the ramps.

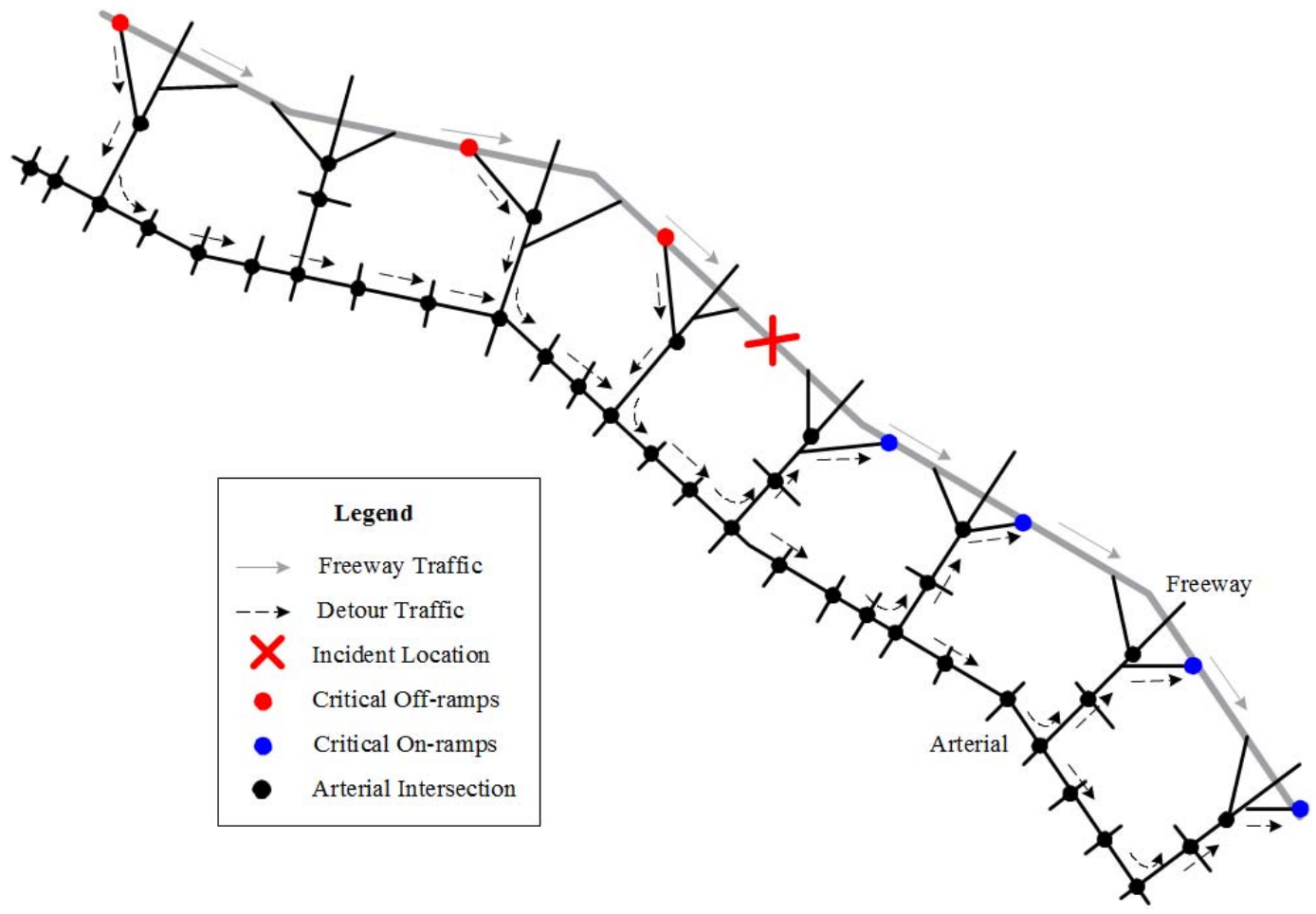


Figure 4.8 Scope of the Extended Model for Integrated Corridor Control

4.4.2. Assumptions for the Extended Model

The key concept of the extended model is to choose a critical set of upstream off-ramps, and dynamically connect them with downstream on-ramps via different segments of the parallel arterial to best utilize the corridor capacity during the incident management. The extended model is developed with the following additional assumptions:

- The detour route (portion of arterial) that connects a given off-ramp and on-ramp is predetermined; and
- For each control interval h , traffic at a selected upstream off-ramp will be detoured to no more than one downstream on-ramp.

4.4.3. Model Formulations

This extended model uses a similar bi-objective optimization as shown in Equations 4.44 and 4.45. The network flow formulations are also similar as those in the Base Model, but with some extension to capture the effects of multi-route detour operations on the corridor network. Key variables and constraints of the elaborated network for applying the extended model are illustrated below.

Key Variables

S_{μ}^{+}, S_{μ}^{-}	Set of on-ramps upstream and downstream of the incident location, respectively
S_{ν}^{+}, S_{ν}^{-}	Set of off-ramps upstream and downstream of the incident location, respectively
μ, ν	Index of the on-ramps and off-ramps, respectively
$\delta_{\nu\mu}^h, \nu \in S_{\nu}^{+}, \mu \in S_{\mu}^{-}, h \in H$	A 0-1 decision variable indicating whether traffic at upstream off-ramp ν will be diverted to downstream on-ramp μ during the control interval h (1 – Yes, 0 – No)
$\bar{\gamma}_{ij}[k], j \in \Gamma^{-1}(i)$	Relative turning proportion of <u>normal</u> arterial traffic from link i to j
$\gamma_{ij}^{\mu}, j \in \Gamma^{-1}(i), \mu \in S_{\mu}^{-}$	A binary value indicating whether <u>detour</u> traffic at link i heading to downstream on-ramp μ will use downstream link j or not
$\bar{N}_i[k]$	Num. of vehicles from <u>normal</u> arterial traffic at link i at step k
$N_i^{\mu}[k], \mu \in S_{\mu}^{-}$	Num. of <u>detour</u> vehicles heading to downstream on-ramp μ at link i at step k . Note that, we have $\bar{N}_i[k] + \sum_{\mu \in S_{\mu}^{-}} N_i^{\mu}[k] = N_i[k]$ holds
$\eta_i[k]$	Fraction of <u>normal</u> arterial traffic in total traffic at link i at step k
$\theta_i^{\mu}[k], \mu \in S_{\mu}^{-}$	Fraction of traffic heading to downstream on-ramp μ within the total detour traffic at step k . Note that, we have $\sum_{\mu \in S_{\mu}^{-}} \theta_i^{\mu}[k] = 1$ holds

$\bar{\lambda}_m^{ij}[k], j \in \Gamma^{-1}(i)$	Percentage of <u>normal</u> arterial traffic in lane group m going from link i to j
$\lambda_m^{i\mu}[k], j \in \Gamma^{-1}(i), \mu \in S_\mu^-$	Percentage of <u>detour</u> traffic in lane group m going from link i to j with destination to on-ramp μ . Note that, we have $\bar{\lambda}_m^{ij}[k] + \sum_{\mu \in S_\mu^-} \lambda_m^{i\mu}[k] = \lambda_m^{ij}[k]$ holds
$\bar{Q}_{ij}[k]$	<u>Normal</u> arterial traffic flows actually depart from link i to link j at step k
$Q_{ij}^\mu[k], \mu \in S_\mu^-$	<u>Detour</u> traffic flows heading to downstream on-ramp μ actually depart from link i to link j at step k . Note that, we have $\bar{Q}_{ij}[k] + \sum_{\mu \in S_\mu^-} Q_{ij}^\mu[k] = Q_{ij}[k]$ holds

Network Flow Constraints

The extended model features its capability in capturing the evolution of detour traffic heading to more than one downstream on-ramps along the detour route with the following sets of constraints:

- The constraints to represent network flow evolution at arterial links are similar to those in the Base Model, except that Equations 4.32 – 4.43 are substituted by Equations 4.56 – 4.69 to accommodate the detour traffic heading to multiple downstream on-ramp $\mu, \mu \in S_\mu^-$.

$$q_i^{in}[k] = \sum_{j \in \Gamma(i)} \bar{Q}_{ji}[k] + \sum_{\mu \in S_\mu^-} \sum_{j \in \Gamma(i)} Q_{ji}^\mu[k] \quad (4.56)$$

$$\rho_i[k] = \frac{\bar{N}_i[k] + \sum_{\mu \in S_\mu^-} N_i^\mu[k] - x_i[k]}{n_i \left(l_i - \frac{x_i[k]}{n_i \cdot \rho^{jam}} \right)} \quad (4.57)$$

$$q_i^{arr}[k] = \min\{\rho_i[k] \cdot v_i[k] \cdot n_i \cdot \Delta t, \bar{N}_i[k] + \sum_{\mu \in S_\mu^-} N_i^\mu[k] - x_i[k]\} \quad (4.58)$$

$$q_m^i[k] = \sum_{j \in \Gamma^{-1}(i)} q_i^{arr}[k] \cdot \left[\eta_i[k] \cdot \bar{\gamma}_{ij}[k] + \sum_{\mu \in S_\mu^-} (1 - \eta_i[k]) \cdot \theta_i^\mu[k] \cdot \gamma_{ij}^\mu \right] \cdot \delta_m^{ij} \quad (4.59)$$

$$\lambda_m^{ij}[k] = \frac{\delta_m^{ij} \cdot \left[\eta_i[k] \bar{\gamma}_{ij}[k] + \sum_{\mu \in S_\mu^-} (1 - \eta_i[k]) \theta_i^\mu[k] \gamma_{ij}^\mu \right]}{\sum_{j \in \Gamma^{-1}(i)} \delta_m^{ij} \cdot \left[\eta_i[k] \bar{\gamma}_{ij}[k] + \sum_{\mu \in S_\mu^-} (1 - \eta_i[k]) \theta_i^\mu[k] \gamma_{ij}^\mu \right]} \quad (4.60)$$

$$\bar{\lambda}_m^{ij}[k] = \frac{\delta_m^{ij} \cdot \eta_i[k] \bar{\gamma}_{ij}[k]}{\sum_{j \in \Gamma^{-1}(i)} \delta_m^{ij} \cdot \left[\eta_i[k] \bar{\gamma}_{ij}[k] + \sum_{\mu \in S_\mu^-} (1 - \eta_i[k]) \theta_i^\mu[k] \gamma_{ij}^\mu \right]} \quad (4.61)$$

$$\lambda_m^{ij\mu}[k] = \frac{\delta_m^{ij} \cdot (1 - \eta_i[k]) \theta_i^\mu[k] \gamma_{ij}^\mu}{\sum_{j \in \Gamma^{-1}(i)} \delta_m^{ij} \cdot \left[\eta_i[k] \bar{\gamma}_{ij}[k] + \sum_{\mu \in S_\mu^-} (1 - \eta_i[k]) \theta_i^\mu[k] \gamma_{ij}^\mu \right]} \quad (4.62)$$

$$\bar{Q}_{ij}[k] = Q_m^i[k] \cdot \bar{\lambda}_m^{ij}[k] \quad (4.63)$$

$$Q_{ij}^\mu[k] = Q_m^i[k] \cdot \lambda_m^{ij\mu}[k], \mu \in S_\mu^- \quad (4.64)$$

$$\bar{N}_i[k+1] = \bar{N}_i[k] + \sum_{j \in \Gamma(i)} \bar{Q}_{ji}[k] - \sum_{j \in \Gamma^{-1}(i)} \bar{Q}_{ij}[k] \quad (4.65)$$

$$N_i^\mu[k+1] = N_i^\mu[k] + \sum_{j \in \Gamma(i)} Q_{ji}^\mu[k] - \sum_{j \in \Gamma^{-1}(i)} Q_{ij}^\mu[k], \mu \in S_\mu^- \quad (4.66)$$

$$s_i[k+1] = N_i - \bar{N}_i[k+1] - \sum_{\mu \in S_\mu^-} N_i^\mu[k+1] \quad (4.67)$$

$$\eta_i[k+1] = \frac{\bar{N}_i[k+1]}{\bar{N}_i[k+1] + \sum_{\mu \in S_\mu^-} N_i^\mu[k+1]} \quad (4.68)$$

$$\theta_i^\mu[k+1] = \frac{N_i^\mu[k+1]}{\sum_{\mu \in S_\mu^-} N_i^\mu[k+1]}, \mu \in S_\mu^- \quad (4.69)$$

Note that, Equations 4.56 – 4.69 are also applicable for the Base Model, in which there is only one element in the set of downstream on-ramps S_μ^- , and $\theta_i^\mu[k]$ is always equal to 1.

- The constraints to capture the movement of vehicles at freeway mainline and ramps are also similar to those in the Base Model, except that Equations 4.21 and 4.30 are modified as in Equations 4.70 and 4.71, respectively, by incorporating the binary variables $\delta_{v\mu}^h$ to reflect the dynamic diversion control decisions.

$$q_{i-1,N(i-1)}[t] = \rho_{i-1,N(i-1)}[t] \cdot v_{i-1,N(i-1)}[t] \cdot n_{i-1,N(i-1)} \cdot [1 - \gamma_v^h - \delta_{v\mu}^h \cdot \beta_v^h \cdot Z_v^h] + q_v^{in}[t] \quad (4.70)$$

$$q_v^{in}[t] = \min \left\{ \rho_{i-1,N(i-1)}[t] \cdot v_{i-1,N(i-1)}[t] \cdot n_{i-1,N(i-1)} \cdot (\gamma_v^h + \delta_{v\mu}^h \cdot \beta_v^h \cdot Z_v^h), \right. \\ \left. Q_v, \frac{s_v[l \cdot t] + \sum_{k=l}^{l(t+1)-1} \sum_{j \in \Gamma^{-1}(v)} Q_{vj}[k]}{\Delta T} \right\} \quad (4.71)$$

Operational Constraints

The operational constraints for various control decision variables are the same as those defined with Equations 4.46 – 4.54 in the Base Model, except that Equation 4.50 and 4.51 is modified as in Equation 4.72 and 4.73 for multiple on-off ramps.

$$R^{\min} \leq R_\mu^h \leq R^{\max}, \mu \in S_\mu^+, h \in H \quad (4.72)$$

$$\beta_v^h \cdot Z_v^h + \gamma_v^h \leq Z^{\max}, v \in S_v^+, h \in H \quad (4.73)$$

In addition, Equation 4.74 defines that traffic at any upstream off-ramp can be detoured to no more than one downstream on-ramp during each control interval h .

$$\sum_{\mu \in S_{\mu}^{-}} \delta_{v\mu}^h \leq 1, \quad \forall v \in S_v^+, h \in H \quad (4.74)$$

The Overall Model

In summary, by incorporating the elaborated network and operational constraints, as well as the new set of decision variables $\{\delta_{v\mu}^h\}$, the mathematical expression of the Extended Model is given below:

$$\begin{aligned} \min \quad & \Phi(s) = \begin{bmatrix} f_1(s) \\ f_2(s) \end{bmatrix} \\ & f_1 : - \left[\sum_{t=1}^H q_{i+1,0}[t] \cdot \Delta T + \sum_{k=1}^H \sum_{i \in S^{OUT}} q_i^{in}[k] \right] \\ & f_2 : \sum_{k=1}^H \left[\sum_{i \in S^U} \sum_{\mu \in S_{\mu}^{-}} N_i^{\mu}[k] + \sum_{v \in S_v^+} \sum_{\mu \in S_{\mu}^{-}} N_v^{\mu}[k] + \sum_{\mu \in S_{\mu}^{-}} N_{\mu}^{\mu}[k] \right] \cdot \Delta t \\ & s.t. \quad s : \{C^h, \Delta_n^h, G_{np}^h, R_{\mu}^h, Z_v^h, \delta_{v\mu}^h, \forall h \in H\} \end{aligned} \quad (4.75)$$

s denotes the feasible solution space defined by Equations 4.1, 4.2, 4.4, 4.5, 4.9, 4.11 – 4.14, 4.17 – 4.20, 4.22 – 4.25, 4.28 – 4.29, 4.31, 4.46 – 4.49, 4.52 – 4.54, and 4.56 – 4.74. $q_{i+1,0}[t]$ is the flow rate entering the freeway link $(i+1)$ downstream of the most outside on-ramp $\mu \in S_{\mu}^{-}$. Other parameters and variables keep the same meanings as in the Based Model.

4.5. Solution Algorithms – A Compromised GA

Note that the formulations for both the base model and the extended model feature a bi-objective optimization framework. The solution of multi-objective model is always situated in its *Pareto Optimal* (non-dominated) set (Eschenauer et al., 1990). A solution $s^* \in S$ is claimed to be *Pareto Optimal* if and only if there is no $s \in S$ such that $\Phi(s) \leq \Phi(s^*)$, and $\Phi(s) < \Phi(s^*)$ for at least one objective. Usually, there exist infinite Pareto optimal solutions for a multi-objective optimization problem, which form the so-called *Pareto Frontier*, as illustrated in Figure 4.9. Decision makers can then select a particular Pareto solution based on the preferred objectives. Thus, the solution procedures for the multi-objective problem shall include two steps:

- Obtaining an evenly distributed subset of its Pareto frontier; and
- Identifying the best solution of the multi-objective problem based on the obtained Pareto frontier and decision preference.

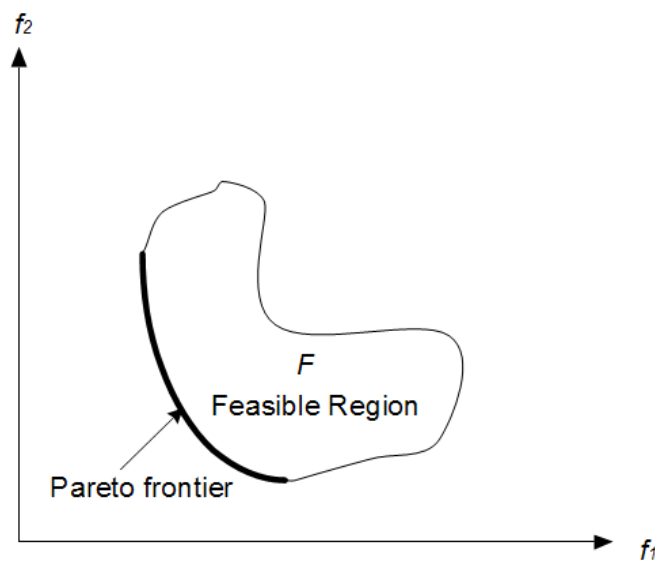


Figure 4.9 Illustration of the Pareto Frontier

However, considering the complex nature of the model proposed in this study, to evaluate the entire Pareto solution set and select the best one will be quite time-consuming and pose a considerable cognitive burden on the potential users. Therefore, this study proposes a heuristic approach to ensure that the solutions are efficient and deployable.

In this regard, this study employed the Genetic Algorithm (GA) based heuristic proposed by Cheng and Gen (1998), and extended it to identify the compromised solution closest to the “ideally best point” of the multi-objective problem rather than to obtain the entire Pareto solution set. This section will briefly present the following extensions proposed in this study:

4.5.1. Regret Value Computation

In the heuristic developed by Cheng and Gen (1998), at each population in the evolution process of GA, the algorithm evaluates the performance of an individual solution by defining a regret value $r(s)$. This study has developed the following equation to compute the regret value for an individual solution s :

$$r(s) = \sqrt{w_1 \cdot \left(\frac{f_1(s) - f_1^{\min}(P)}{f_1^{\max}(P) - f_1^{\min}(P)} \right)^2 + w_2 \cdot \left(\frac{f_2(s) - f_2^{\min}(P)}{f_2^{\max}(P) - f_2^{\min}(P)} \right)^2}, s \in P \quad (4.76)$$

$s \in P$ represents the solution s in the current population P ; w_m ($m = 1, 2$) is the weight assigned to objective function m to emphasize its degree of importance.

$f_m^{\min}(P) = \min\{f_m(s) \mid s \in P\}$ and $f_m^{\max}(P) = \max\{f_m(s) \mid s \in P\}$ represent the minimum and the maximum values of the objective function at the current population P , respectively. Note that Equation 4.76 defines the normalized distance from the

solution s to the “ideally best” point in the current population P . Therefore, the smaller the regret value is, the better the individual will be in the population.

The reason for using the normalized values in Equation 4.76 is that the value of the first objective in the proposed model is expressed in number of vehicles, whereas the second objective value is measured on a vehicle-min scale. Therefore, two objectives cannot be compared or assigned weights directly. In order to solve the proposed optimal control model with the compromised GA-based approach, one needs to normalize the objective functions to a common satisfaction scale.

4.5.2. Decoding of Control Variables

To generate feasible control parameters which satisfy the operational constraints, one needs to develop the following decoding scheme:

I. Signal control variables: According to the phase structure shown in Figure 4.7, a total number of NP_n fractions ($\lambda_j^h, j = 1 \dots NP_n$) are generated for the controller at intersection n during each control interval h from decomposed binary strings, where NP_n is the number of phases of intersection n . Those fractions are used to code the green times and offsets as shown in the following equations:

$$\Delta_n^h = (C^h - 1) \cdot \lambda_{NP}^h \quad (4.77)$$

$$G_{np}^h = G_{np}^{\min} + (C^h - \sum_{j \in P_n} G_{nj}^{\min} - \sum_{j \in P_n} I_{nj}) \cdot \lambda_p^h \cdot \prod_{j=1}^p (1 - \lambda_{j-1}^h), \quad (4.78)$$

$$p = 1 \dots NP_n - 1, n \in S_N$$

$$G_{np}^h = G_{np}^{\min} + (C^h - \sum_{j \in P_n} G_{nj}^{\min} - \sum_{j \in P_n} I_{nj}) \cdot \prod_{j=1}^p (1 - \lambda_{j-1}^h), \quad (4.79)$$

$$p = NP_n, n \in S_N$$

Given the common cycle length C^h , Equation 4.77 would result in an offset value that lies between 0 and the cycle length minus one. The green times are assigned to each phase within a feasible range by Equations 4.78 and 4.79, in which λ_0^h was set to zero to accommodate the case when $j = 1$.

Equation 4.80 constrains the common cycle length generated through the binary string within the maximum and minimum allowable values.

$$C^h = C_{\min} + (C_{\max} - C_{\min}) \cdot \lambda_c^h \quad (4.80)$$

λ_c^h is a random real number fraction transformed from the decomposed binary string.

II. Diversion and metering rates: Equations 4.81 and 4.82 constrain the diversion and metering rates generated within the allowable range:

$$Z_v^h = \frac{(Z^{\max} - \gamma_v^h)}{\beta_v^h} \cdot \lambda_v^h, \quad v \in S_v^+ \quad (4.81)$$

$$R_\mu^h = R^{\min} + (R^{\max} - R^{\min}) \cdot \lambda_\mu^h, \quad \mu \in S_\mu^+ \quad (4.82)$$

$\{\lambda_v^h, v \in S_v^+, h \in H\}$ and $\{\lambda_\mu^h, \mu \in S_\mu^+, h \in H\}$ are fractions generated through the decomposed binary strings.

III. Detour route choice (for the Extended Model): To ensure that the population of solutions for $\{\delta_{v\mu}^h\}$ satisfy the constraint defined by Equation 4.74, this study randomizes an integer vector $(\mu_1^h, \dots, \mu_v^h, \dots, \mu_{S_v^+}^h)$, where $\mu_v^h |_{v \in S_v^+}$ is the index of

incident downstream on-ramp to which traffic from upstream off-ramp ν is detoured during control interval h . Therefore, we have:

$$\delta_{\nu\mu}^h = \begin{cases} 1, & \text{if } \mu_\nu^h \neq 0 \\ 0, & \text{o.w.} \end{cases}$$

Note that the set of $\{\delta_{\nu\mu}^h\}$ obtained from the above approach is sure to satisfy the constraints defined by Equations 4.74.

By employing the aforementioned three sets of decoding schemes, the population of solutions $s : \{C^h, \Delta_n^h, G_{np}^h, R_\mu^h, Z_\nu^h, \delta_{\nu\mu}^h, \forall h \in H\}$ randomized from the binary strings is always assured to be feasible after each genetic evolution.

A step-by-step description of the solution procedures is illustrated in Figure 4.10.

Note that, the proposed heuristic can efficiently address the complex nature of the proposed optimization model in this study, and ensure that the solutions are efficient and deployable.

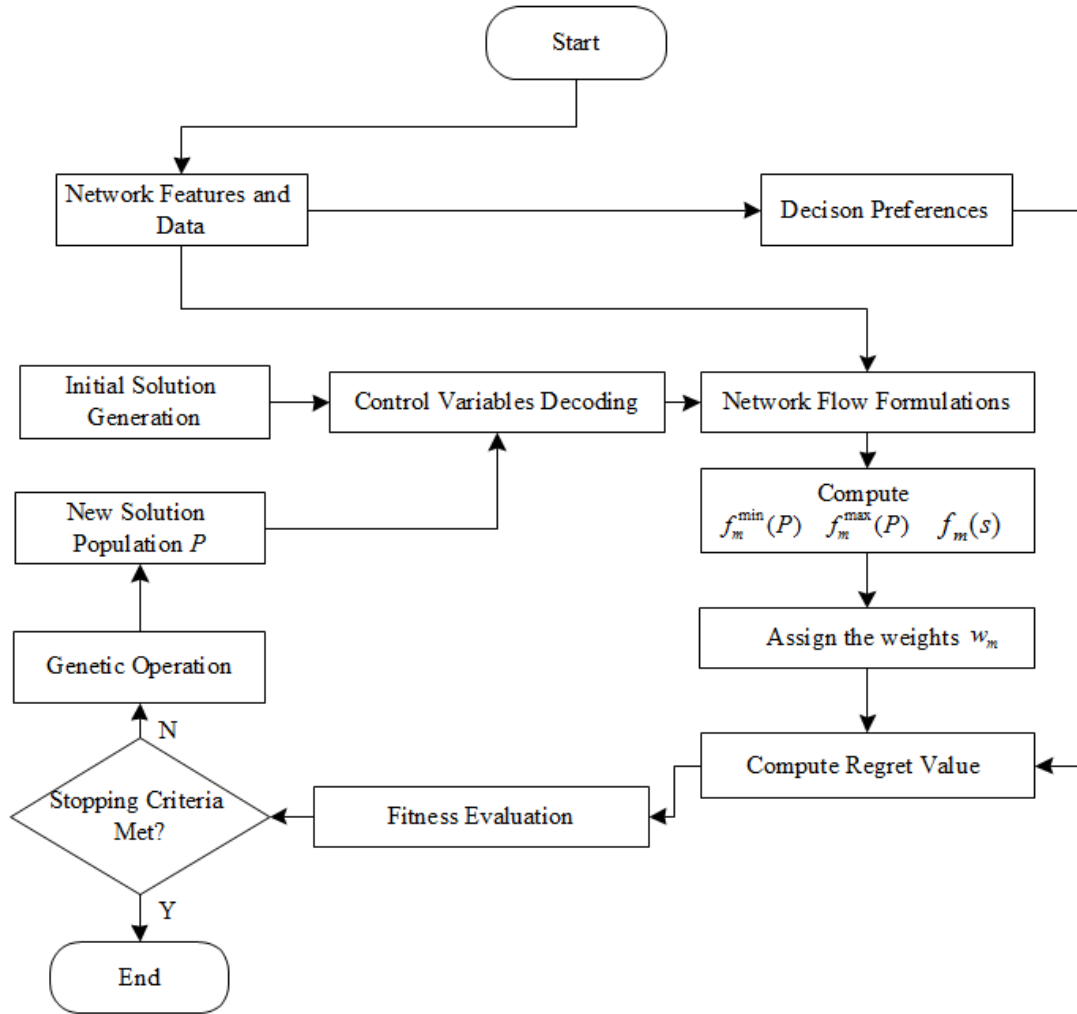


Figure 4.10 Flowchart of the GA-based Compromised Heuristic

4.6. A Successive Optimization Framework for Real-time Model Application

Despite the efficiency of the GA-based heuristic proposed in Section 4.5, real-time application of the proposed large-scale, non-linear and multi-objective control model remains a challenge due to the significant increase in the number of decision variables over different control intervals. In addition, solving such a large-scale control system in one time requires reliable projection of traffic conditions over the entire control horizon, which is also quite difficult due to the expected fluctuation of

traffic flows and discrepancy of driver responses to control actions under non-recurrent congestion. To contend with the above critical issues, this section presents a successive optimization framework for real-time application of the proposed integrated control model, in which the model input and control strategy are regularly updated to improve the computing efficiency and effectiveness under time-varying traffic conditions and potential system disturbance. The main ingredients of the successive optimization framework include two parts: 1) the on-line estimation module for critical model parameters; and 2) a variable-time-window rolling horizon scheme for update of the control strategies.

4.6.1. Real-time Estimation Or Projection of Model Parameters

This module functions to estimate and project real-time traffic states from the surveillance system and feedback to the optimization model to update control strategies. The critical traffic state variables that need to be estimated or predicted in real time include:

- Density distribution;
- Traffic flow rates at demand entry points;
- Queue length distribution;
- Turning fractions; and
- Driver compliance rates to the diversion control.

There are many effective approaches in the literature for real-time identification of traffic flows and density distribution, based on on-line traffic measurements (Payne et al., 1987; Bhouri et al., 1988; Wu, 1999c). The recent

advances in traffic sensor technologies have also provided reliable tracking of queue evolution at an individual-movement level (Smadi et al., 2006).

For turning fractions, Section 4.3.2 has proposed a network-wide approach to project the impact of detoured traffic on arterial turning movements, from which the composite turning proportion can be estimated or predicted as follows:

$$\gamma_{ij}[k] = \frac{\bar{Q}_{ij}[k] + \sum_{\mu \in S_{\mu}^{-}} Q_{ij}^{\mu}[k]}{\sum_{j \in \Gamma^{-1}(i)} \left[\bar{Q}_{ij}[k] + \sum_{\mu \in S_{\mu}^{-}} Q_{ij}^{\mu}[k] \right]} \quad (4.83)$$

$\gamma_{ij}[k]$ represents the composite turning proportion from link i to link j at time interval k , and other parameters are same as in Section 4.3.2.

In addition to the network-wide approach with Equation 4.83, it is notable that the identification of turning fractions can also be made from local measurements of associated link or movement flows to overcome the fluctuation of traffic patterns among neighboring movements (Davis and Lan, 1995; Mirchandani et al., 2001). Therefore, the traffic control system can employ the following simple convex combination of the above two estimators to produce a more reliable estimation or projection of the turning proportions (Wu, 1999c):

$$\gamma_{ij}[k] = \alpha \cdot \gamma'_{ij}[k] + (1 - \alpha) \cdot \gamma''_{ij}[k] \quad (4.84)$$

where, α is a weighting parameter between 0 and 1 that can be determined based on field calibrations; $\gamma'_{ij}[k]$ and $\gamma''_{ij}[k]$ are the projected turning proportions from Equation 4.83 and local measurement approaches, respectively.

It should be noted that reliable projection of turning proportions is also conditioned on how drivers respond to the diversion control under the given corridor network structure and traffic conditions. In real-world applications, one can employ real-time traffic measurements from the surveillance system to produce a reliable estimation of driver compliance rates in the current and previous control intervals, which will provide on-line feedback to the optimization model so as to adjust the set of diversion rates.

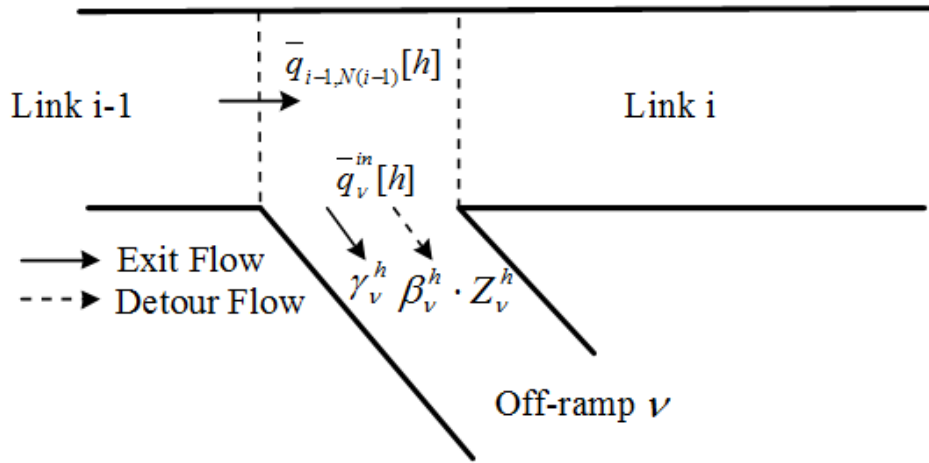


Figure 4.11 Real-time Estimation of Diversion Compliance Rates

As shown in Figure 4.11, the diversion compliance rate at off-ramp ν during the control interval h , denoted by $\hat{\beta}_\nu^h$, can be easily estimated by the following equation:

$$\hat{\beta}_\nu^h = [\bar{q}_\nu^-[h] / \bar{q}_{i-1, N(i-1)}^-[h] - \gamma_\nu^h] / Z_\nu^h \quad (4.85)$$

where, $\bar{q}_\nu^-[h]$ and $\bar{q}_{i-1, N(i-1)}^-[h]$ represent the on-line measurement of flow rates at the off-ramp ν and its upstream freeway mainline link during the control interval h ,

respectively; γ_v^h is the normal exit rate for off-ramp v during the control interval h ; Z_v^h is the applied diversion rate during the control interval h ;

The estimated driver compliance rates from Equation 4.85 are only for current and previous control intervals. However, one can still project compliance rates in the future time horizon by applying time series analysis approaches or by data-mining of historical driver response patterns to the diversion control.

4.6.2. A Variable-Time-Window Rolling Horizon Scheme

A key issue for developing such a rolling horizon framework is to keep the consistency between the variation of arterial signal timings and the update of control time interval. The following two types of strategies are commonly employed in the literature: 1) arterial signal timings are represented with G/C ratios and updated at every constant time interval, or 2) a constant network cycle length is pre-set to keep consistency with the control update interval, and green splits as well as offsets are optimized under the given cycle length. However, some limitations embedded in those approaches may limit their applications:

- Representation of arterial signal timings with G/C ratios is not ready for implementation. It still needs an additional interface with a compatible microscopic local control controller to determine the resulting signal phasing, green times, and offsets;
- A pre-set network cycle length may not be able to accommodate the traffic fluctuation under incident conditions; and

- A constant control update time interval may not be able to accommodate the variation of signal control parameters, thus may cause the loss of some phases.

To overcome the above drawbacks and make the optimization outputs deployable, this study has developed the following variable-time-window rolling horizon scheme:

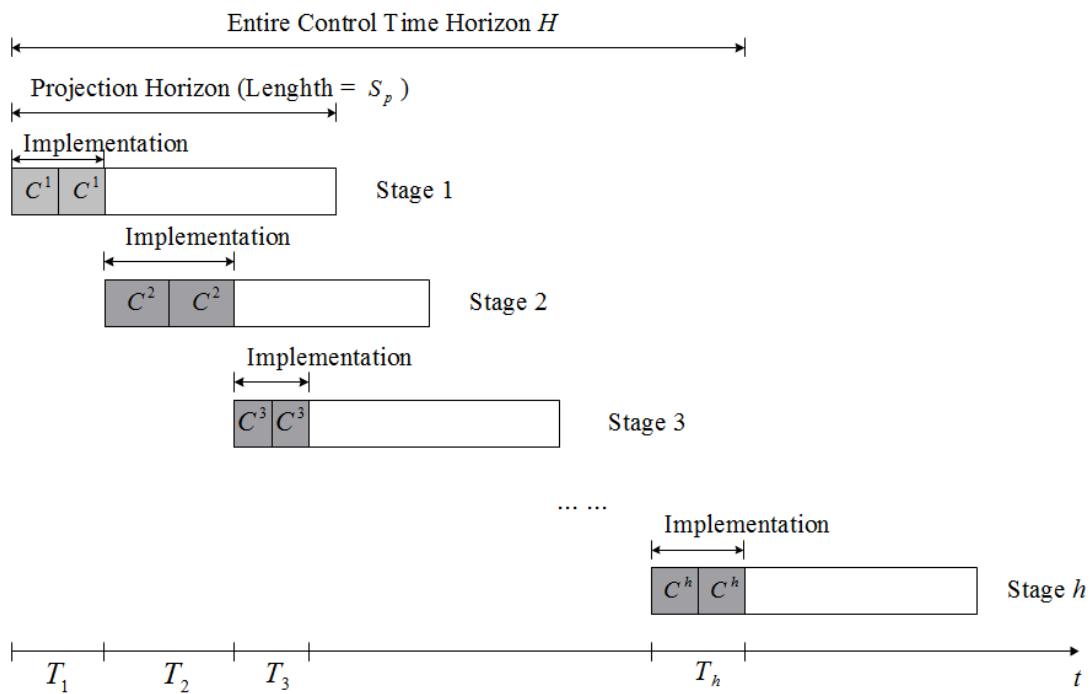


Figure 4.12 Illustration of the Variable-Time-Window Rolling Horizon Scheme

- Control plans are optimized over successive stages, S_p , as shown in Figure 4.12, but implemented only within the control interval T_h ($T_h < S_p$),

which is an integer multiple of the optimal cycle length in that stage, i.e.

$$T_h = c \cdot C^h ;$$

- Once the control plan is implemented, the state of the traffic within the corridor network is updated using real-time measurements from Section 4.6.1, and the optimization process starts all over again with the prediction and the control horizon shifted forward by T_h ; and
- The optimization process terminates when $\sum_h T_h \geq H$.

Note that, the proposed scheme employs a variable rolling time window that can accommodate the variation of signal timing parameters, and thus can significantly improve the effectiveness of the optimization model under time-varying traffic conditions. In real-world applications, the lengths of the prediction horizon (S_p) and the control interval (T_h) need to be carefully chosen in order to make a trade-off between the computational complexity and the controller accuracy. The larger the S_p is, the further the controller can foresee the potential impact of certain events. However, a larger S_p implies more computational complexity and dependency on prediction. For the choice of T_h , a similar trade-off exists. The smaller the value is, the more frequent the control decision variables need to be re-optimized, which may significantly increase the computational complexity of the optimization process. On the other hand, a larger value of T_h may not accurately accommodate traffic variation.

4.7. Closure

Chapter 4 has presented the formulations for design of integrated corridor control strategies. A brief summary of research activities in each section is reported below:

- Section 4.2 has proposed a lane-group-based concept to serve as the underlying network flow model for the arterials and ramps, which can accurately and efficiently capture the operational characteristics of traffic in the overall corridor optimization process when properly integrated with the freeway model.
- Section 4.3 has proposed the Base Model for design of integrated corridor control, which includes a segment of the freeway mainline experiencing an incident. With a network enhancement that can precisely project the time-varying impacts of detour traffic on the existing demand patterns, an effective multi-objective control model is proposed to determine the best set of control strategies that can efficiently explore the control effectiveness under different policy priorities between the target freeway and available detour routes.
- Section 4.4 has proposed the Extended Model, which incorporates multiple detour routes comprising several on-ramps, off-ramps, and different segments of parallel arterials for integral operations. With a proper network enhancement approach, the extended model features its

effectiveness in accommodating various operational complexities caused by the interactions between multiple diversion routes.

- Section 4.5 has proposed a compromised GA-based heuristic that can yield sufficiently reliable solutions for application of the proposed models.
- Section 4.6 has developed a successive optimization framework for real-time application of the proposed integrated control model. This framework has embedded an on-line module for critical model parameter estimation and prediction, which has captured the fluctuation of required input data in the control model formulations. This module is further integrated with a variable-time-window rolling horizon scheme so that on-line feedback from the surveillance system can be used for the controller to regulate future plans and improve the computing efficiency.

Chapter 5: Case Studies for Integrated Control Strategies

This chapter presents numerical test results for the proposed integrated control model and its solution algorithm to illustrate their operational performance with respect to the total delay, throughput, travel times, and volume distribution on both the freeway and its neighboring arterial. A segment along the I-95 North corridor and a hypothetical corridor network are respectively used for evaluating the Base Model and the Extended Model. The sensitivity of the control performance with respect to the variation of diversion compliance rates has also been investigated.

5.1. Numerical Test of the Base Model

5.1.1. Experimental Design

To evaluate the performance of the base model, a single segment corridor shown in Figure 5.1 is selected for the case study. Assuming that an incident occurs on the freeway mainline segment (between node 26 and 44), traffic will detour to MD198 and then follow MD216 back to the freeway. The proposed control model will update the control measures, including diversion rate at node 27, signal timings at intersections along MD198 and 216 (nodes 68, 69, 65, 67, and 99), and metering rate at node 26. The entire test period is designed to cover 35 minutes, which consists of the following 3 periods: 5 min for normal operations (no incident), 20 min with incident, and 10 min recovery period (incident cleared). A total of four scenarios are designed as follows for the experiment (see Table 5.1 for volume levels):

- I: Volume level-I with 1 lane blocked;
- II: Volume level-I with 2 lanes blocked;
- III: Volume level-II with 1 lane blocked; and
- IV: Volume level-II with 2 lanes blocked.

Table 5.1 Volume Levels for the Case Study of Base Model

Demand Entries	Level I (vph)	Level II (vph)
8101	4680	7800
8025	614	1024
8017	564	940
8077	554	924
8078	725	1208
8076	200	400
8080	210	384
8074	550	916
8021	200	400
8028	246	510
8022	187	312
8024	390	684

5.1.2. Geometric and Network Traffic Flow Characteristics

Within the control area shown in Figure 5.1, I-95 mainline has 4 lanes in the northbound direction. Among the detour routes, the off-ramp from I-95 North to MD198 East has 2 lanes, and MD198 East is an arterial street with 3 lanes in each direction. MD216 is an arterial street with 2 lanes in each direction, and the on-ramp from MD216 to I-95 North has 1 lane. The lane channelization at each intersection is shown in Table 5.2.

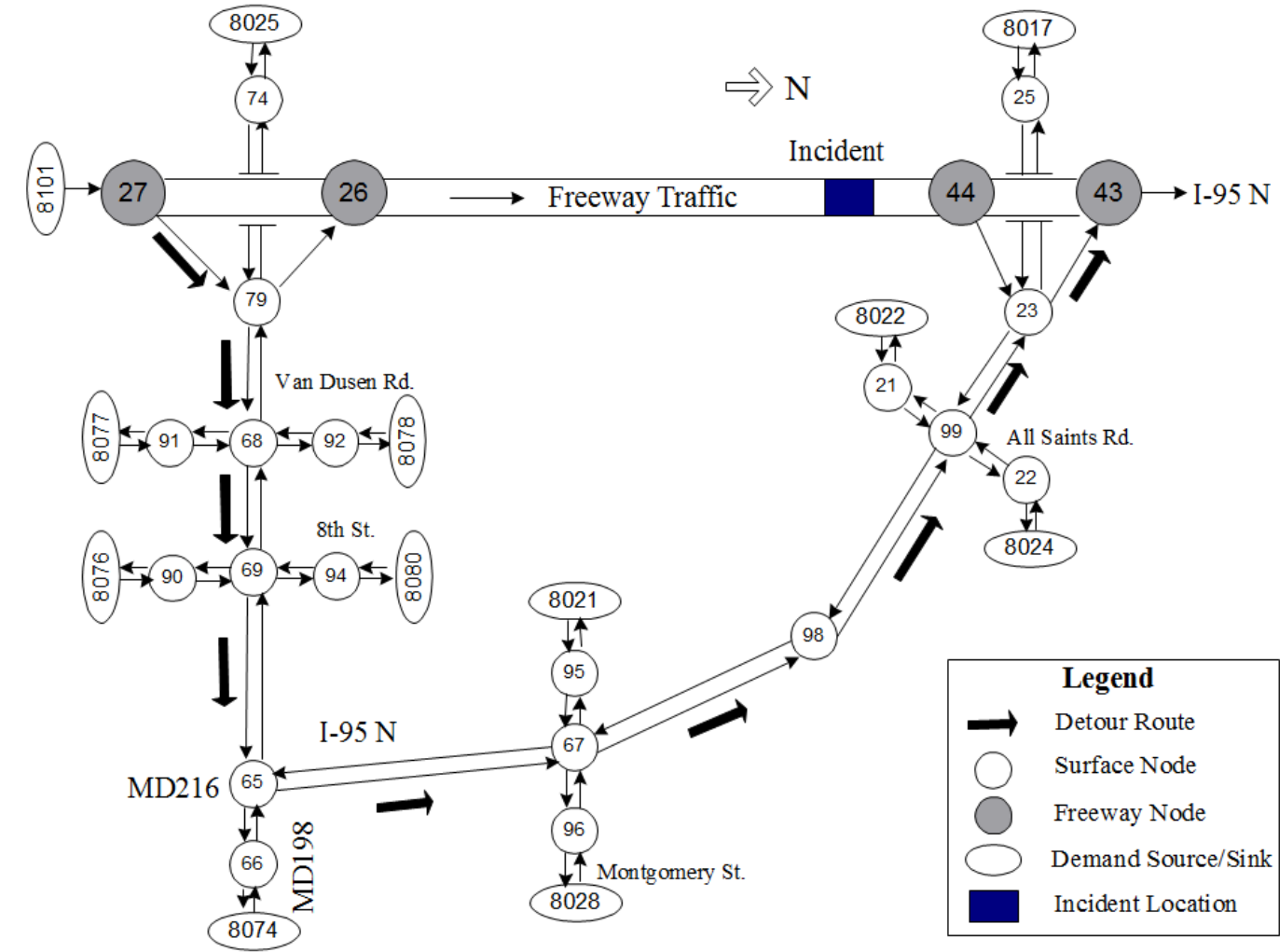
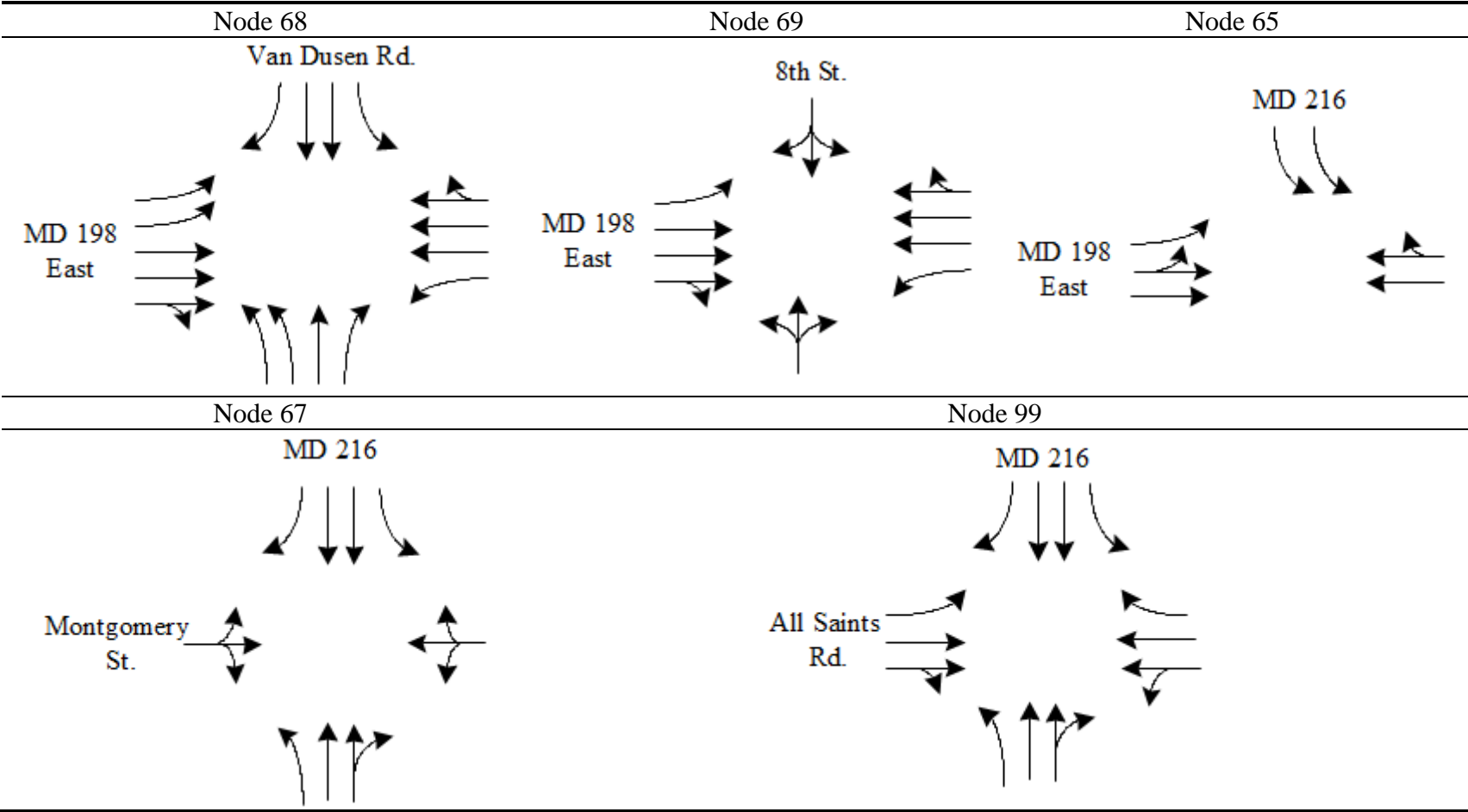


Figure 5.1 Layout of the Corridor Segment for Case Study of the Base Model

Table 5.2 Lane Channelization at Intersection Approaches of the Detour Route



All other parameters related to the network flow models in the case study are summarized as follows:

- Update time steps for the arterial (Δt) and the freeway (ΔT) are set to be 1s and 5s, respectively;
- Each freeway segment is set to be 800ft;
- Jam density ρ^{jam} is set to be 210veh/mile/lane, and the minimum density ρ^{min} is set to be 20veh/mile/lane;
- Free flow speed is set at 65mph for freeway mainline, 45mph for on-off ramps, and 50mph for arterials;
- The minimum speed at arterials corresponding to the jam density is set to 5mph;
- Discharge capacity: freeway (2200vplph), arterial link (1800vplph), ramps (1900vplph);
- Average vehicle length is set to be 24 ft to compute the storage capacity of arterial links;
- Traffic flow model parameters: α (3.0), β (2.0), α_f (1.78), τ (27s), η (6 mile² / h), κ (20.8 veh/mile/lane);
- Normal exiting rate at the off-ramp to MD198 East, $\gamma_{v^+}^h$, is 0.0875 for the entire control time horizon;
- Driver compliance rates to the detour operation, $\beta_{v^+}^h$, is assumed at 100% level over entire control time horizon if the detour travel time is less or comparable to the freeway travel time;

5.1.3. Traffic Control Parameters

- Minimum and maximum cycle length for arterial intersections: C^{\min} (60s), C^{\max} (160s);
- Minimum green time per phase: G_{np}^{\min} (7s), clearance time I_{np} (5s)
- Minimum and maximum ramp metering rates: R^{\min} (0.1), R^{\max} (1.0);
- Maximum diversion rate Z^{\max} (0.25);
- The phase diagrams for each intersection along the detour route are shown in Table 5.3.

Table 5.3 Phase Diagram of Intersections along the Detour Route

Node ID	Phase Diagram			
68				
69				
65				
67				
99				

5.1.4. Optimization Model Settings

Parameters in the compromised GA-based heuristic are summarized below:

- The population size is set at 50;
- The maximum number of generation is set at 200;
- The crossover probability is set at 0.5;
- The mutation probability is set at 0.03; and
- ε is set to be 0.1 to keep proper selection pressure to the ideally best point.

Key parameters in the successive optimization framework are summarized as:

- The length of the projection horizon S_p is set to be 4-min, and the control time interval $T_h = C^h$; and
- If the GA optimization cannot converge before the control process rolling to the next optimization horizon, plans from the previous control interval will be implemented.

Since the two control objectives are normalized to the same scale, the weights of importance w_1 / w_2 are assigned to them from 10/0 to 0/10 at an increment of 1 to reflect the trade-off between the preference of traffic management decision makers and detoured travelers.

5.1.5. Numerical Results and Analyses

This study has coded the proposed model and the successive optimization procedure in Visual C++ 2005, with the embedded GA-based heuristic coded by the

MIT GA C++ Library v.2.4.6 (Wall, 1999). The optimized control plans obtained from the proposed base model are evaluated through the following steps:

- **Step I** - Evaluate the performance of the proposed model with systematically varied weights to provide operational guidelines for decision makers in best weighting importance between both control objectives under each given scenario;
- **Step II** - With a set of properly selected weights from Step I, compare the model performance with the following two control strategies:
 - A. No control;
 - B. Diversion control with rates determined by a static user-equilibrium (UE) assignment between freeway and arterial, and re-timing of arterial signals with TRANSYT-7F based on volumes from the assignment results. On-ramp metering is operated with ALINEA; and

The microscopic simulator CORSIM was employed as an unbiased evaluator for model performance. To overcome the stochastic nature of simulation results, an average of 30 simulation runs has been used.

Step I:

Table 5.4 summarizes the performance of the proposed multi-objective model under different scenarios and weights of importance. One can observe the following primary findings:

Table 5.4 Performance of the Proposed Model under Different Scenarios with Various Decision Preferences

Scenarios		I		II		III		IV	
Objective Function Value		f1	f2	f1	f2	f1	f2	f1	f2
Decision Making Preferences w_1 / w_2	10/0	3126	0.0	2863	1135.3	3461	2044.4	2773	2473.2
	9/1	3124	0.0	2854	1103.0	3450	1980.0	2761	2452.1
	8/2	3124	0.0	2847	1094.2	3425	1784.3	2723	2268.6
	7/3	3122	0.0	2832	1025.9	3376	1511.7	2672	2073.6
	6/4	3125	0.0	2808	919.5	3333	1355.3	2628	1857.6
	5/5	3128	0.0	2680	691.2	3293	1182.3	2540	1576.8
	4/6	3125	0.0	2641	513.4	3253	946.1	2457	1285.2
	3/7	3127	0.0	2612	362.9	3203	712.3	2400	1136.8
	2/8	3124	0.0	2576	257.5	3169	556.0	2340	888.4
	1/9	3122	0.0	2538	191.2	3103	436.6	2286	583.2
0/10	3124	0.0	2512	0.0	3087	0.0	2267	0.0	

f1 – Total Freeway Corridor Throughput (in vehs); f2 – Total Time Spent by the Detour Traffic (in veh-mins).

a) For Scenario I, the performance of the multi-objective model is not sensitive to the weight variation, as shown in Figure 5.2. This is probably due to the fact that the existing capacity of the freeway can accommodate the demand in the Volume-I level without detour operations, and the ideally best point was reached. The slight fluctuation of the system objective function values is probably due to the convergence of GA within different control intervals;

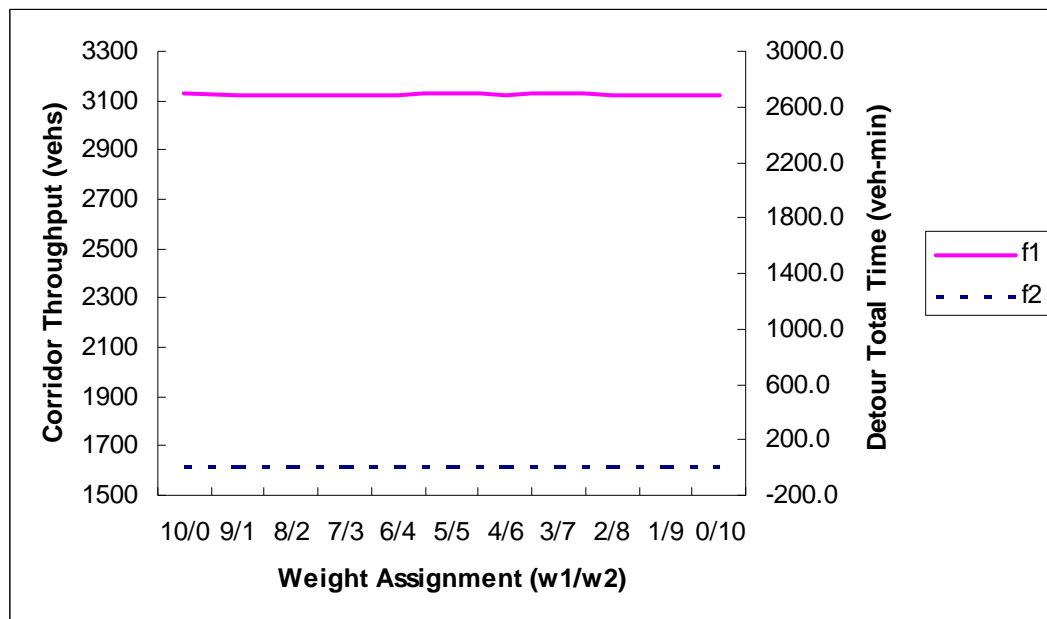


Figure 5.2 MOE Changes under Different Weight Assignment (Scenario I)

b) For Scenario II, the performance of the multi-objective model is not sensitive within a specific range. For example, the performance of the model seems quite stable as long as $w_1 > w_2$, as shown in Figure 5.3. That is probably due to the fact that the under-saturated arterial can accommodate sufficient detour traffic volume as long as the freeway

system is given the priority. However, when $w_1 \leq w_2$, the total corridor throughput exhibits a dramatic drop (from 2808 to 2680, as highlighted in Table 5.4) due to the priority switching from the freeway to the arterial. When the arterial is given the highest priority (0/10), the corridor throughput will be at the lowest level (2512);

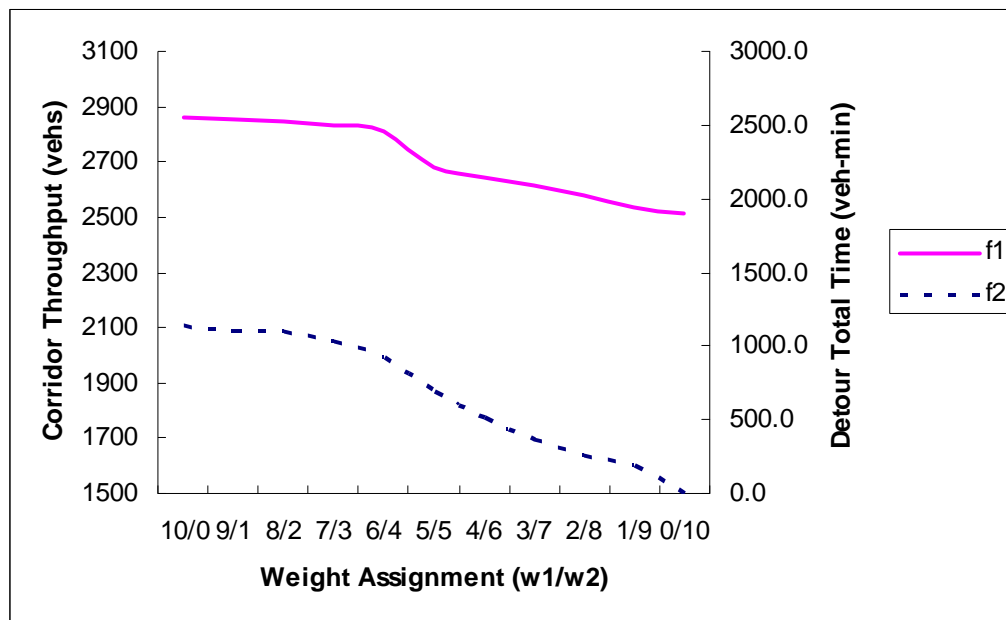


Figure 5.3 MOE Changes under Different Weight Assignment (Scenario II)

- c) For Scenarios III and IV, the performance of the model is sensitive to every step of the weight adjustment between objective functions (see Figure 5.4 and 5.5). Every improvement of the performance for one objective will be at the cost of the other.

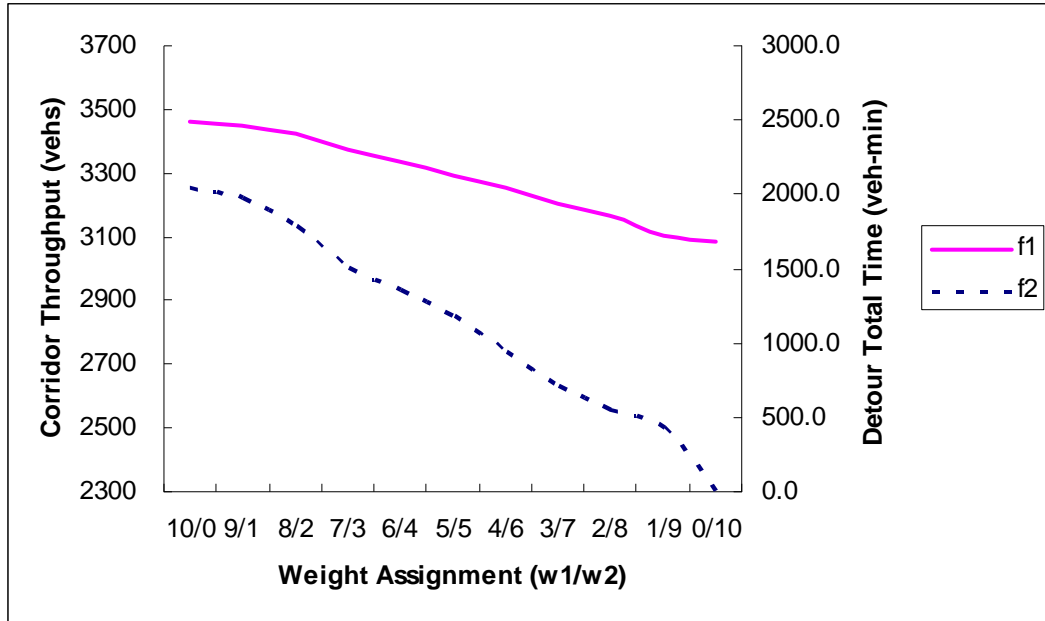


Figure 5.4 MOE Changes under Different Weight Assignment (Scenario III)

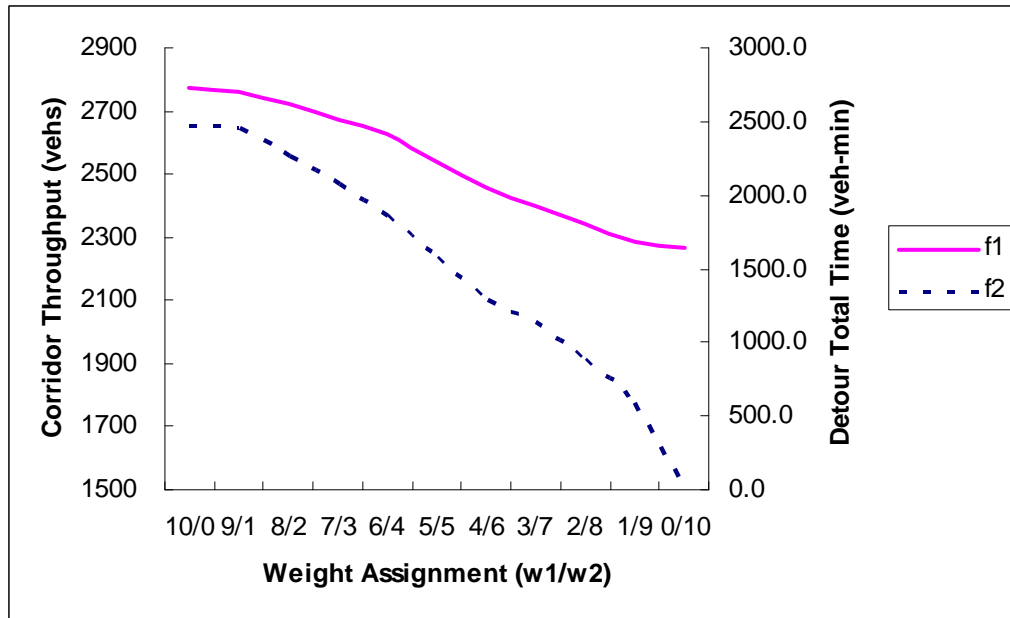


Figure 5.5 MOE Changes under Different Weight Assignment (Scenario IV)

To further assist traffic operators in best weighting the importance between system performance and travelers' preferences, this study has also investigated the time-varying travel time patterns on both the detour route and the freeway mainline under different scenarios (see Figures 5.6 – 5.8) except Scenario I. The following findings can be reached:

- With the weight assignment changing from $w_1/w_2 = 10/0$ to $w_1/w_2 = 0/10$, the ratio of detour travel time to freeway travel time decreases under all scenarios;
- The commonly used control objective of maximizing the total corridor throughput (i.e. $w_1/w_2 = 10/0$) may result in a significant unbalance of travel time between the detour route and the freeway mainline which could cause unacceptable driver compliance rates and degrade the control performance; and
- There exists a threshold in the weight assignment for each scenario, below which the assumed level of driver compliance rates can be achieved. For example, this case study assumes a 100% driver compliance rate if the detour travel time is less than or comparable to the freeway travel time, which indicates that the weight assignment must be set at a critical value to ensure the ratio of detour travel time to freeway travel time is less than or around 1.0. For Scenario I, one can set $w_1/w_2 = 10/0$ to maximize the utilization of residual freeway capacity without detour operations. For Scenario II (see Figure 5.6), one can still set $w_1/w_2 = 10/0$ to fully utilize

the available capacity in the arterial while keeping a high level of driver compliance rates. For Scenario III (see Figure 5.7), one needs to set $w_1 / w_2 = 6/4$ or lower to ensure acceptable driver compliance rates. For Scenario IV (see Figure 5.8), one needs to set $w_1 / w_2 = 5/5$ or lower to ensure acceptable driver compliance rates.

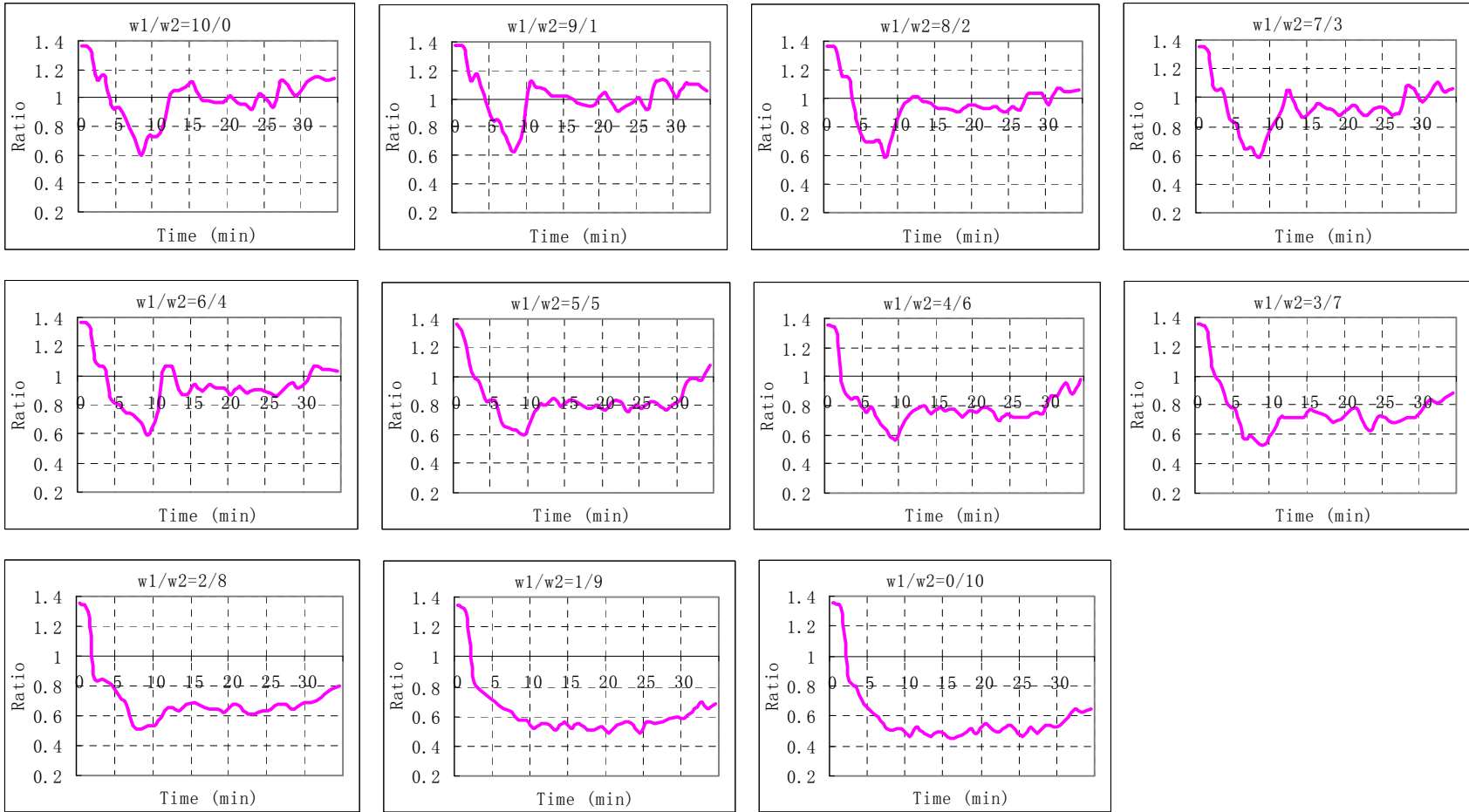


Figure 5.6 Time-varying Detour Travel Time over Freeway Travel Time Ratio (Scenario II)

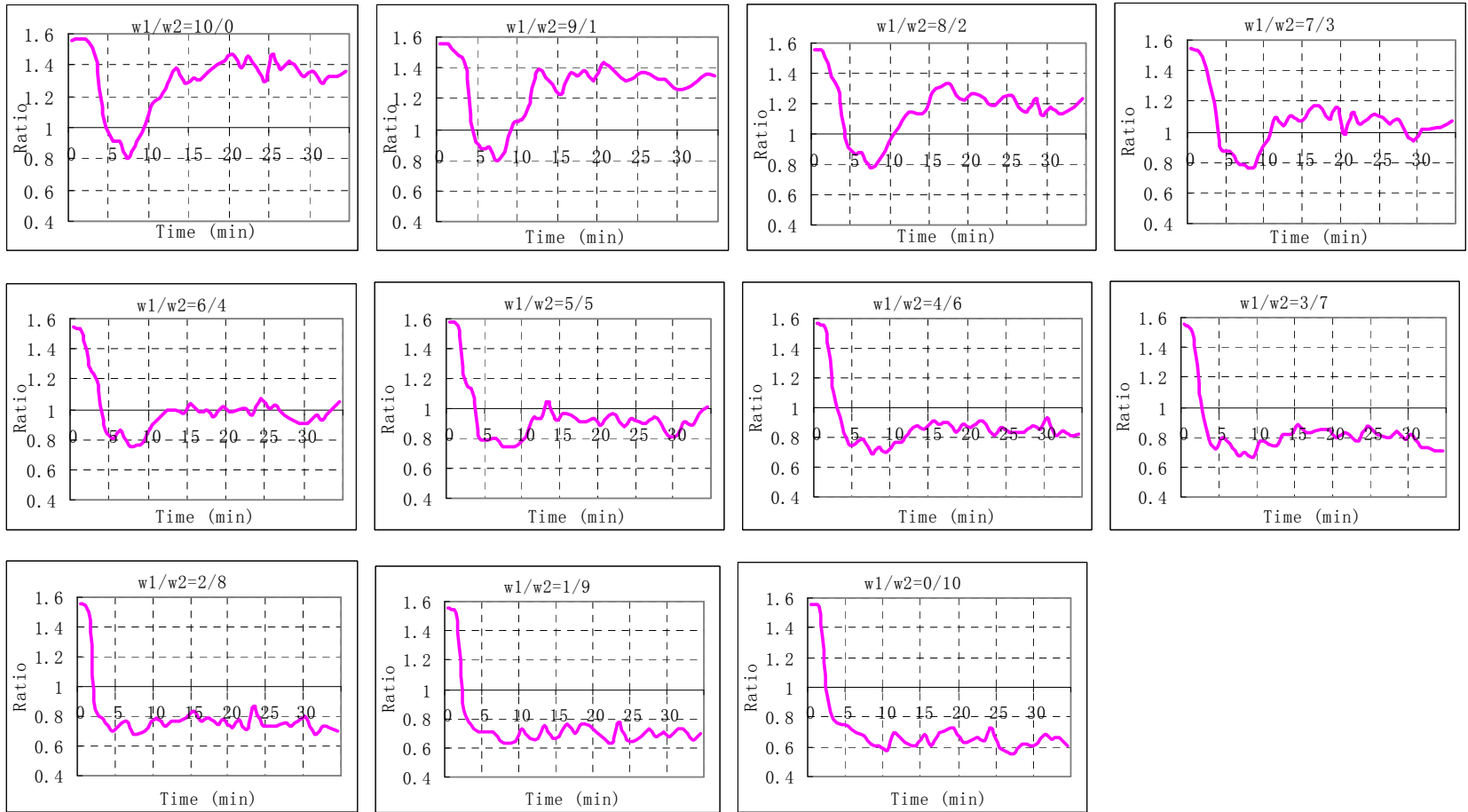


Figure 5.7 Time-varying Detour Travel Time over Freeway Travel Time Ratio (Scenario III)

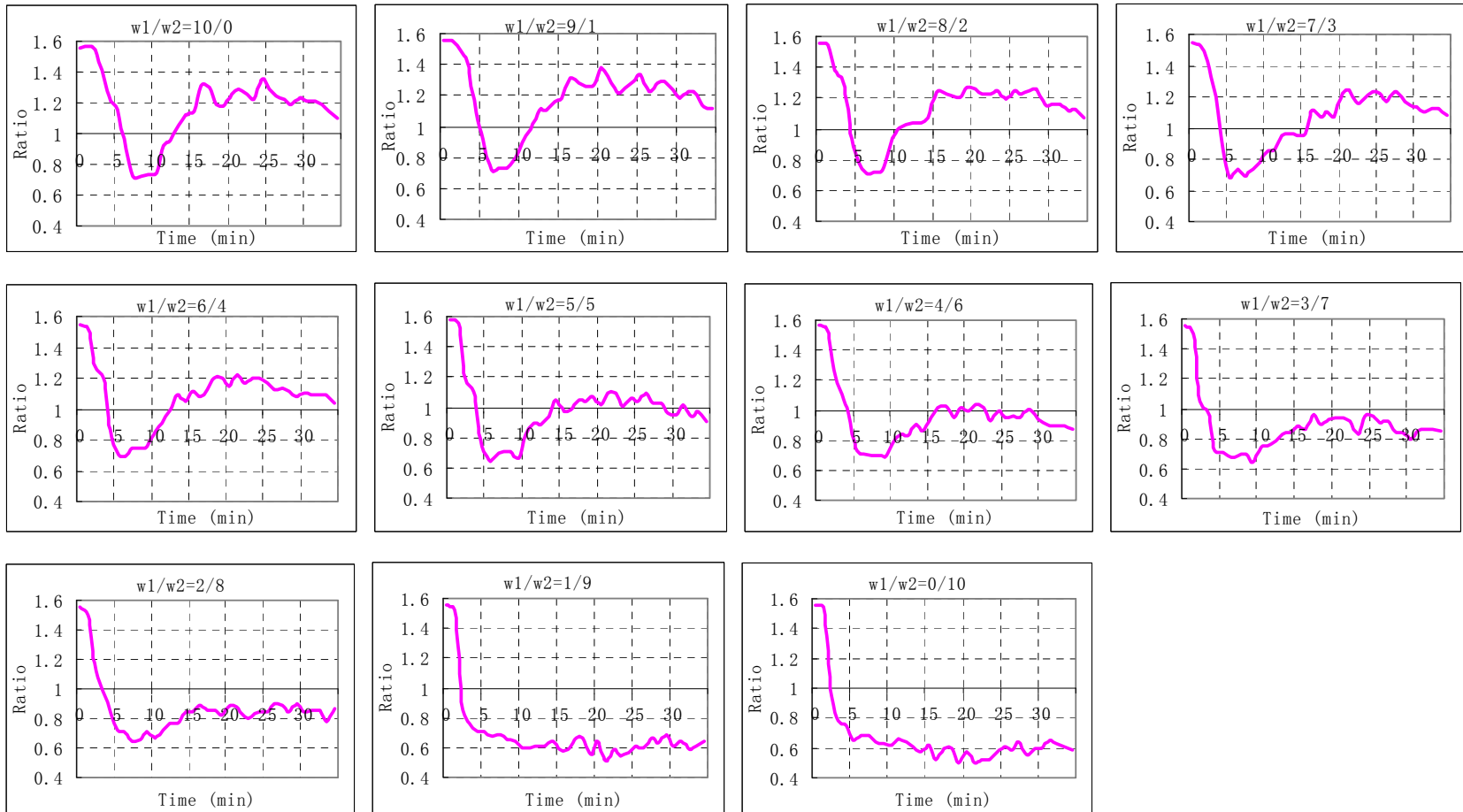


Figure 5.8 Time-varying Detour Travel Time over Freeway Travel Time Ratio (Scenario IV)

Step II:

This study has also compared the performance of the proposed model with other control strategies with respect to the total corridor throughput increases and the total spent time savings under all scenarios. The control strategies for comparison are:

- Control A: No control (the base line);
- Control B: Diversion control with rates determined by a static user-equilibrium (UE) assignment between the freeway and arterial, and re-timing of arterial signals with TRANSYT-7F based on volumes from the assignment results. On-ramp metering is operated with ALINEA.

Based on the analysis results from Step I, the weights of control objectives for the four test scenarios are set as follows to ensure balanced traffic conditions between the primary freeway and detour route:

- Scenario I: $w_1 / w_2 = 10/0$;
- Scenario II: $w_1 / w_2 = 10/0$;
- Scenario III: $w_1 / w_2 = 6/4$;
- Scenario IV: $w_1 / w_2 = 5/5$;

Figure 5.9 – Figure 5.16 illustrate the comparison results. The following findings can be reached:

- The proposed model can outperform Control A and Control B for all scenarios in terms of both total time savings and total throughput increases at the assumed level of driver compliance rates.
- In Scenario I (see Figure 5.9 and 5.10), since the existing capacity of the freeway can accommodate traffic without detour operations, the proposed model outperforms Control A probably due to the fact that the proposed model can produce slightly better signal timings in the arterial than TRANSYT-7F under light traffic conditions. Control B, however, has exhibited its performance worse than Control A, which is caused by the extra amount of traffic detoured to the arterial set by the static UE.
- In Scenario II (see Figure 5.11 and 5.12), the proposed model compared with Control A, exhibits a substantial improvement since it aims to maximize the total corridor throughput ($w_1/w_2 = 10/0$), which also results in a relatively low total spent time. However, the improvement over Control B is relatively low, that is probably due to the static UE employed in Control B which can also provide good utilization of the excessive capacity in the arterial. and
- In Scenarios III and IV (see Figures 5.13 – 5.16), the proposed model significantly outperforms both Control A and Control B due to its integrated control function and the embedded traffic flow equations which are capable of capturing the dynamic interactions between freeway and surface streets under saturated conditions.

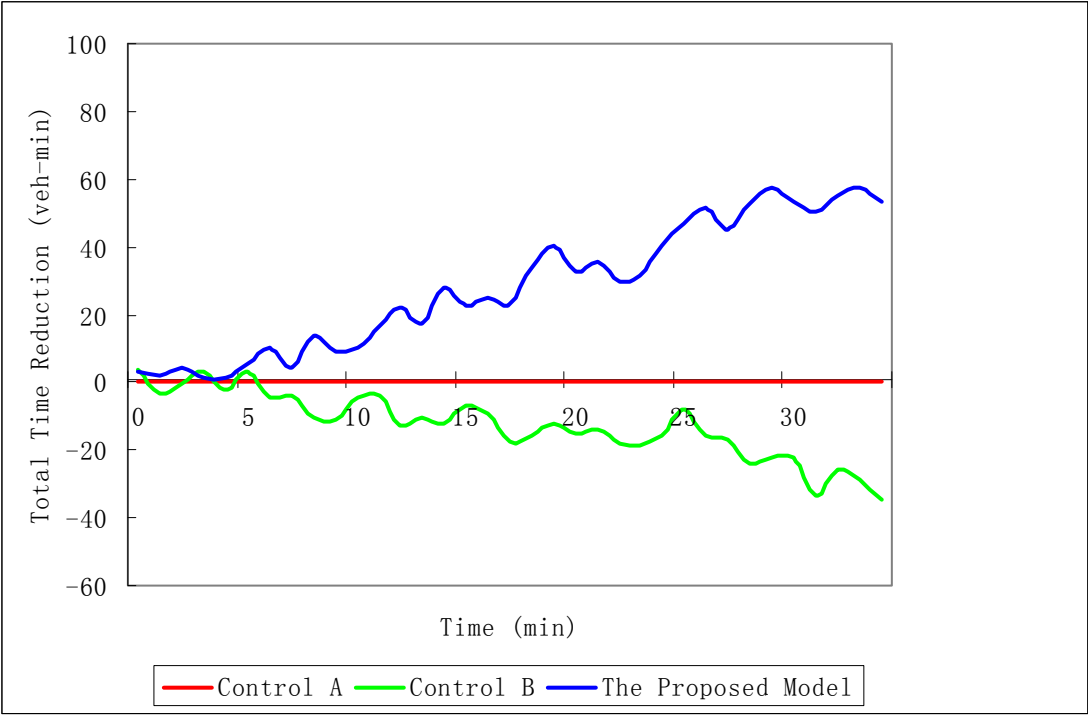


Figure 5.9 Time-varying Total Time Savings (Scenario I)

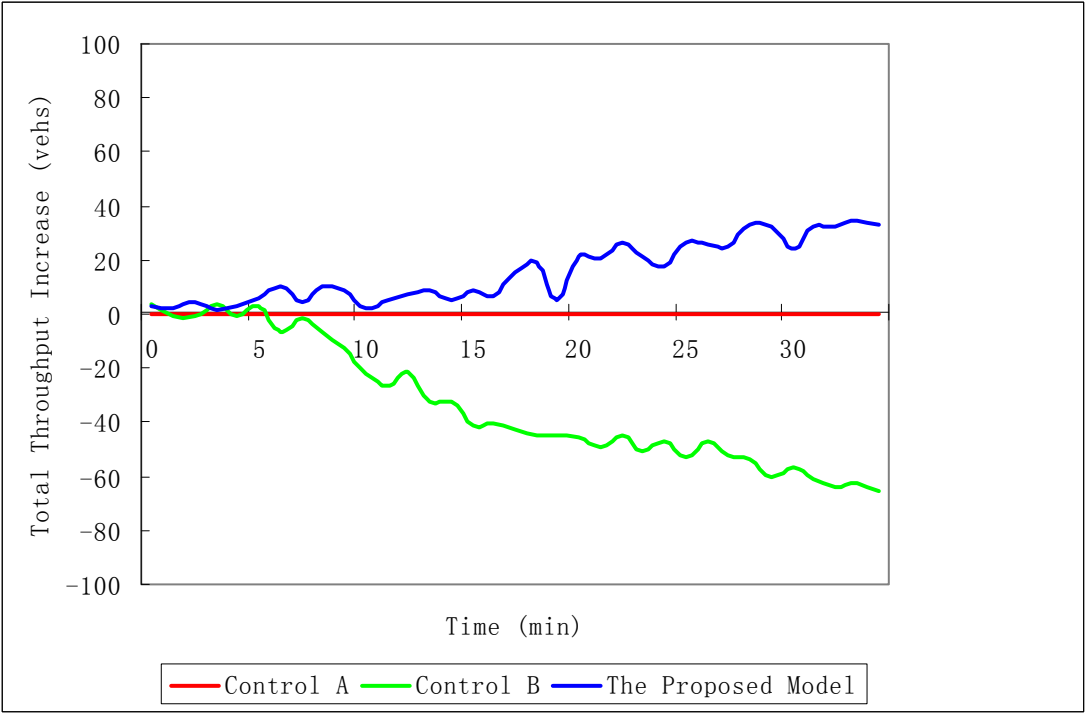


Figure 5.10 Time-varying Total Throughput Increases (Scenario I)

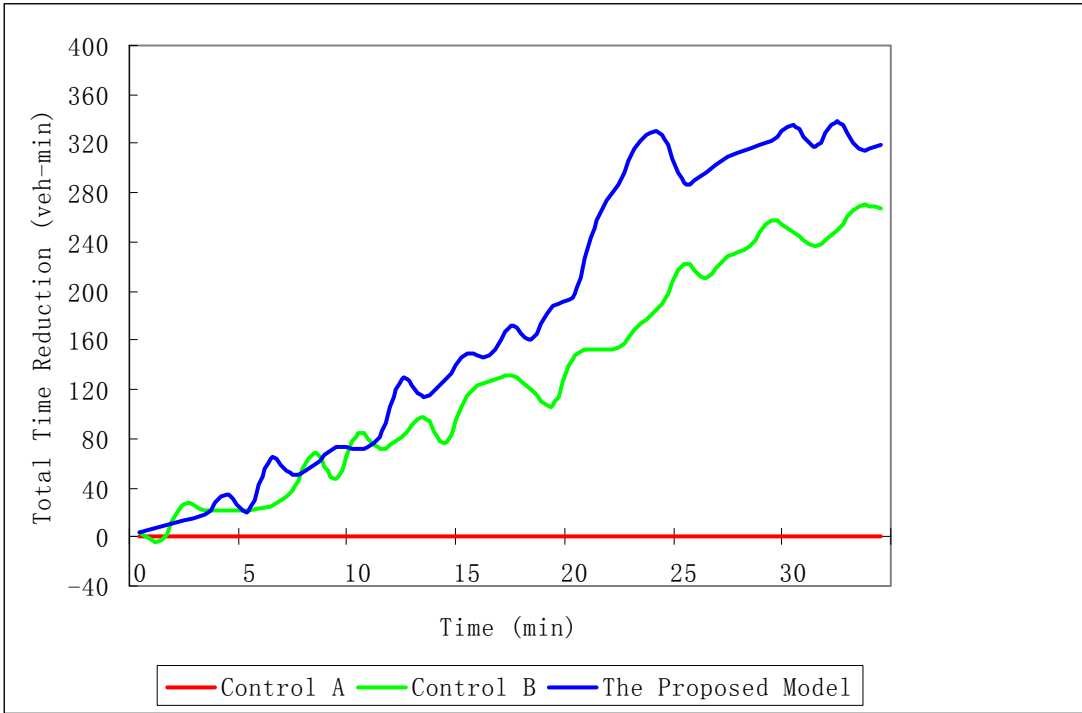


Figure 5.11 Time-varying Total Time Savings (Scenario II)

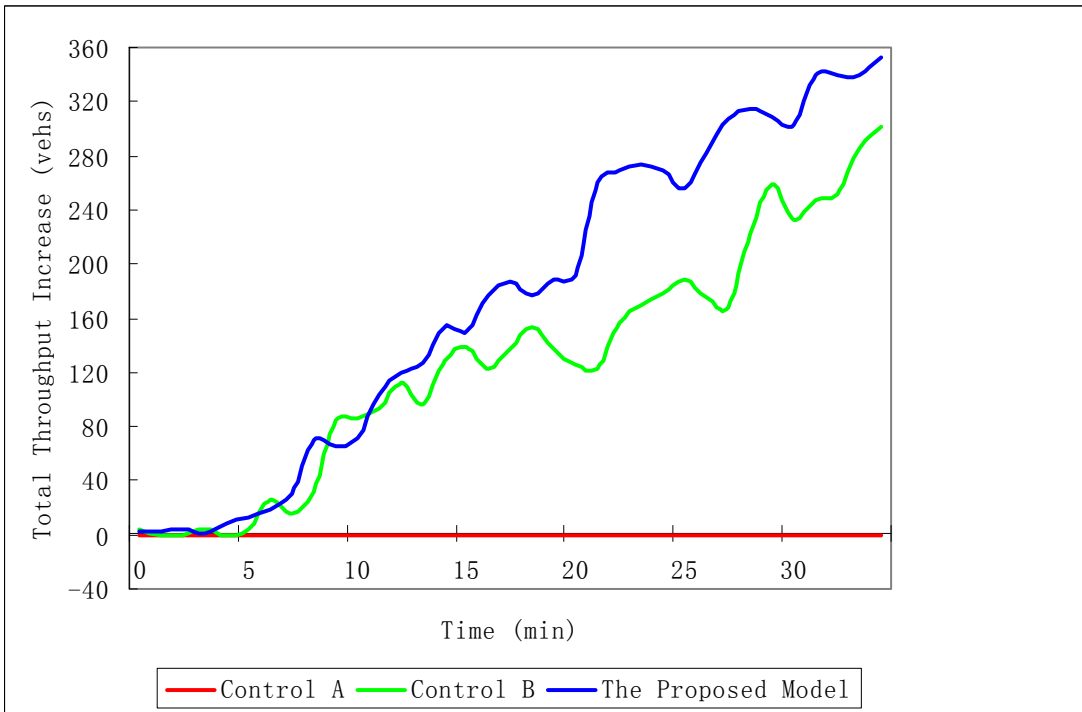


Figure 5.12 Time-varying Total Throughput Increases (Scenario II)

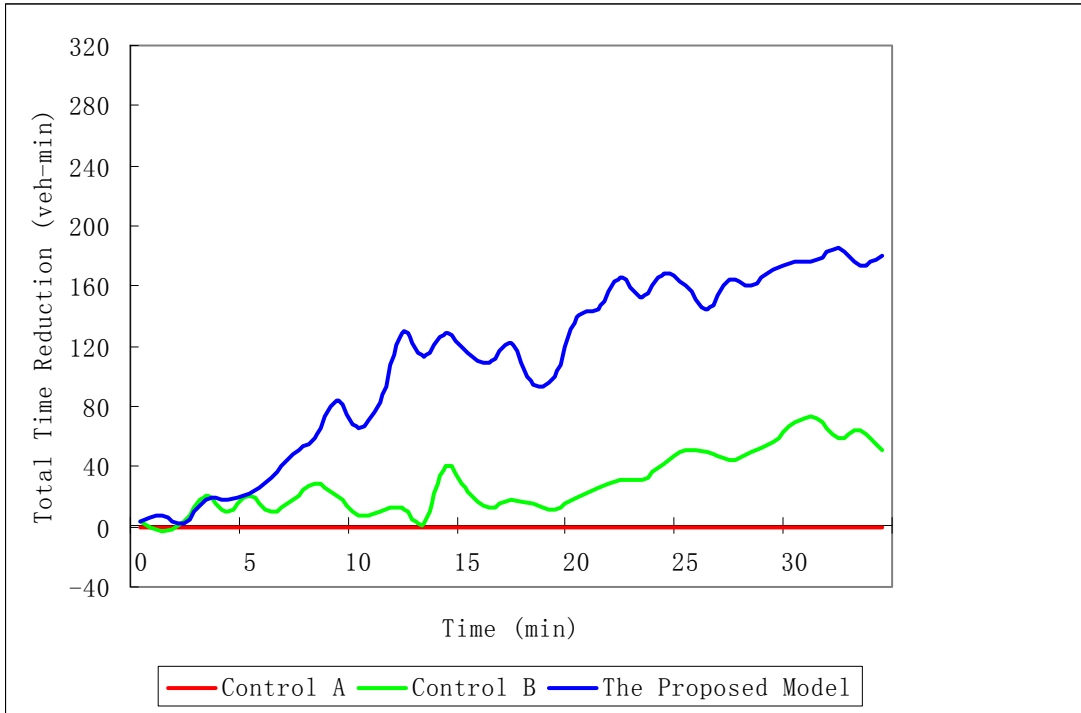


Figure 5.13 Time-varying Total Time Savings (Scenario III)

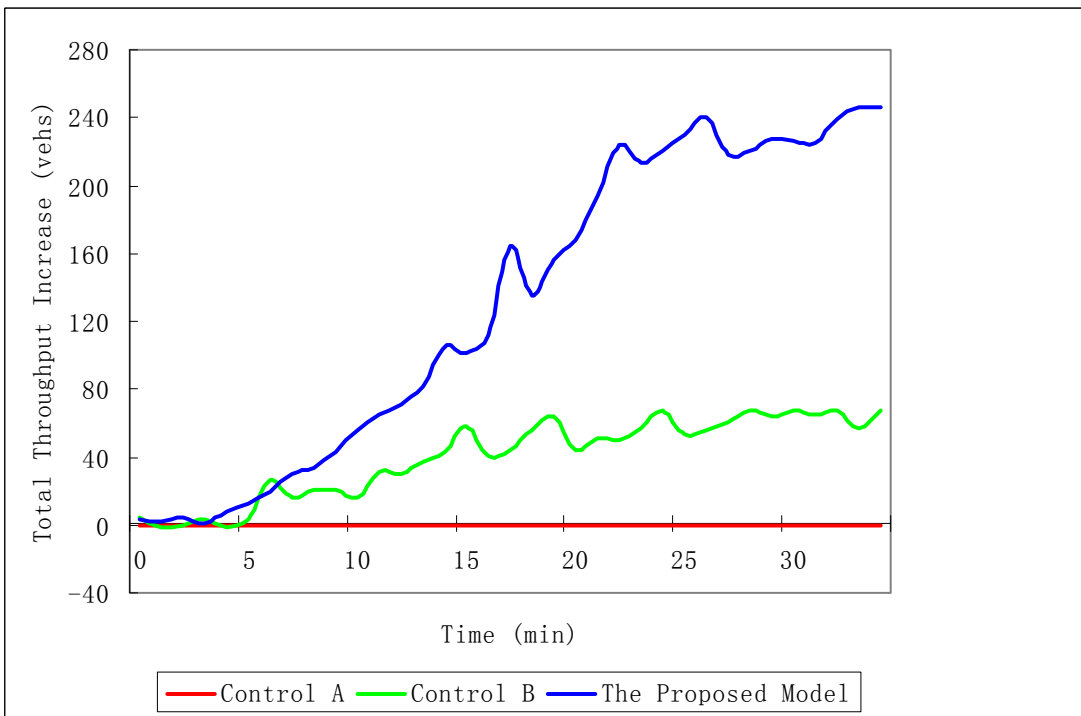


Figure 5.14 Time-varying Total Throughput Increases (Scenario III)

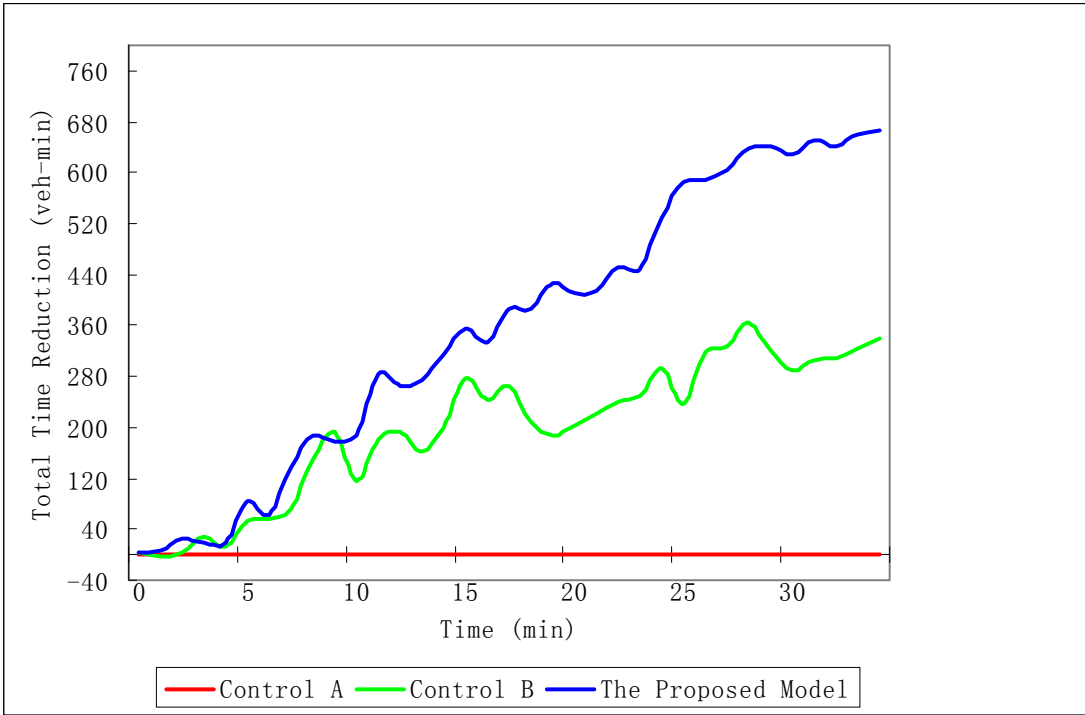


Figure 5.15 Time-varying Total Time Savings (Scenario IV)

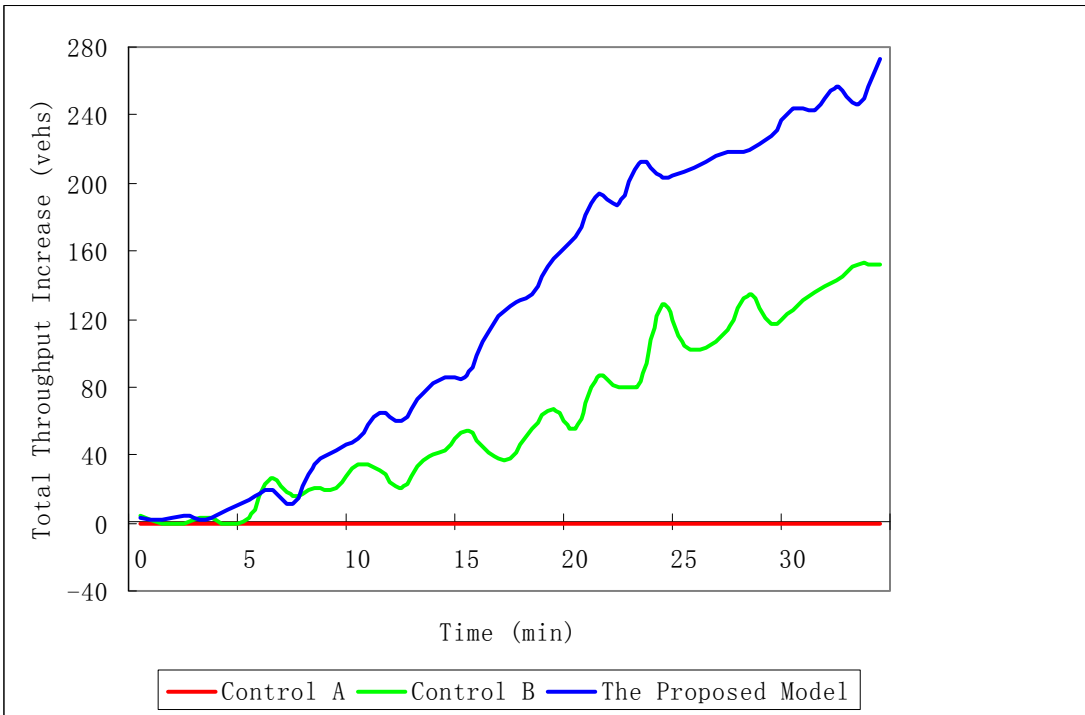


Figure 5.16 Time-varying Total Throughput Increases (Scenario IV)

5.1.6. Summary

Based on the above analysis results, one can reach the following conclusions:

- For under-saturated scenarios, the performance of the multi-objective model is not quite sensitive to the weight assignment. Increasing the total corridor throughput by detouring traffic will not excessively degrade the traffic conditions at the arterial. Therefore, maximizing the total corridor throughput in those scenarios, will be an effective decision;
- For oversaturated scenarios, the entire system performance becomes sensitive to the weigh assignment. A single control objective of maximizing the total corridor throughput tends to favor the freeway mainline by detouring traffic to the arterial, which may cause over-congestion in the arterial and discourage the drivers for detour operations. In these scenarios, decision makers need to carefully set the weight assignment, based on the corridor network structure and driver behavioral characteristics to maximize the utilization of corridor capacity while maintaining balanced traffic conditions between the freeway and arterial system; and
- With properly selected weights of importance between control objectives, the proposed model outperforms the state-of-practice control strategies with better utilized available corridor capacity especially under saturated conditions.

5.2. Numerical Test of the Extended Model

5.2.1. Experimental Design

In Section 5.1, the operational effectiveness and efficiency of the proposed base model has been validated through an example of a single corridor segment. This section will focus on the following aspects:

- Investigate the performance of the extended model with systematically varied weights to assist decision makers in determining an appropriate control area for integrated control operations on a multi-segment corridor network; and
- Compare the operational performance of the extended model with the base model under a given incident scenario.

A segment of 12-mile hypothetical corridor, including a total of 12 freeway exits and 36 arterial intersections, is employed for the experimental analyses (see Figure 5.17). Assuming that an incident occurs on the freeway mainline section (between Exit 6 and 7), traffic will detour via different on-ramps, off-ramps, and different portions of the parallel arterial to circumvent the incident location. The proposed control model will determine a set of critical off-ramps and on-ramps for detour operations, and update the control measures, including diversion rates at critical off-ramps, signal timings at all related intersections, and metering rates at upstream on-ramps. The entire experiment period is designed to cover 60 minutes, including a 5-min for normal operations (no incident), a 40-min with incident, and a

15-min recovery period (incident cleared). The data used for model inputs is summarized as follows:

- Freeway entry volumes: 3000 vph;
- Normal arterial entry volumes: 500 vph for arterial (80% for through and right-turn, 20% for left-turn); 200 vph for the side streets (40% for left-turn, 40% for right-turn, and 20% for through);
- Normal exiting rate at the off-ramps is 0.05 for the entire control time horizon;
- Driver compliance rates to the detour operation at all off-ramps are assumed at the 100% level over entire control time horizon;
- The number of lanes on the affected freeway mainline: 2;
- The number full lanes at the arterial: 2;
- The number of left-turn lanes at arterial: 1;
- The number of lanes at off-ramps and on-ramps: 1;
- Minimum and maximum cycle length for arterial intersections: C^{\min} (60s), C^{\max} (160s);
- Minimum green time per phase: G_{np}^{\min} (7s), clearance time I_{np} (5s);
- Minimum and maximum ramp metering rates: R^{\min} (0.1), R^{\max} (1.0);
- Maximum diversion rate Z^{\max} (0.4);
- Each arterial intersection has four phases with the left-turn lag in the arterial direction and split phases for the side streets;

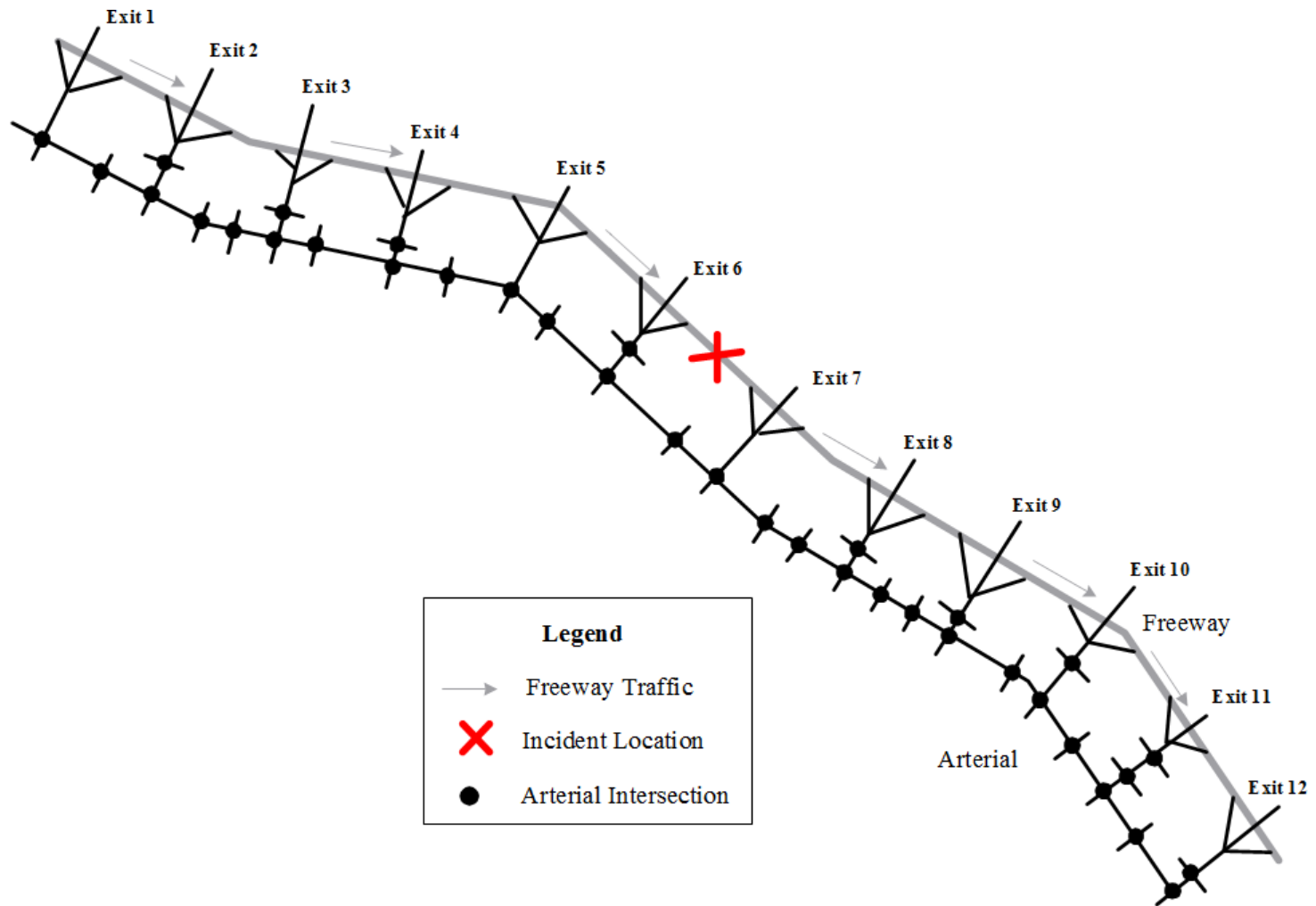


Figure 5.17 A Hypothetical Corridor Network for Case Study

- All other parameters related to the network flow models are the same as the base model;
- The GA population size is set at 100;
- The maximum number of generation is set at 200;
- The crossover probability is set at 0.6;
- The mutation probability is set at 0.02;
- ε is kept the same as in the base model;
- The length of the projection horizon S_p is set to be 10-min, and the control time interval $T_h = 2C^h$;
- The weights of importance w_1 / w_2 are varying from 10/0 to 0/10 with a step of 1.

5.2.2. Numerical Analyses and Findings

To evaluate the performance of the proposed extended model, this experimental analysis will be focused on the following critical issues:

I - The control area (critical off-ramps and on-ramps involved) generated from the proposed model under different weight assignment settings, and its impact on the system MOEs.

Figures 5.18 – 5.22 present the variation of the control area (shown in the blue color) with the weight assignment for w_1 / w_2 ranging from 10/0 to 0/10 for the study corridor network.

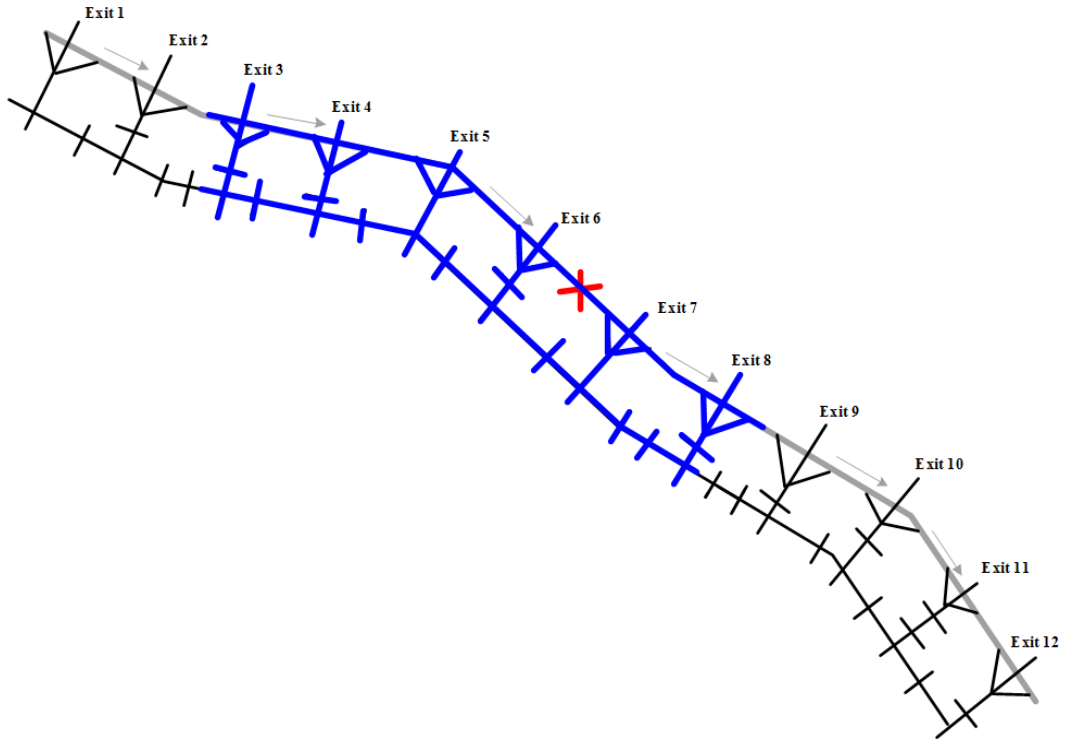


Figure 5.18 The Control Area ($w_1/w_2 = 10/0$ and $9/1$)

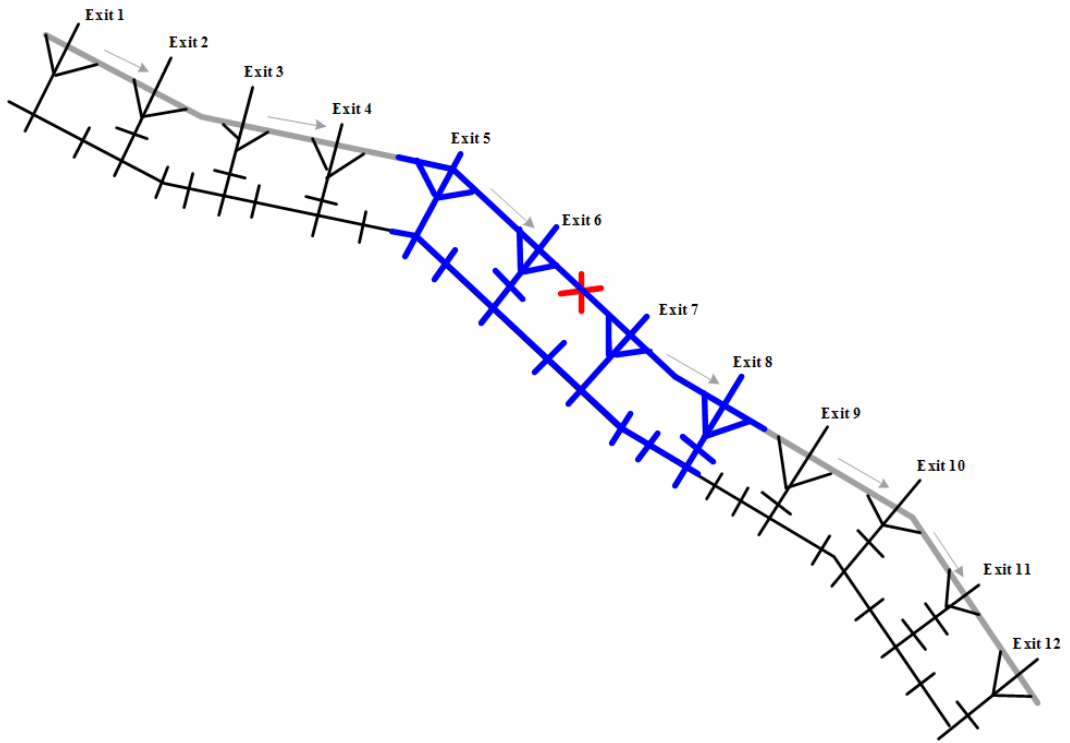


Figure 5.19 The Control Area ($w_1/w_2 = 8/2, 7/3$ and $6/4$)

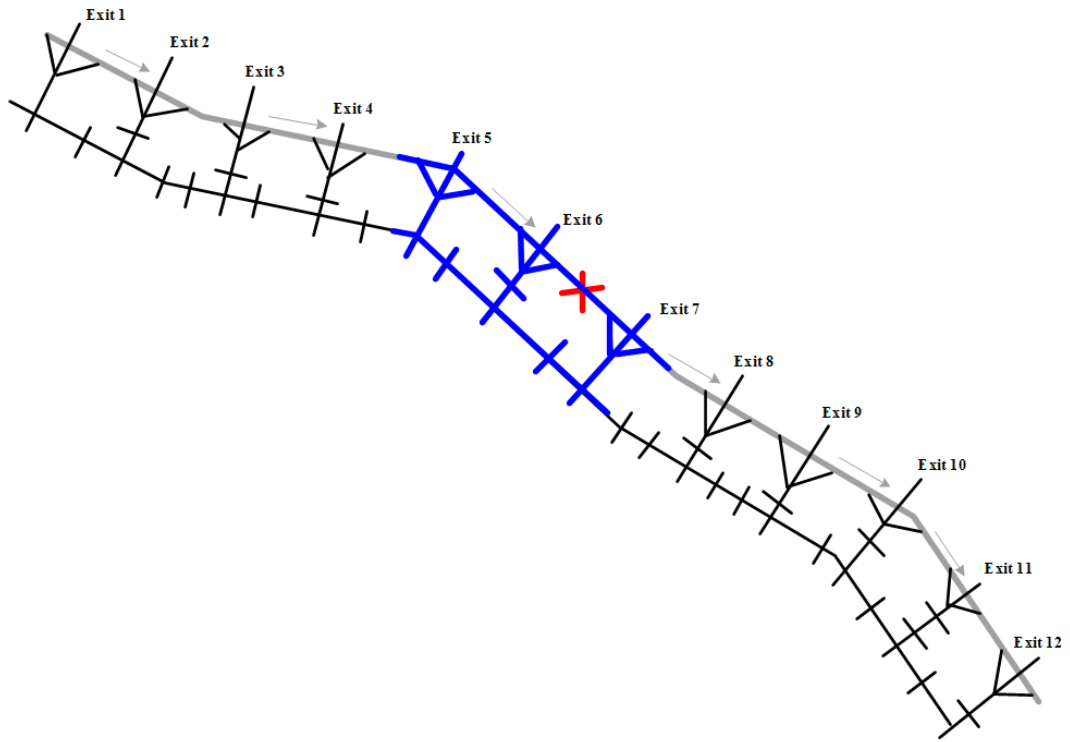


Figure 5.20 The Control Area ($w_1/w_2 = 5/5, 4/6, \text{ and } 3/7$)

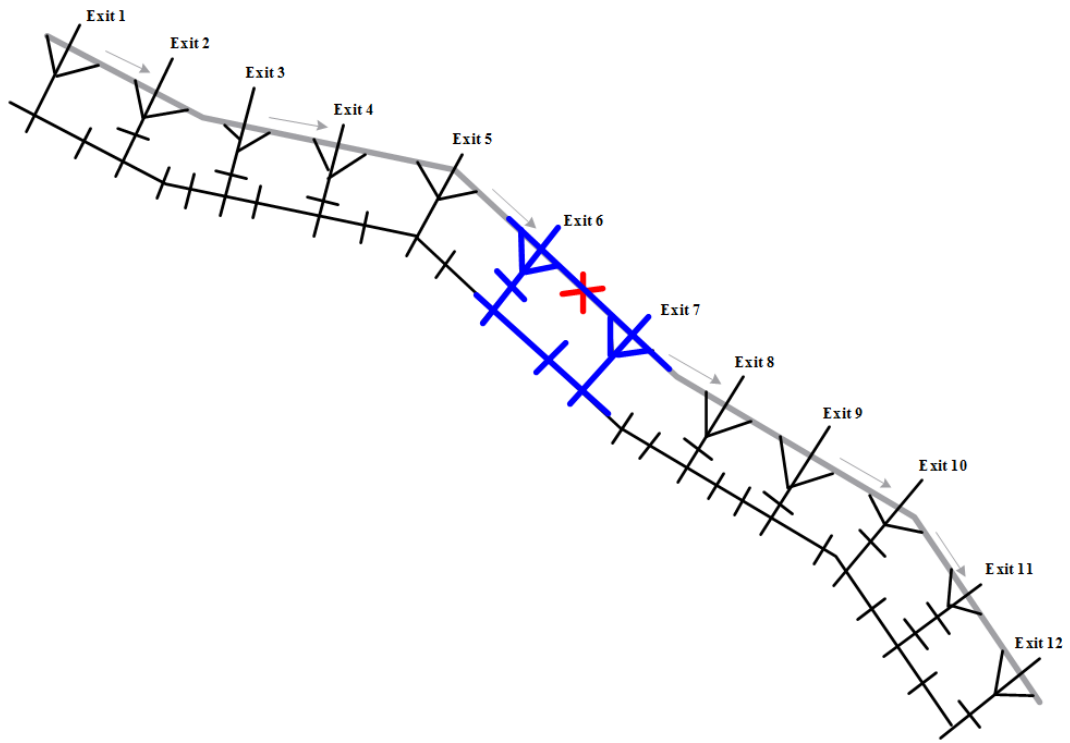


Figure 5.21 The Control Area ($w_1/w_2 = 2/8 \text{ and } 1/9$)

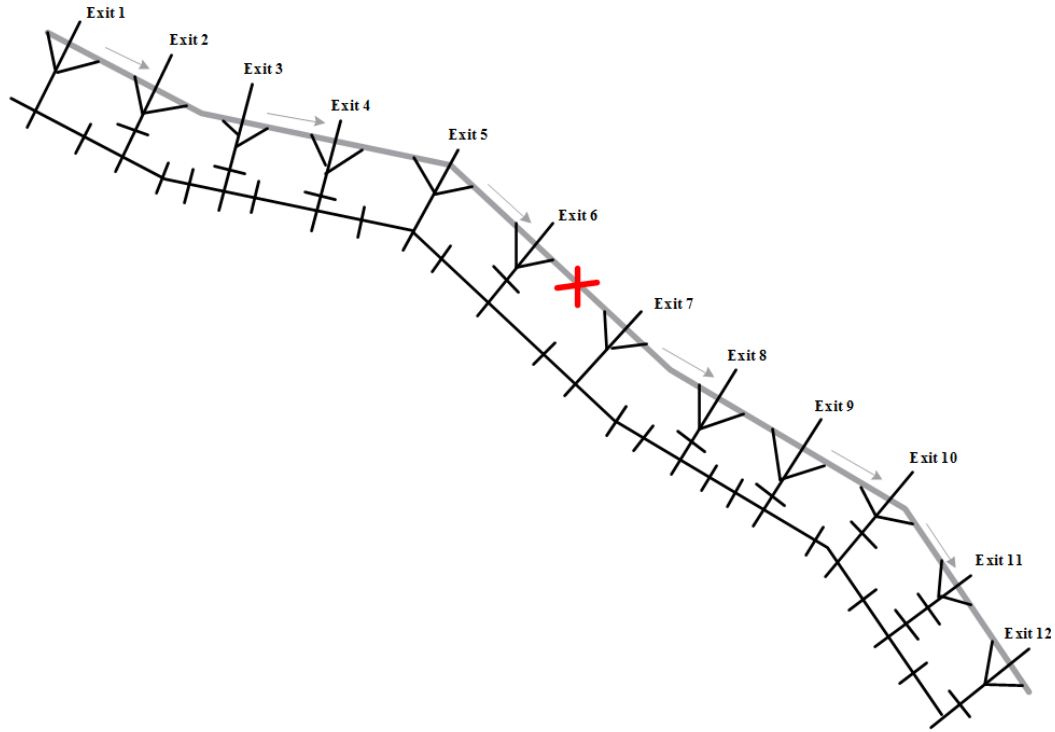


Figure 5.22 The Control Area ($w_1/w_2 = 0/10$, no detour)

The impact of the control area variation on the corridor system MOEs is summarized in Table 5.5, and illustrated in Figures 5.23 – 5.25. Comparison between the results yields the following observations:

- With the weight assignment between two control objectives varying from 10/0 to 0/10, the generated control area shrinks and the total diversion rates decrease;
- Depending on the traffic conditions and corridor network structure, there exists a critical control area beyond which the total corridor throughput no longer increases. For example, although the study network covers a 12-

exit stretch, only 4 upstream exits and 2 downstream exits are used to yield the maximal corridor throughput (see Figure 5.18);

- The number of incident downstream on-ramps used to divert traffic back to the freeway is less than that of incident upstream off-ramps, which is expected since the higher capacity at incident-free freeway links may encourage detour traffic to come back to freeway whenever it is available; and
- Compared with the control area generated by maximizing the total corridor throughput (i.e., $w_1 / w_2 = 10/0$), the one obtained by setting $w_1 / w_2 = 8/2$ seems more appropriate for the example corridor network due to its compact size and shorter distances for detour operations (see Figure 5.18 and 5.19), which can significantly save the manpower and control resources. Most importantly, it can substantially reduce the required total diversion rates as well as the total spent time by the detour traffic (12.3% and 19.8%, respectively, as shown in Table 5.5 and Figures 5.24 – 5.25) at the relatively low reduction in the total corridor throughput (3.2% as shown in Table 5.5 and Figure 5.23). In real-world applications, traffic operators can refer to the same procedure to determine a proper control area, and achieve the maximal control benefits under the given incident scenario.

Table 5.5 Model Performance with Various Decision Preferences

w_1 / w_2	Corridor System MOE		
	Total Corridor Throughput (vehs)	Total Diversion Rates (vph)	Total Time Spent by Detour Traffic (veh-min)
10/0	3352	1379	4573.8
9/1	3297	1340	4441.5
8/2	3244	1209	3667.4
7/3	3198	1176	3330.5
6/4	3077	1030	2937.8
5/5	2835	799	2231
4/6	2764	701	1842.7
3/7	2694	596	1544.1
2/8	2570	404	987.5
1/9	2476	288	694.3
0/10	2226	0	0.0

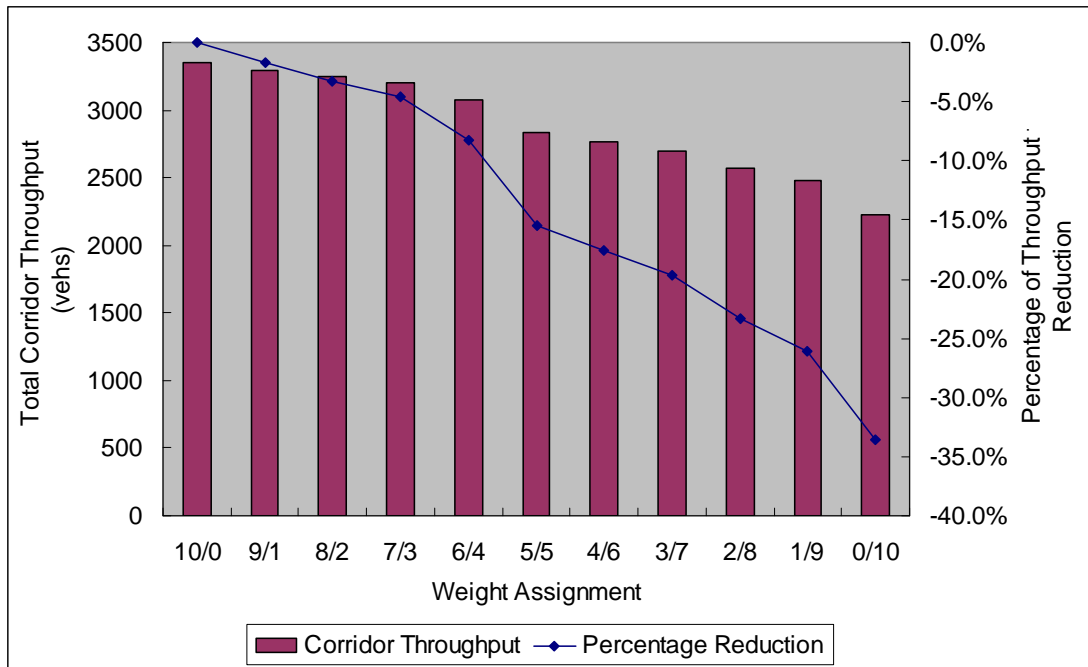


Figure 5.23 The Impact of Weight Assignment on Corridor Throughput

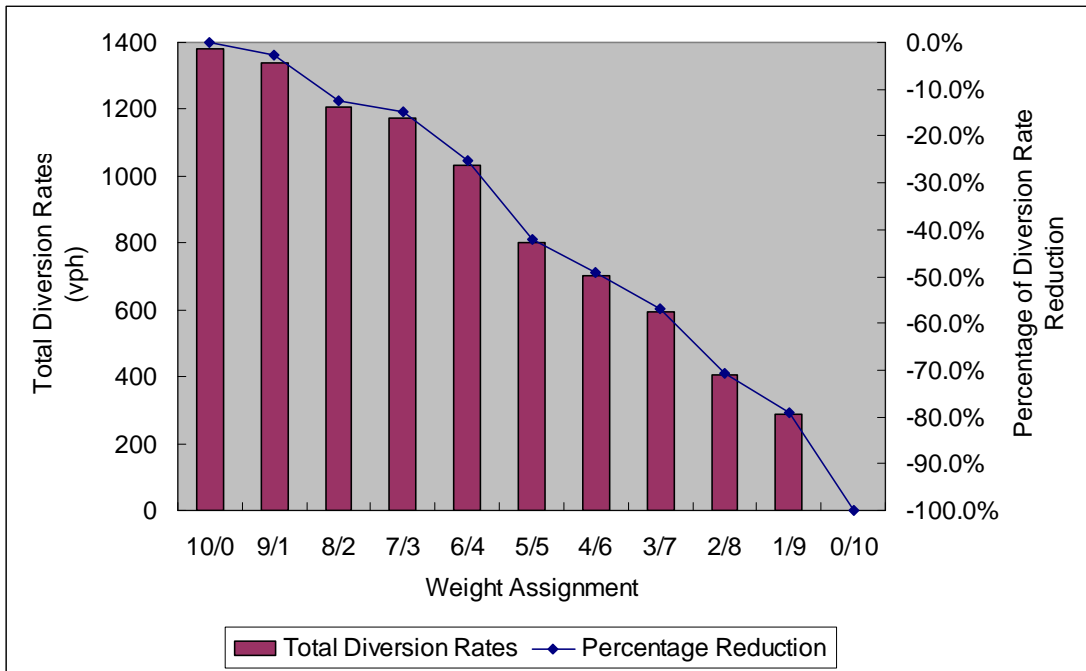


Figure 5.24 The Impact of Weight Assignment on Total Diversion Rates

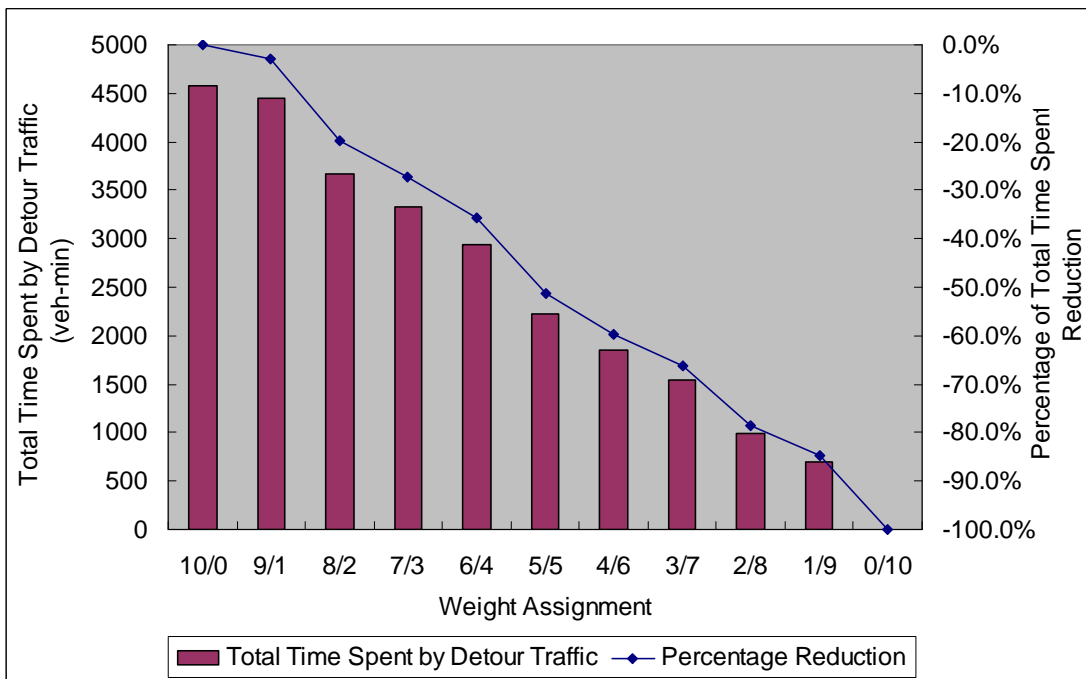


Figure 5.25 The Impact of Weight Assignment on Total Time by Detour Traffic

To further explore the results of diversion plans, this experimental analysis has also yielded the distribution of diversion flows over different off-ramps and on-ramps within the control area under various weights between two control objectives. The comparison results, as shown in Table 5.6 and Figures 5.26 – 5.29, have indicated that:

- The diversion flows are not evenly distributed over the upstream off-ramps. An off-ramp closer to the incident location has carried more diversion flows (see Figures 5.26 – 5.29). This is reasonable as traffic tends to take off-ramps closer to the incident segment to reduce the extra travel distances caused by the detour operations;
- Similarly, the on-ramp closer to the incident location has also received more detoured flows. This again confirms the previous findings that detour traffic prefers to employ the on-ramp closer to the incident location to come back to the freeway so as to best use of the high capacity at incident-downstream freeway links.

Table 5.6 Distribution of Diversion Flows at Off-ramps and On-ramps

Freeway		Decision Making Preferences w_1 / w_2										
		10/0	9/1	8/2	7/3	6/4	5/5	4/6	3/7	2/8	1/9	0/10
Off-ramps (vph)	Exit 1	-	-	-	-	-	-	-	-	-	-	-
	Exit 2	-	-	-	-	-	-	-	-	-	-	-
	Exit 3	119	75	-	-	-	-	-	-	-	-	-
	Exit 4	188	185	-	-	-	-	-	-	-	-	-
	Exit 5	505	478	564	501	332	207	128	38	-	-	-
	Exit 6	567	602	645	685	698	592	573	558	404	288	-
On-ramps (vph)	Exit 7	618	606	594	621	664	707	648	564	388	279	-
	Exit 8	467	453	417	366	236	-	-	-	-	-	-
	Exit 9	-	-	-	-	-	-	-	-	-	-	-
	Exit 10	-	-	-	-	-	-	-	-	-	-	-
	Exit 11	-	-	-	-	-	-	-	-	-	-	-
	Exit 12	-	-	-	-	-	-	-	-	-	-	-

- No Diversion Flows

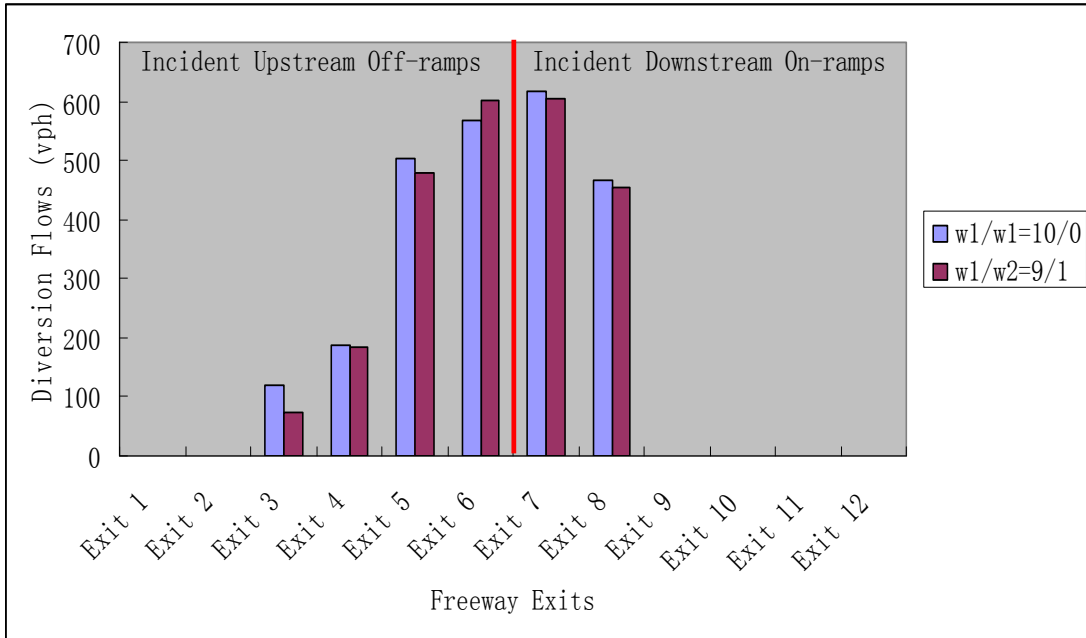


Figure 5.26 Distribution of Diversion Flows ($w1/w2 = 10/0$ and $9/1$)

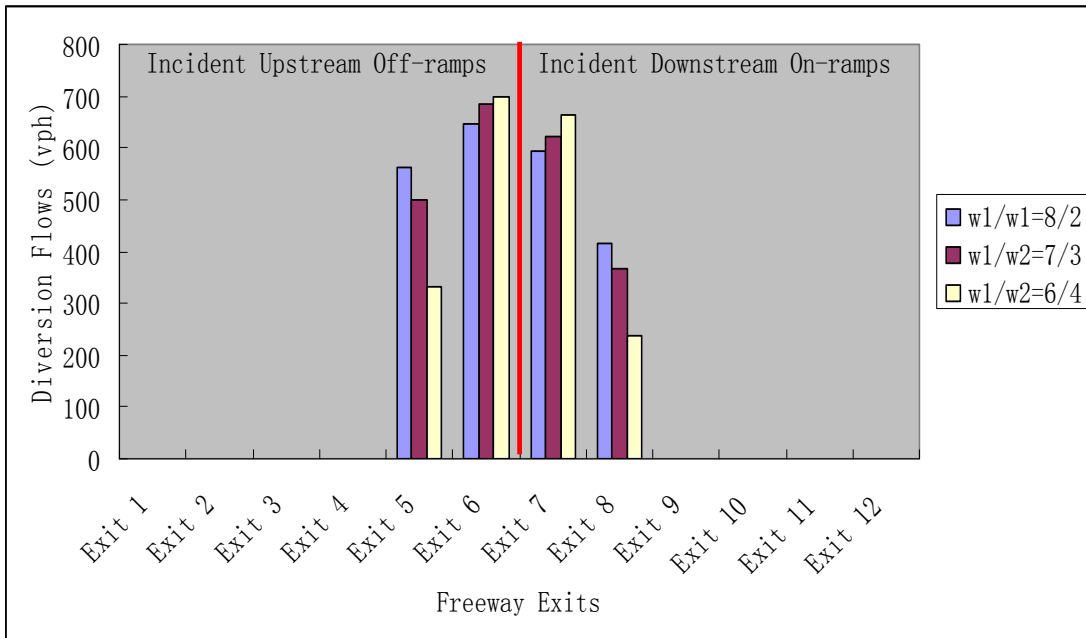


Figure 5.27 Distribution of Diversion Flows ($w1/w2 = 8/2$, $7/3$ and $6/4$)

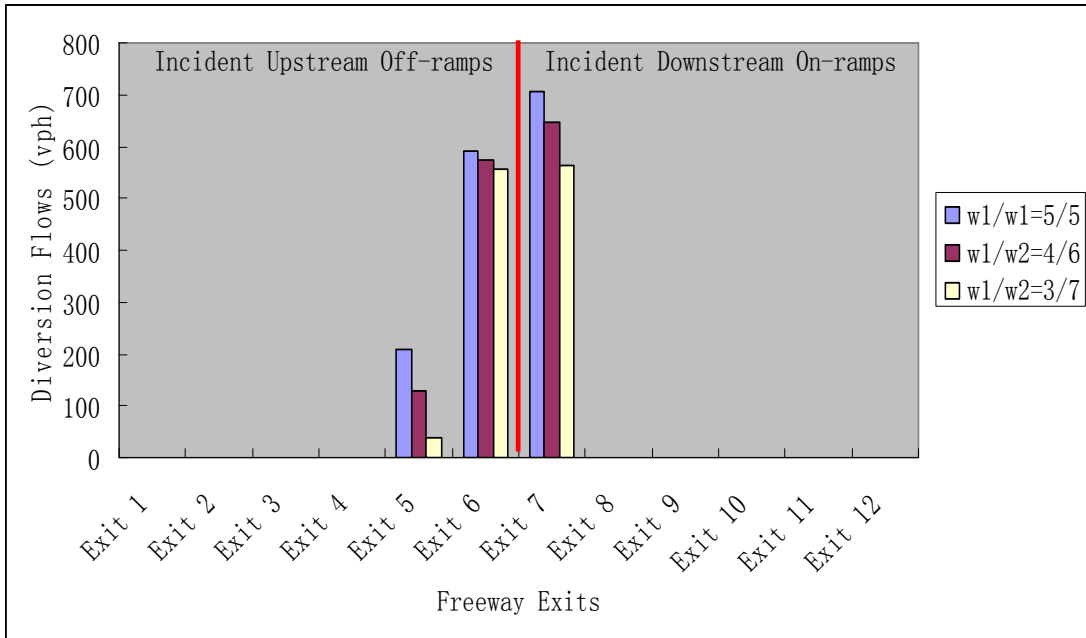


Figure 5.28 Distribution of Diversion Flows (w1/w2 = 5/5, 4/6, and 3/7)

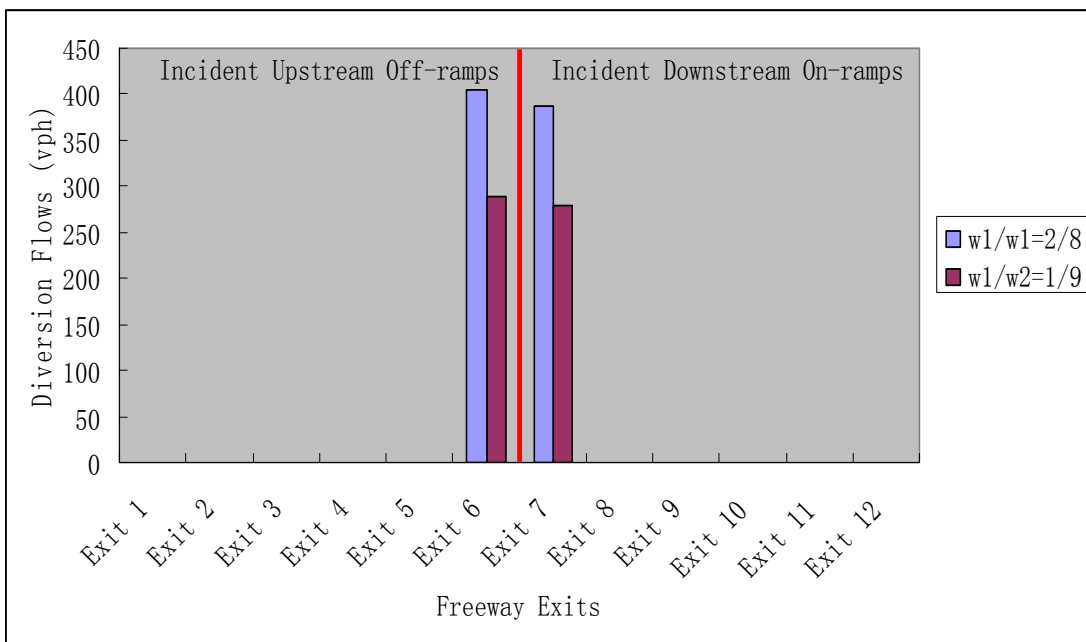


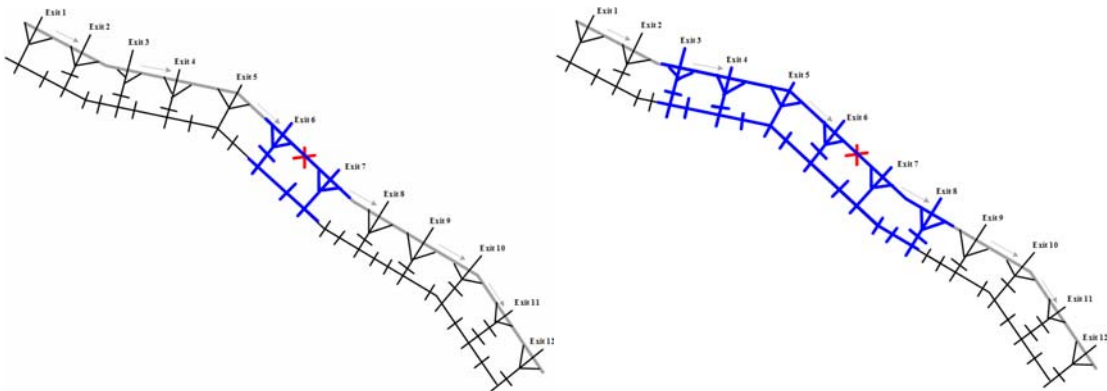
Figure 5.29 Distribution of Diversion Flows (w1/w2 = 2/8 and 1/9)

II – Comparison of the extended model performance with the base model under the same incident scenario and the same control objective.

In this analysis, the corridor network shown in Figure 5.17 and the same experimental design are employed for comparison. The performance of the following two control models is compared using CORSIM:

- Model 1 - The base model with only one segment between exits 6 and 7 as the control area, and the control objective is to maximize the total corridor throughput; and
- Model 2 - The extended model with the control objective of maximizing the total corridor throughput;

Figure 5.30 illustrates the control areas represented by the above two models.



(a) Control Area of Model 1

(b) Control Area of Model 2

Figure 5.30 Control Areas Represented by the Model 1 and 2

Table 5.7 summarizes the comparison results between the two models in terms of the following four types of performance indices:

- Total diversion rates
- Total corridor throughput
- Average detour link total queue time
- Average side street link total queue time

Table 5.7 Comparison Results between Models 1 and 2

Performance Indices	Model 1	Model 2	Improvement over Model 1
Total diversion rates (vph)	984	1379	+40.1%
Total corridor throughput (vehs)	2917	3352	+14.9%
Average detour link total queue time (veh-min)	547.2	416.8	-23.8%
Average side street link total queue time (veh-min)	833.7	575.9	-30.9%

Comparison between the results in Table 5.7 yields the following observations:

- The extended model outperforms the base model in terms of the total corridor throughput (i.e., 3352 versus 2917, a +14.9% increase) due to the fact that using only one corridor segment is subject to the limitation of flow capacity at the ramp or the intersection turning lane. However, with multiple ramps for integrated control, one can overcome this limitation by balancing the detour traffic load over multiple ramps and intersection

turning lanes, which results in a higher rate of diversion flows (1379 versus 984) and better utilized network capacity;

- The advantage of the extended model is also indicated by the significantly decreased average total queue time on detour links (547.2 versus 416.8, a 23.8% decrease) and at the side street links (833.7 versus 575.9, a 30.9% decrease). Compared with the base model, this result is desirable as it encourages traffic to follow the detour operations, and avoids the excessive delays to the side street traffic.

5.3. Sensitivity Analyses

Conditioned on a 100% level of diversion compliance rates, the proposed integrated control model outperforms other control strategies with respect to both the total spent time savings and the total corridor throughput increases. However, during real-world operations, driver behavioral patterns are usually subject to time-varying fluctuations. Therefore, the sensitivity of the control performance with respect to the variation of diversion compliance rate needs to be investigated.

To address the above critical issue, this section has evaluated the performance of the integrated control model under two previously designed experimental scenarios (Scenarios II and IV in Section 5.1.1), with the diversion compliance rates at the 95%, 90%, 85%, 80%, and 70% levels, respectively. Table 5.8 has summarized the results of the sensitivity analyses.

Table 5.8 Sensitivity Analysis With Respect To The Variation of Diversion Compliance Rates

Diversion Compliance Rates	Incident Scenario	System MOEs			
		Total Time Spent Savings (veh-min)	Improvement over Control B	Total Throughput Increases (vehs)	Improvement over Control B
100%	Scenario II	319.14	19.0%	352	17.7%
	Scenario IV	667.03	95.6%	273	79.6%
95%	Scenario II	303.82	23.8%	337	24.3%
	Scenario IV	630.00	89.5%	254	77.0%
90%	Scenario II	275.04	21.4%	308	22.5%
	Scenario IV	500.99	104.9%	216	80.9%
85%	Scenario II	242.25	26.7%	289	28.0%
	Scenario IV	444.00	113.4%	198	81.4%
80%	Scenario II	199.21	30.6%	250	32.9%
	Scenario IV	264.00	120.4%	161	86.2%
70%	Scenario II	179.36	33.8%	232	41.0%
	Scenario IV	220.00	127.0%	139	90.7%

As illustrated in Table 5.8, the performance of the integrated control model declines with the decrease of the diversion compliance rates. For example under Scenario II, the savings of total spent time drop from 319.14 to 179.39 with the decrease of diversion compliance level from 100% to 70%, and the increases of total corridor throughput decline from 352 to 232 similarly. Such patterns can also be observed under the incident Scenario IV. However, the improvement of the model performance over Control B seems not to be sensitive to the decrease of the diversion compliance rates (see the highlighted cells in Table 5.8 for Scenario II), which has indicated the potential for an application of the proposed model in the traffic environment with significant discrepancy in driver behavioral patterns.

5.4. Closure

This chapter has illustrated the potential application of the proposed model with a segment along the I-95 northbound corridor and a hypothetical corridor network, respectively.

The numerical analyses presented in this chapter have shed some light on the guideline development for best use the proposed integrated control models with respect to the corridor operational efficiency under various non-recurrent congested scenarios. Through the extensive information produced from the developed integrated control model, the responsible agency can implement effective strategies in a timely manner at all control points, including off-ramps, arterial intersections, and on-ramps.

Chapter 6: Enhanced Control Strategies for Local Bottlenecks

6.1. Introduction

This chapter presents the enhanced formulations for the lane-group-based traffic flow model proposed in Chapter 4, which is designed to capture the complex interrelations between the queue overflow in each lane group and its impacts on the neighboring lanes. This is due to the fact that detoured traffic often incurs the volume surge at local intersections and off-ramps. Through proper integration with the signal optimization model, the enhanced set of formulations is designed to prevent the formation of local bottlenecks with optimized signal plans. The remaining chapter is organized as follows: Section 6.2 presents the formulations for the enhanced lane-group-based model as well as numerical results to demonstrate its strengths over the base model proposed in Chapter 4. Section 6.3 illustrates the enhanced network flow model for producing optimal signal plans, and its performance effectiveness in comparison with the results from TRANSYT-7F (version 8) under various traffic conditions. The last section summarizes the research efforts in this chapter.

6.2. The Enhanced Network Formulations for Local Bottlenecks

The set of formulations for modeling arterial network flows proposed in Chapter 4 is focused on the dynamic evolution of physical queues with respect to the signal status, arrival rate, and departure rate, but not the blockage due to queue spillback from neighboring lane groups. For example, left turn traffic with

insufficient left-turn bay capacity could block the through traffic, and vice versa during detour operations.

This section proposes a set of enhanced network formulations for arterials or off-ramps using the lane group concept. Grounded on those equations proposed in Chapter 4, this enhanced model contains some additional formulations to capture the queue spillback impacts and interactions between different lane groups.

6.2.1. Model Formulations

Additional Model Parameters

To facilitate the presentation of the enhanced model formulations, this section summarizes the notations used hereafter:

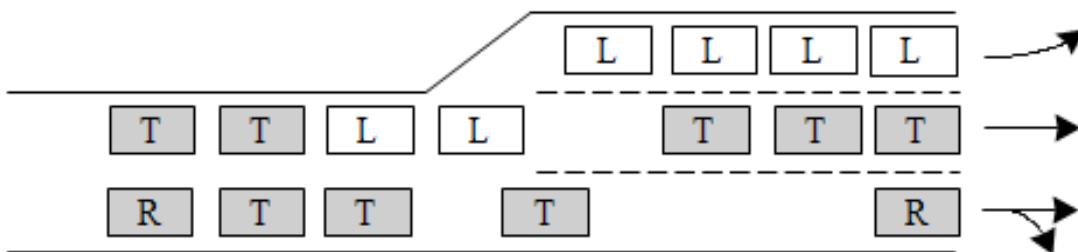
N_m^i	Storage capacity of lane group m at link i (vehs)
$\Omega^i[k]$	Blocking matrix between lane groups at link i
$\omega_{m'm}^i[k] \in \Omega^i[k]$	Blocking coefficient between lane group m' and m at time step k
$\phi_{m'm}$	A constant between 0 and 1 that is related to driver's response to lane blockage and geometry features for lane group m' and m
$q_m^{i,pot}[k]$	Flows likely to merge into lane group m of link i at time step k (vehs)
$\tilde{x}_m^i[k]$	The number of arriving vehicles bound to lane group m but queued outside the approach lanes at link i due to blockage at time step k (vehs)

Additional Model Formulations

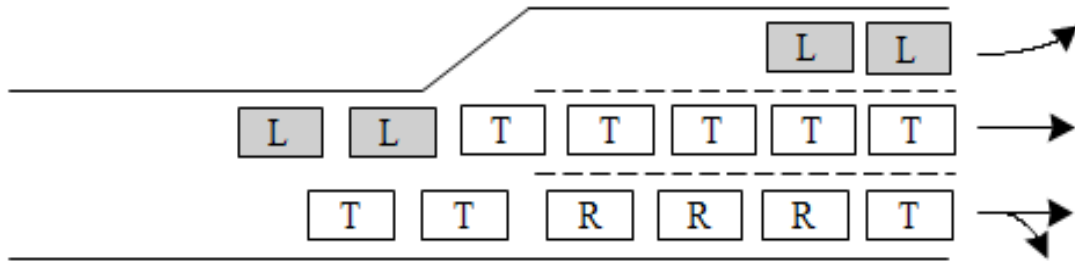
In modeling the process of traffic merging into lane groups, it is noticeable that after vehicles arrive at the end of a link queue, they will try to change lanes and merge into different lane groups based on their destinations. Most previous studies assume that the arriving vehicles could always merge into their destination lanes without being blocked. However, such an assumption may not be realistic under the following scenarios: (1) the intended lane group has no more space to accommodate vehicles (e.g., a fully occupied left-turn bay); and (2) the overflowed queues from other lane groups may block the target lane group (shown in Figure 6.1). Therefore, arriving vehicles that could not merge into their destination lane group m due to either overflows or blockage will form queues on the through lanes upstream to the target approach, denoted by $\tilde{x}_m^i[k]$ (see Figure 6.2).

To illustrate such scenarios, it should be noted that the number of vehicles allowed to merge into lane group m at time step k depends on the available storage capacity of the lane group, and is given by:

$$\max\{N_m^i - x_m^i[k], 0\} \quad (6.1)$$



i) Left-turn lane group partially blocks the right-through lane group



ii) Right-through lane group completely blocks the left-turn lane group

Figure 6.1 Blockages between Lane Groups

The aforementioned blocking impacts between different lane groups can further be classified as complete blockage or partial blockage (shown in Figure 6.1). In order to model such interactions, this study has defined a blocking matrix for each arterial link i , denoted by $\Omega^i[k]$. The matrix element, $\omega_{m'm}^i[k]$, takes a value between 0 and 1 to depict the percentage of merging capacity reduction for lane group m due to queue spillback at lane group m' at time step k . It is defined as follows:

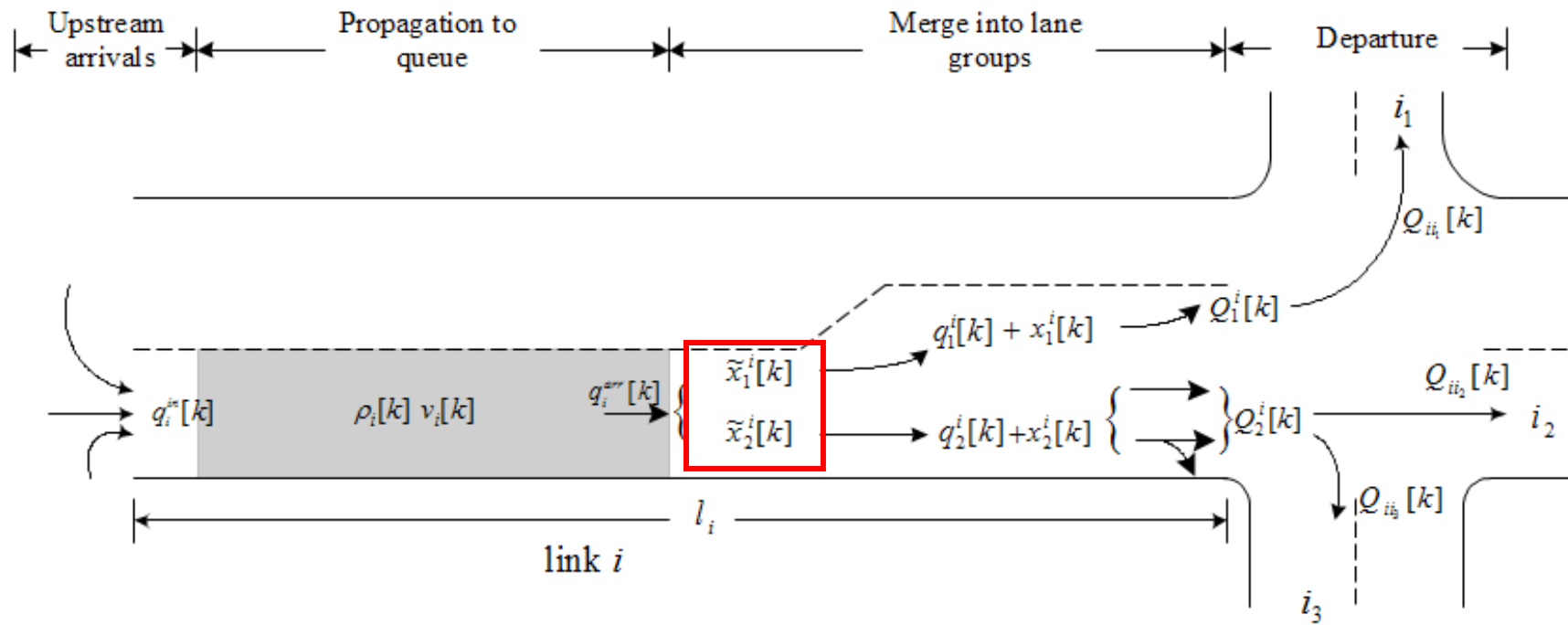


Figure 6.2 Enhanced Traffic Flow Dynamics along an Arterial Link Considering Lane Group Queue Interactions

$$\omega_{m'm}^i[k] = \begin{cases} 1 & x_{m'}^i[k] > N_{m'}^i, \text{complete blockage} \\ \phi_{m'm} \cdot \frac{q_{m'}^{i,pot}[k]}{\sum_{m \in S_i^M} q_m^{i,pot}[k]} & x_{m'}^i[k] > N_{m'}^i, \text{partial blockage} \\ 0 & \text{no blockage or } x_{m'}^i[k] \leq N_{m'}^i \end{cases} \quad (6.2)$$

$$q_m^{i,pot}[k] = \tilde{x}_m^i[k] + \sum_{j \in \Gamma^{-1}(i)} q_i^{arr}[k] \cdot \gamma_{ij}[k] \cdot \delta_m^{ij} \quad (6.3)$$

$q_i^{arr}[k]$ is the total flow arriving at the end of queue of link i at time step k ; $\gamma_{ij}[k]$ is the turning fraction going from link i to j ; δ_m^{ij} is a binary value indicating whether traffic going from link i to j uses lane group m . Hence, one can approximate $[\tilde{x}_m^i[k] + \sum_{j \in \Gamma^{-1}(i)} q_i^{arr}[k] \cdot \gamma_{ij}[k] \cdot \delta_m^{ij}]$ as the potential level of flows that may merge into lane group m at time step k , denoted as $q_m^{i,pot}[k]$.

At each time step, the model will evaluate each element in the blocking matrix once a queue spillback occurs in a lane group. For the complete blockage or no blockage cases, $\omega_{m'm}^i[k]$ can be easily determined to 1 or 0, based on the geometric features of the approach (shown in Figure 6.1-ii). For the partial blockage case, $\omega_{m'm}^i[k]$ can be approximated by $\phi_{m'm} \cdot q_{m'}^{i,pot}[k] / \sum_{m \in S_i^M} q_m^{i,pot}[k]$. Where, $\phi_{m'm}$ is a constant parameter between 0 and 1 that is related to driver's response to lane blockage and geometry features, and $q_{m'}^{i,pot}[k] / \sum_{m \in S_i^M} q_m^{i,pot}[k]$ approximates the fraction of merging lanes occupied by the overflowed traffic from lane group m' at time step k .

Taking the link shown in Figure 6.1 as an example, there are two lane groups in the link: left-turn and right-through (named as L and R-T, respectively). Therefore,

the blocking matrix at time step k is constructed as
$$\begin{bmatrix} / & \omega_{L,R-T}^i[k] \\ \omega_{R-T,L}^i[k] & / \end{bmatrix}.$$

Where $\omega_{L,R-T}^i[k]$ and $\omega_{R-T,L}^i[k]$ will be updated as follows:

$$\omega_{L,R-T}^i[k] = \begin{cases} \phi_{L,R-T} \cdot \frac{q_L^{i,pot}[k]}{q_L^{i,pot}[k] + q_{R-T}^{i,pot}[k]}, & \text{if } x_L^i[k] > N_L^i, \text{ L partially blocks R-T;} \\ 0 & \text{if } x_L^i[k] \leq N_L^i \end{cases}$$

$$\omega_{R-T,L}^i[k] = \begin{cases} 1 & \text{if } x_{R-T}^i[k] > N_{R-T}^i \\ 0 & \text{if } x_{R-T}^i[k] \leq N_{R-T}^i \end{cases}, \text{ R-T completely blocks L;}$$

Considering the impact of blocking matrix, the number of vehicles allowed to merge into lane group m at time step k is restricted by:

$$q_m^{i,pot}[k] \cdot \left[1 - \sum_{m' \in S_i^M \wedge m' \neq m} \omega_{m'm}^i[k] \right] \quad (6.3)$$

According to the definition of $\omega_{m'm}^i[k]$, $1 - \sum_{m' \in S_i^M \wedge m' \neq m} \omega_{m'm}^i[k]$ is the residual fraction

of capacity to accommodate those potential merging vehicles to lane group m .

Finally, the number of vehicles allowed to merge into lane group m at time step k should be the minimum of Equations 6.1 and 6.3, and is given by:

$$q_m^i[k] = \min \left\{ \max \{ N_m^i - x_m^i[k], 0 \}, q_m^{i,pot}[k] \cdot \left[1 - \sum_{m' \in S_i^M \wedge m' \neq m} \omega_{m'm}^i[k] \right] \right\} \quad (6.4)$$

To keep the flow conservation on a target approach lane or a given link, the lane group based queues are advanced as follows:

$$x_m^i[k+1] = x_m^i[k] + q_m^i[k] - Q_m^i[k] \quad (6.5)$$

And, queues exceeding the approach lanes due to overflows or blockages are advanced as follows:

$$\tilde{x}_m^i[k+1] = \tilde{x}_m^i[k] - q_m^i[k] + \sum_{j \in \Gamma^{-1}(i)} q_i^{arr}[k] \cdot \gamma_{ij}[k] \cdot \delta_m^{ij} \quad (6.6)$$

Then, the total number vehicles queued at link i can be approximated as:

$$x_i[k+1] = \sum_{m \in S_i^M} (x_m^i[k+1] + \tilde{x}_m^i[k+1]) \quad (6.7)$$

Note that, the above enhanced formulations can be modified with the same procedure used in Section 4.3.2 or Section 4.4.3 to accommodate the impact of traffic from single or multiple detour routes.

6.2.2. Model Validation

Intersection for Experimental Analysis

This section presents the results of performance evaluation for the enhanced model with a real-world intersection (MD212 and Adelphi Rd., Maryland) under various demand scenarios using a microscopic simulator, VISSIM. Figure 6.3 shows the geometric configuration and lane channelization of the target intersection, and Table 6.1 lists its signal timings. The reason for choosing this intersection as a test site is due to its existence of both shared lanes and left-turn bays. Also, severe blockages often occur between its left-turn and right-through traffic at eastbound and westbound approaches during the peak hours.

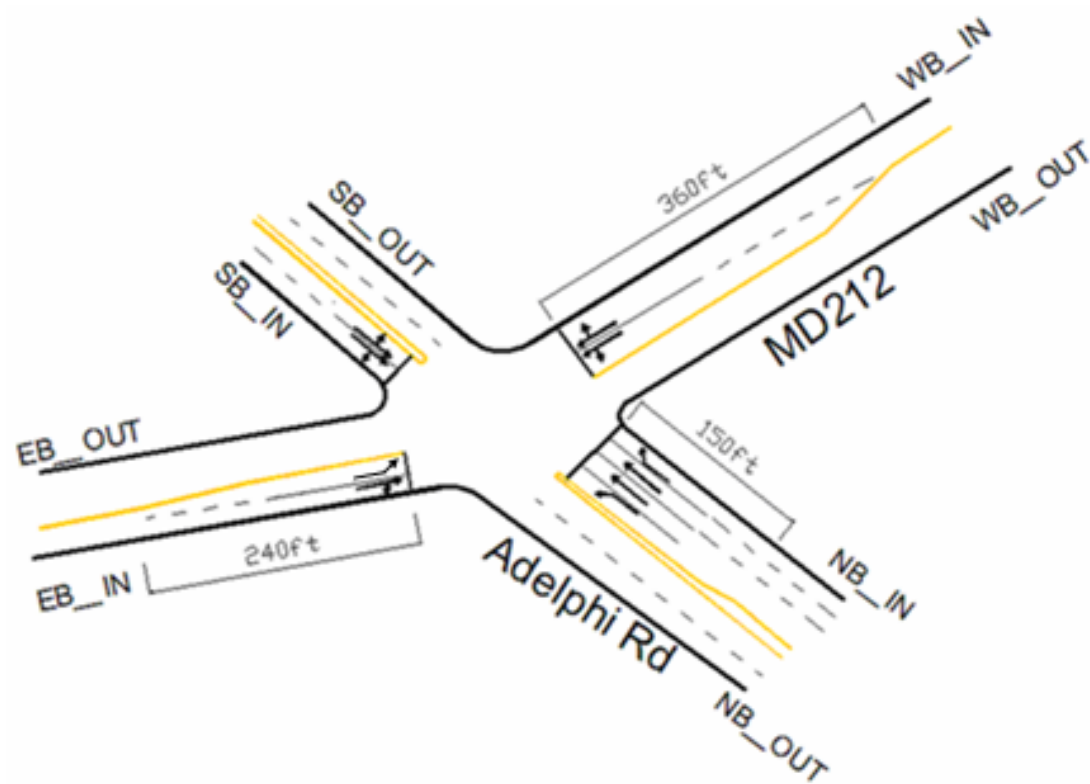


Figure 6.3 A Graphical Illustration of the Target Intersection for Model Validation (MD212@Adelphi Rd.)

Table 6.1 Signal Settings for the Target Intersection

Phases	I	II	III
Green Time (secs)	44	35	49
Yellow Time (secs)	3	3	3
All-red Time (secs)	1	1	1
Turning Movements			

Simulation Calibration and Model Parameter Fitting

To make sure that VISSIM can reliably replicate driver behavioral patterns and traffic conditions at the target intersection, this study has calibrated those parameters with field data during a period of two hours in the morning (7:30 am to 9:30 am). Due to the limitation of data availability, traffic data used for calibrating the target intersection are only traffic volumes for all movements at a time interval of 5 minutes.

To facilitate calibration of the enhanced network flow model, the parameters vector for link i is shown as follows:

$$\theta_i = [Q_i, \rho_i^{jam}, \rho_i^{\min}, v_i^{free}, v_i^{\min}, \alpha, \beta, Q_i^m, \Omega^i] \quad (6.8)$$

Let $[Q_{ij}[t]]$ denote the model-output values of departure volumes for movement from link i to j , and $[\bar{Q}_{ij}[t]]$ represent the field measured values then θ_i is chosen for each link i to minimize the quadratic errors between the model-output and the field collected values of traffic volumes for all movements of that intersection:

$$L(\theta) = \frac{1}{n^U n^T} \sum_{i \in S^U} \sum_{t=1}^{n^T} (Q_{ij}[t] - \bar{Q}_{ij}[t])^2 \quad (6.9)$$

Where, n^U is the number of links and $t = 1, \dots, n^T$ is the sampling intervals (5 minutes in this study). To avoid the local optimal or abnormal values from the non-linear optimization process for parameter fitting, some parameters can be pre-fixed or bounded by commonly used equations or practices. For example, the discharging capacity for lane group m shall be bounded around the values computed from the

Highway Capacity Manual (HCM). Table 6.2 summarizes the model parameter values after calibration.

Experimental Design

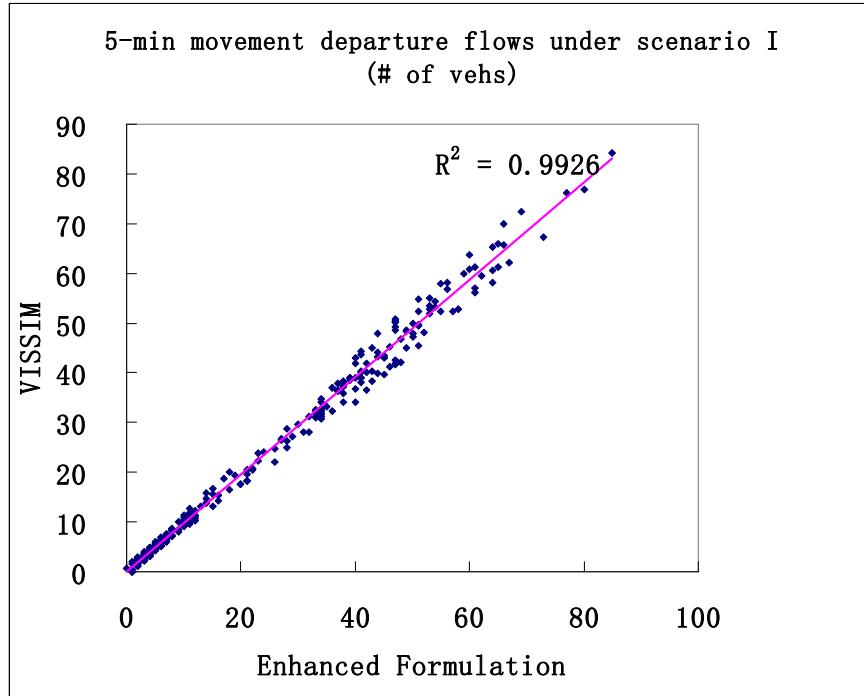
After the calibration for the VISSIM and the enhanced network flow model, this study has designed four scenarios with their volumes increased at an increment of 10 percent (denoted by I, II, III, and IV) and two scenarios at the 10 percent decreasing rate (denoted by V and VI) from the current intersection demand level. Simulation outputs from VISSIM serve as the base line for performance evaluation of the enhanced model under all those experimental scenarios.

Validation Results and Discussion

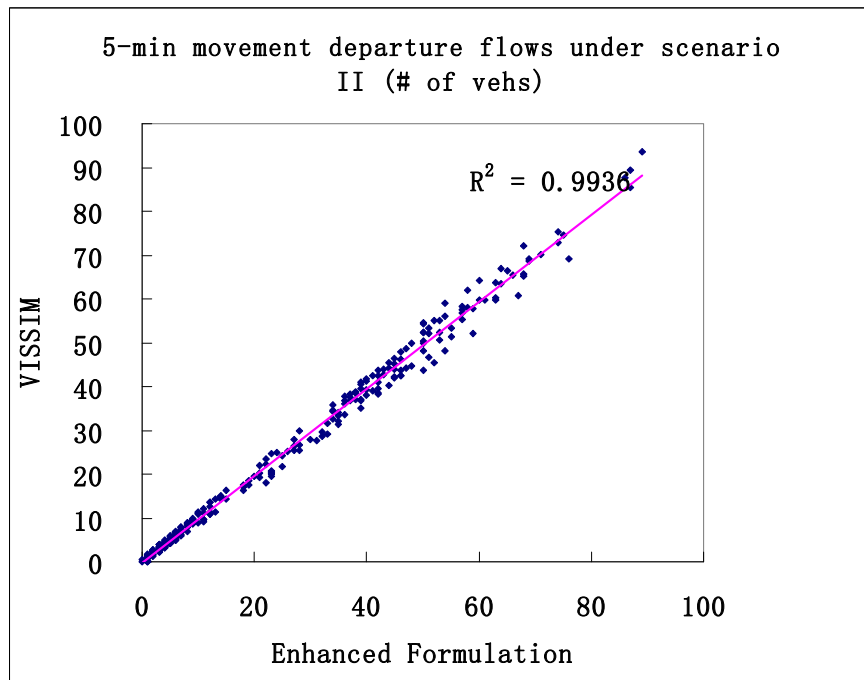
Figure 6.4 show the comparison results of each 5-minute departure flows for all movements from VISSIM simulation results and the enhanced model under each experimental scenario. From correlation coefficients shown in Figure 6.4, it is observable that there exists high consistency between the results from the VISSIM and the enhanced model for all experimental scenarios. Using VISSIM results as the true values for departure flows, the Root Mean Square Errors (RMSE) and maximal errors of 5-min movement departure flows for the enhanced model are summarized in Table 6.3 in comparison with the base model proposed in Chapter 4.

Table 6.2 Parameter Fitting Results for All Intersection Links

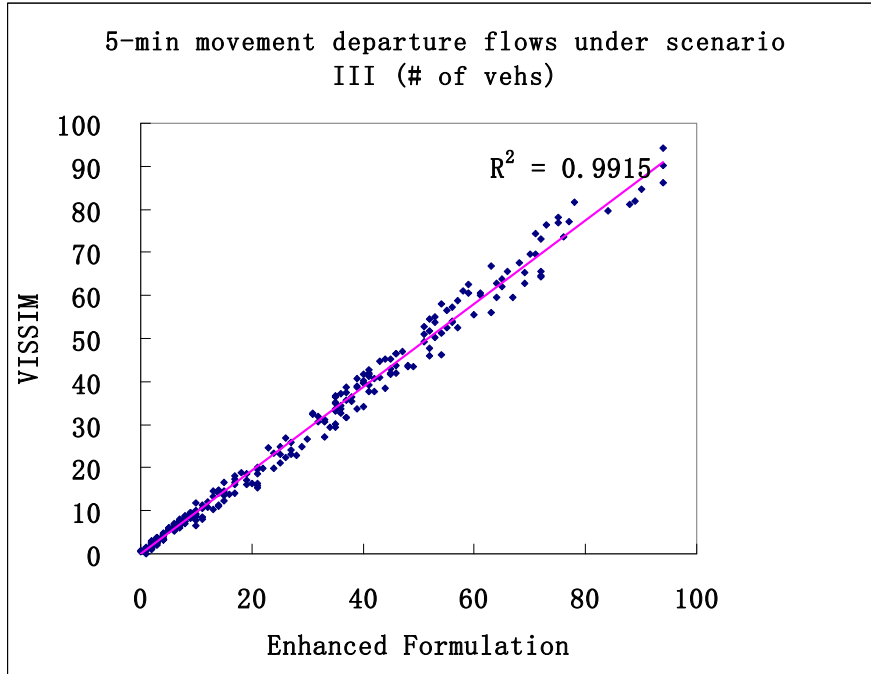
Links	Q_i (veh/hr)	ρ^{jam}, ρ^{min} (veh/mile/lane)	v^{min} (mph)	v_i^{free} (mph)	α	β	$[Q_i^m]$ (veh/hr)	$\Omega^i [k]$ (blocking matrix)
EB_IN	1873			35			$\begin{bmatrix} L & R-T \\ 647 & 1805 \end{bmatrix}$	$\begin{matrix} L & R-T \\ L \begin{bmatrix} / & 1.0 \\ 1.0 & / \end{bmatrix} \\ R-T \end{matrix}$
EB_OUT	1881			35			1881	Not applicable
WB_IN	1857			35			$\begin{bmatrix} L & R-T \\ 935 & 1844 \end{bmatrix}$	$\begin{matrix} L & R-T \\ L \begin{bmatrix} / & 1.0 \\ 1.0 & / \end{bmatrix} \\ R-T \end{matrix}$
WB_OUT	1870			35			1870	Not applicable
		185, 16	5		3.25	1.96		
NB_IN	5105			30			$\begin{bmatrix} L & T & R \\ 533 & 3540 & 1581 \end{bmatrix}$	$\begin{matrix} L & T & R \\ L \begin{bmatrix} / & 0.18 \cdot \frac{q_L^{i,pot} [k]}{\sum_{m \in S_i^M} q_m^{i,pot} [k]} & 0 \\ 1.0 & / & 0 \\ 0 & 0 & / \end{bmatrix} \\ T \\ R \end{matrix}$
NB_OUT	3580			30			3580	Not applicable
SB_IN	3556			30			$\begin{bmatrix} L-T-R \\ 2520 \end{bmatrix}$	Not applicable
SB_OUT	3580			30			3580	Not applicable



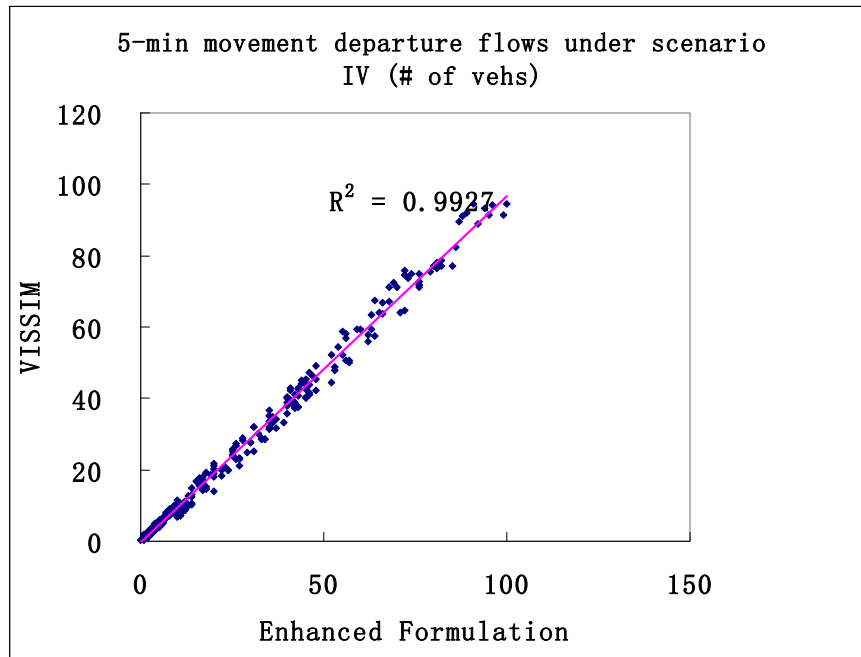
(i)



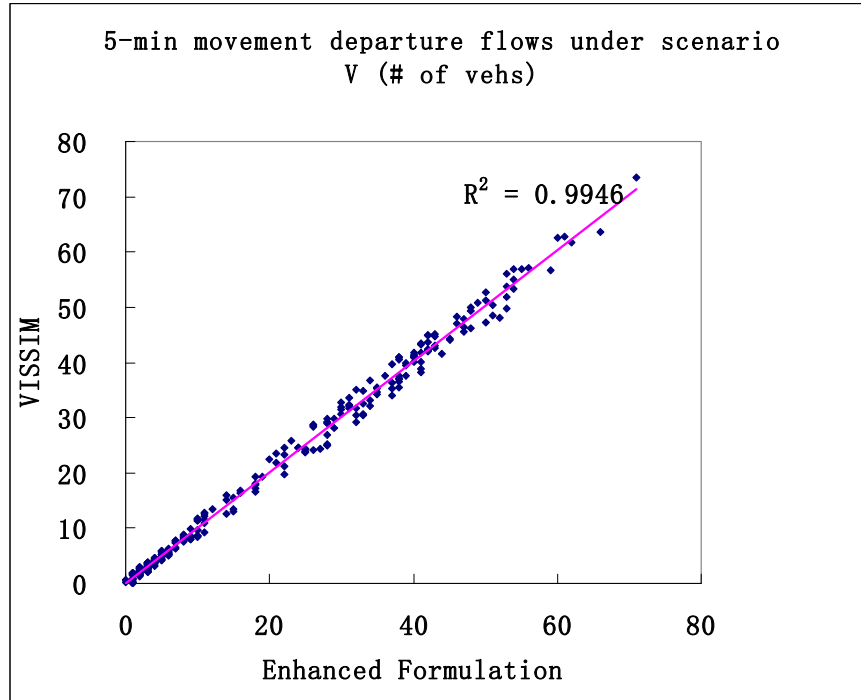
(ii)



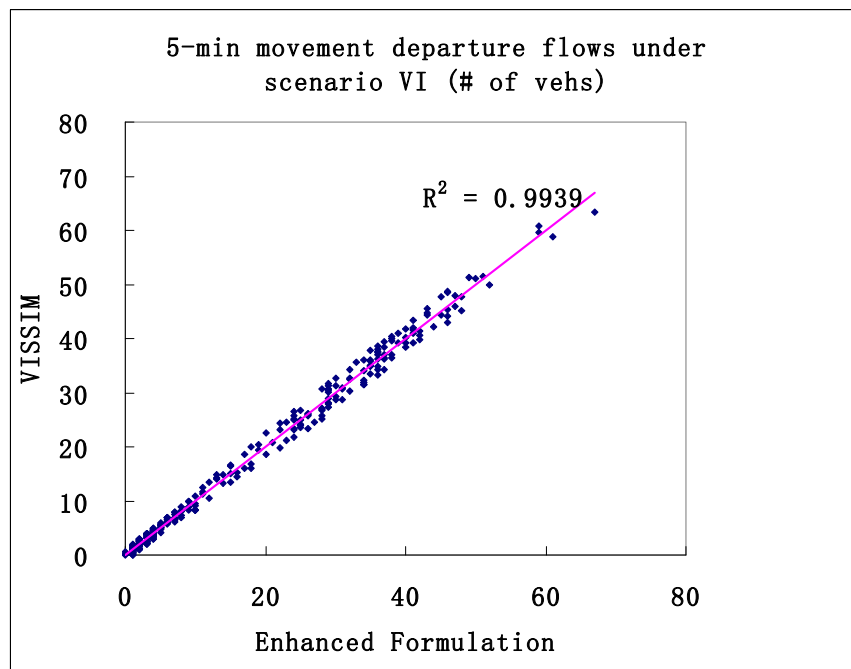
(iii)



(iv)



(v)



(vi)

Figure 6.4 Comparison of 5-minute Movement Departure Flows (VISSIM v.s. The Enhanced Formulation)

Table 6.3 Comparison between the Base Model and the Enhanced Model in 5-min Departure Flows (in # of vehicles)

Movements	Results	Scenarios											
		I		II		III		IV		V		VI	
		B	E	B	E	B	E	B	E	B	E	B	E
Northbound	I	0.67	0.67	0.72	0.65	1.04	0.79	1.82	0.95	0.66	0.66	0.6	0.6
Left	II	1	1	1	1	3	1	3	2	1	1	1	1
Northbound	I	2.13	1.26	2.41	1.51	2.42	1.63	3.37	1.94	1.06	1.06	1.04	1.03
Through	II	3	2	4	2	4	3	5	3	3	3	3	3
Northbound	I	0.62	0.62	0.7	0.64	0.79	0.69	1.13	0.86	0.61	0.61	0.59	0.59
Right	II	1	1	2	1	2	2	2	1	1	1	1	1
Southbound	I	1.17	1.17	1.44	1.42	1.7	1.7	1.81	1.81	0.96	0.96	0.86	0.86
Left	II	2	2	2	2	3	3	3	3	2	2	2	2
Southbound	I	2.06	2.06	2.45	2.45	2.71	2.71	2.53	2.53	2.02	1.99	1.95	1.95
Through	II	3	3	3	3	4	4	4	4	3	3	3	3
Southbound	I	0.53	0.53	0.61	0.61	0.67	0.67	0.97	0.97	0.51	0.51	0.48	0.49
Right	II	1	1	1	1	1	1	2	2	1	1	1	1
Eastbound	I	1.72	1.02	2.94	1.34	3.63	1.63	4.79	1.86	0.96	0.96	0.85	0.85
Left	II	4	2	4	2	7	3	8	3	2	2	2	2
Eastbound	I	1.58	1.12	1.7	1.28	2.52	1.45	3.67	1.62	0.94	0.93	0.82	0.82
Through	II	3	2	3	2	4	2	6	2	2	2	2	2
Eastbound	I	0.71	0.71	0.75	0.72	0.76	0.76	0.76	0.74	0.69	0.69	0.5	0.5
Right	II	1	1	1	1	1	1	1	1	1	1	1	1
Westbound	I	2.15	1.23	2.77	1.47	3.6	1.68	4.67	1.87	1.19	1.19	1.05	1.05
Left	II	3	2	5	2	6	3	7	3	2	2	2	2
Westbound	I	2.21	1.03	2.58	1.18	3.25	1.35	3.46	1.53	0.95	0.95	0.84	0.84
Through	II	3	2	4	2	5	2	6	2	2	2	2	2
Westbound	I	0.65	0.55	0.65	0.56	0.96	0.56	0.98	0.58	0.52	0.52	0.53	0.52
Right	II	1	1	1	1	2	1	2	1	1	1	1	1
Overall	I	1.55	1.27	1.76	1.41	3.43	1.53	4.08	1.65	1.35	1.34	1.12	1.12
Intersection	II	4	3	5	3	7	4	8	4	3	3	3	3

Note: I – RMSE; II – Max. Error; B – Base Model Proposed in Chapter 4; E – Enhanced Model Formulations;

From Table 6.3, one can identify the following findings:

- Compared with VISSIM simulation results, the RMSEs of the enhanced model formulations with respect to 5-min movement departure flows are within 2 vehicles, and the maximal errors are within 4 vehicles for all experimental scenarios (see highlighted cells at the bottom of Table 6.3);
- For under-saturated scenarios (V and VI), the enhanced model shows no significant improvement over the base model due likely to the lack of spillback or blockages in intersections approaches; and
- For near-saturated or over-saturated conditions (I, II, III, and IV), the enhanced model in comparison with its based model, can significantly overcome its deficiencies, especially for the eastbound and westbound approaches which exhibit severe blockages during the scenarios III and IV, as highlighted in Table 6.3. These results clearly show the promising property of the enhanced model under the scenarios of having lane blockages.

6.3. Signal Optimization with the Enhanced Network Formulations

Based on the above enhanced network formulations for lane-blockage at arterial intersections, this section presents the model for optimizing signal timings so as to further improve the system operational performance.

6.3.1. The Signal Optimization Model and Solution

During under-saturated traffic conditions, Equation 6.10 represents the objective of the control model for minimizing the total time for all vehicles in the target arterial over the entire time horizon H of analysis. For over-saturated conditions, the control model aims at maximizing the total throughput, i.e., the total number of vehicles that can go through the control area. Since the throughput equals the total number of vehicles entering the outgoing links, one can also state the control objective as Equation 6.11.

$$\min \quad \sum_{k=1}^H \left[\sum_{i \in S^U} N_i[k] + \sum_{r \in S_r} w_r[k] \right] \cdot \Delta t \quad (6.10)$$

$$\max \quad \sum_{k=1}^H \sum_{i \in S^{OUT}} q_i^{in}[k] \quad (6.11)$$

In Equations 6.10 and 6.11, all notations represent the same meanings as stated in Chapter 4. The same set of decision variables in Chapter 4 are employed to represent arterial signal timings, including:

- $\{C^h, h \in H\}$: Common cycle length for all intersections in the control interval h ;
- $\{\Delta_n^h, \forall n \in S_N, h \in H\}$: Offset of intersection n for each control interval h ;
- and
- $\{G_{np}^h, \forall n \in S_N, p \in P_n, h \in H\}$: Green time for phase p of intersection n for each control interval h ;

The network flow constraints proposed in Chapter 4 are enhanced to capture flow interactions at local bottlenecks by substituting Equations 4.8, 4.13, and 4.14 by Equations 6.4 – 6.7, and the operational constraints, denoted by Equations 4.46 – 4.49 and Equations 4.52 – 4.54, are kept to bound the signal control parameters within a reasonable range.

A Genetic Algorithm (GA)-based heuristic is developed to yield efficient model solutions for signal settings. Equations 4.77 – 4.80 are used to code the green times, cycle length, and offsets. The procedure of the solution algorithm is shown in Figure 6.5.

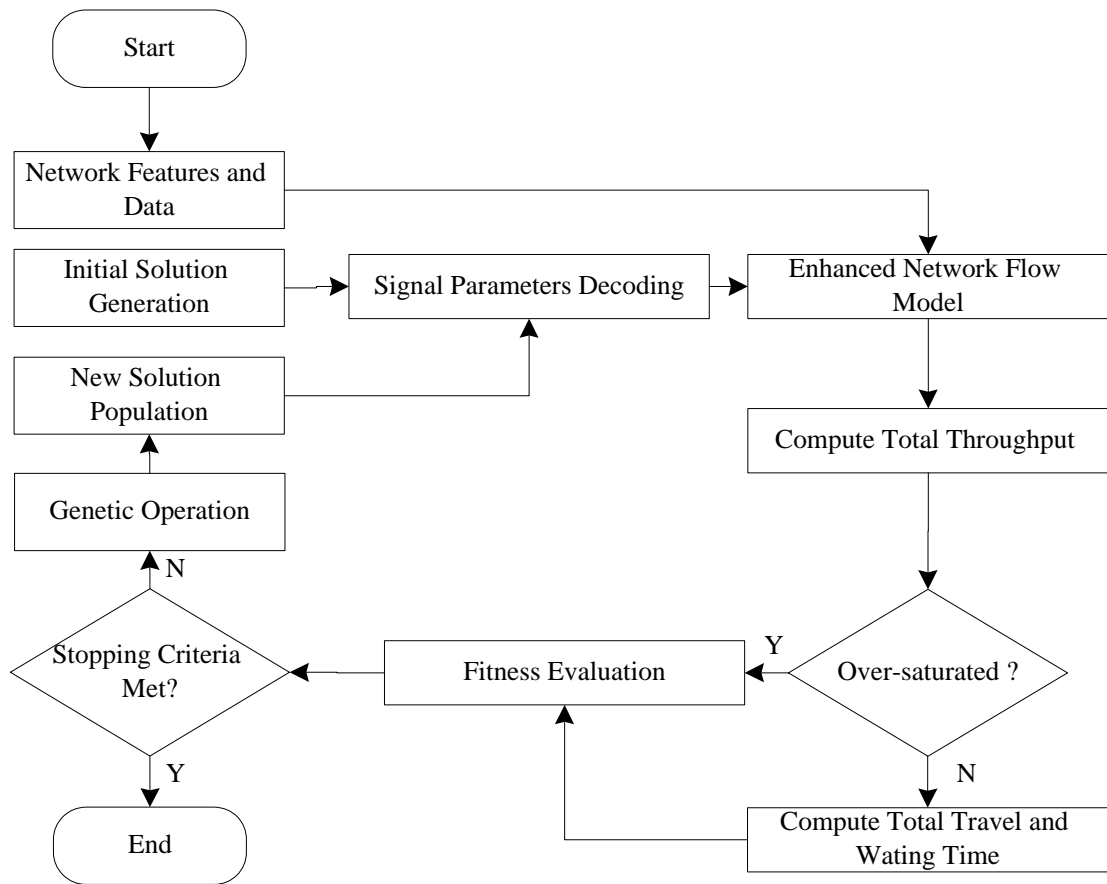


Figure 6.5 Flowchart of the Solution Algorithm for Signal Optimization

6.3.2. Numerical Test of the Enhanced Signal Optimization Model

Experimental Design

To illustrate the effectiveness of the enhanced signal optimization model, this study has employed a simple arterial, consisting of four intersections for numerical tests. Basic layouts of the arterial and phase configurations are shown in Figure 6.6. The spacing between intersections in the arterial is set to be 400ft. To test the capability of the enhanced model with respect to capturing blockages between different lane-groups under oversaturated conditions, all links along the arterial direction are designed to have one full lane for right-through traffic and an exclusive pocket of 100ft for left-turn traffic.

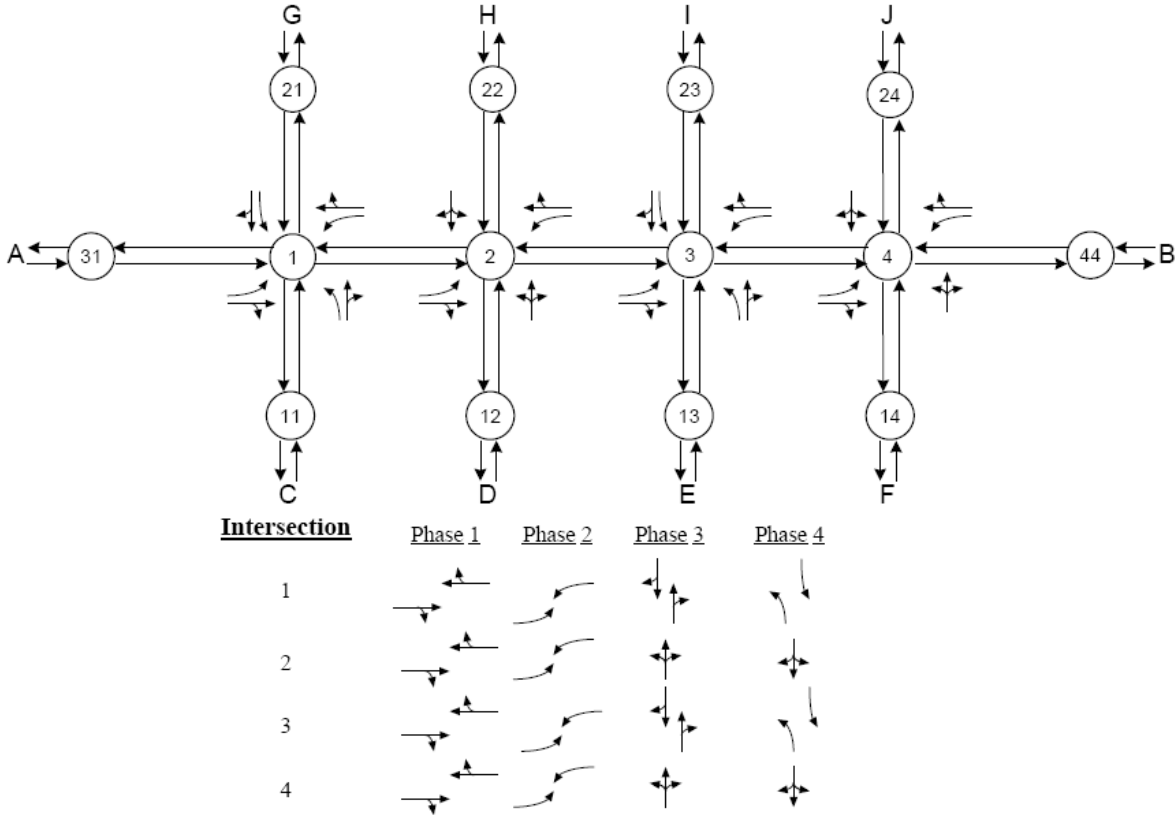


Figure 6.6 Experimental Arterial Layout and Phase Settings

The turning fractions for all intersection approaches are set to be 30% left-turn, 60% through, and 10% right-turn. This numerical test includes 10 demand entries (A-J) and three volume levels (low, medium, and high) designed to test the performance of enhanced signal optimization model. Table 6.4 summarizes all experimental scenarios.

Table 6.4 Experimental Scenarios for Model Evaluation

Demand Scenario	Degree of Saturation	Demand Entries (in vph)									
		A	B	C	D	E	F	G	H	I	J
low	0.4	400	400	300	200	300	200	300	200	300	200
medium	0.8	600	600	450	300	450	300	450	300	450	300
high	1.2	1000	1000	750	500	750	500	750	500	750	500

Optimization Model Settings

The network flow model parameters for case studies are given below:

- The free flow speeds are set to be 40 mph for arterial and 30 mph for side streets, and the minimum density is set to be 20 veh/mile/lane;
- Jam density is set to be 205 veh/mile/lane, and the minimum speed is 5 mph;
- Speed-density function parameter α, β are set to be 3.0 and 2.0, respectively;
- An average vehicle length of 25 ft is used to calculate the storage capacity of left-turn bay; and

- Complete blocking matrix is used to model the blockage effect between right-through and left-turn lane-groups since there exists only one full lane in the link.

The signal timing parameters are given as:

- Common network cycle length is between $C_{\min}, C_{\max} = 48s, 150s$;
- Minimal green time $G_{np}^{\min} = 7s$;and
- Inter-green time $I_{np} = 5s$.

The GA optimization is performed with the following parameters:

- The population size is 30;
- The maximum number of generation is 200;
- The crossover probability is 0.5; and
- The mutation probability is 0.03.

Experimental Results and Discussion

In this section, the optimal signal plans obtained from the enhanced model will be compared with plans from TRANSYT-7F using CORSIM as an unbiased evaluator. With TRANSYT-7F, the phase settings shown in Figure 6.6 were set as the input, and the network cycle length was optimized over a range of 48s to 150s. Stepwise simulation options with default disutility and performance indices are selected. Default run-control parameters were used for the optimization process, and network parameter values were set to reflect the experimental arterial features. To

contend with the problem that the hill-climbing algorithm in TRANSYT (version 8) does not necessarily reach a global optimum, this study has specified different optimization node sequences within the input file (sometimes can avoid the local optimal solution). The best signal timing plans obtained from this process were selected as the final candidate for comparison.

Since TRANSYT-7F release 8 can model the turn-bay spillover effects, this study has coded left-turn bays on arterial links with the Record Type 291 (Link Data Further Continuation) in order to obtain a fair comparison between the enhanced model and TRANSYT-7F with respect to capturing the queue interactions. For the high-demand scenario (degree of saturation above 1.0), the spillback penalty functions were used to accommodate queue blocking or spillback effects. The optimization processes for both TRANSYT-7F and the enhanced optimization model were implemented for one hour with a 5-min initialization interval. The optimized signal timing plans were then input to CORSIM for comparison. To overcome the stochastic nature of simulation results, an average of 20 simulation runs has been used. For the MOE comparison, since CORSIM computes the total delays or average delays only for departed vehicles, it is not technically rigorous to use delay as the MOE for over-saturated conditions. Hence, the total delay is used as the MOE for under-saturated conditions, and throughput and total queue time are for over-saturated conditions, as suggested by previous studies (Park et al., 1999).

Tables 6.5 – 6.6 show the optimization and comparison results from the enhanced model and TRANSYT-7F under different demand levels defined by Table 6.4.

Table 6.5 Signal Timings from the Enhanced Model and TRANSYT-7F

Demand Scenarios	Intersection	Cycle Length (s)		Offset (s)		Start of Green (s)							
		I ^a	II ^b	I	II	Phase I		Phase II		Phase III		Phase IV	
						I	II	I	II	I	II	I	II
Low	1			17	7	0	0	16	22	28	35	40	53
	2			11	8	0	0	13	21	27	33	39	49
	3	52	65	18	3	0	0	13	23	25	35	39	53
	4			9	2	0	0	15	21	27	33	39	49
Medium	1			10	6	0	0	21	30	33	44	58	67
	2			5	6	0	0	24	27	36	40	53	60
	3	70	80	9	3	0	0	22	29	34	43	55	66
	4			4	0	0	0	21	25	34	40	53	60
High	1			7	25	0	0	24	42	45	61	77	94
	2			2	0	0	0	26	38	43	55	72	83
	3	93	111	6	24	0	0	26	40	45	58	77	93
	4			1	1	0	0	29	36	45	55	72	83

^a The enhanced model; ^b TRANSYT-7F.

Table 6.6 Comparison of CORSIM Simulation Results

Scenarios	MOEs	Simulation Results from CORSIM (1 hour)		
		The Enhanced Model	TRANSYT-7F	Improvement ^a (%)
Low-demand	Total Delay (veh-min)	1728.6	1794.6	-3.7
	Total Queue Time (veh-min)	1327	1410.4	-5.9
	Total Throughput (veh)	2798	2807	-0.3
Medium-demand	Total Delay (veh-min)	3307.2	3358.2	-1.5
	Total Queue Time (veh-min)	2607.8	2680.7	-2.7
	Total Throughput (veh)	4206	4219	-0.3
High-demand	Total Queue Time (veh-min)	10625.9	13089.6	-18.8
	Total Throughput (veh)	5737	5574	+2.9

^a Improvement is calculated by $(MOE_{proposed\ model} - MOE_{TRANSYT-7F}) / MOE_{TRANSYT-7F}$

Based on the results reported in Tables 6.5 and 6.6, one can reach the following findings:

- For the low- and medium-demand scenarios, the enhanced model proposed by this study can yield a shorter cycle length under the objective of minimizing the total time in the network. The enhanced model outperforms TRANSYT-7F in terms of total system delay and queue times, but yields less system throughput (shown in Table 6.6) due to the relatively larger percentage of lost time in the cycle length.
- For the high-demand scenario, severe blockages between lane groups (right-through and left-turn) and upstream-downstream links in the network can be observed from the CORSIM simulation animations. Even though TRANSYT-7F tends to select longer cycle lengths to maximize the phase capacity for this scenario, it has adversely increased the likelihood of blockages due to the higher arrival rates to downstream links. In contrast, the enhanced approach can capture those blockage effects explicitly, and then select the most suitable cycle length to accommodate the traffic conditions. As shown in Table 6.6, the enhanced model yields less queue time and a larger throughput than that with TRANSYT-7F under the high-demand scenario.

To investigate the performance of the offset and split settings generated by the enhanced model, this study has compared the queue time for each intersection approach under different demand scenarios, as shown in Figure 6.7 through Figure

6.9. Under the low- and medium-demand scenarios (see Figure 6.7 and Figure 6.8), the enhanced model can achieve the arterial progression performance comparable to that with TRANSYT-7F, as most of the Eastbound and Westbound approaches (arterial direction) produced less queue time. For the side streets, the enhanced model outperforms TRANSYT-7F since all Northbound and Southbound approaches produced less queue time. This is due to the fact that the enhanced model minimizes not only the total system travel time but also the total system queue time, which results in the reduction of side street queue time without significant impact on the arterial progression.

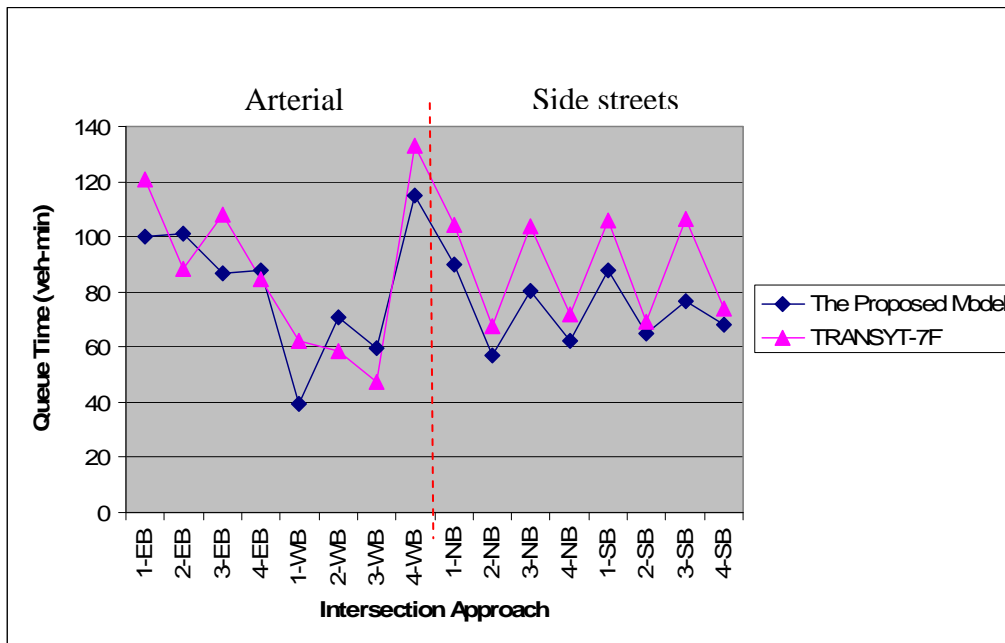


Figure 6.7 Queue Times of Approaches under the Low-demand Scenario

Under the high-demand scenario (see Figure 6.9), the enhanced model provides better arterial progression than TRANSYT-7F does (all Eastbound and Westbound approaches produce less queue time) due to its embedded dynamic traffic flow equations which are capable of handling blocking effects under oversaturated

conditions. For side streets, the enhanced model's performance is also comparable to that by TRANSYT-7F because the control objective has been switched to maximizing the total system throughput, which may cause longer waiting time on the side streets.

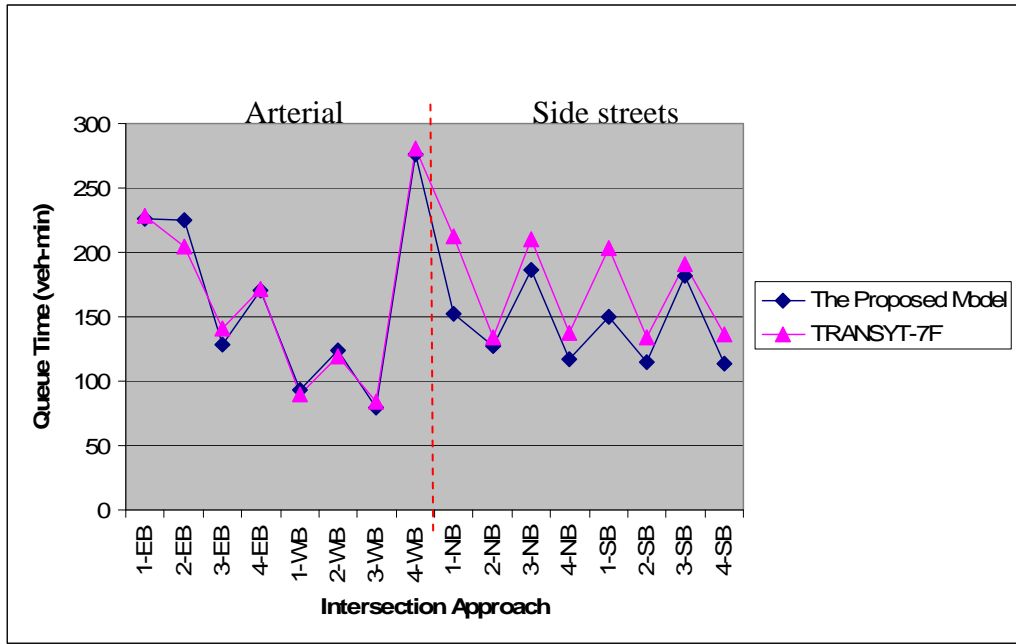


Figure 6.8 Queue Times of Approaches under the Medium-demand Scenario

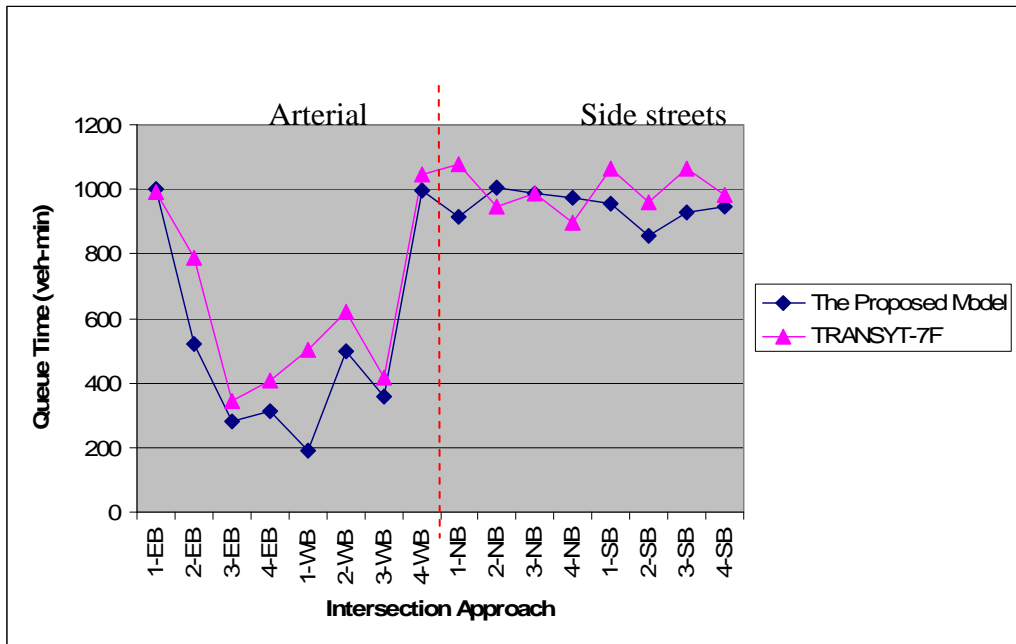


Figure 6.9 Queue Times of Approaches under the High-demand Scenario

In summary, one can reach the following conclusions by comparing the performance measures of the enhanced model and TRANSYT-7F under different demand scenarios:

- The enhanced model outperforms TRANSYT-7F in terms of total system queue time for all experimental demand scenarios;
- For under-saturated traffic conditions (low- and medium-demand scenarios), the enhanced model can produce better signal timings than TRANSYT-7F with respect to total system delay and total queue time. Furthermore, the enhanced model not only can obtain an arterial progression performance comparable to TRANSYT-7F, but also can effectively mitigate the congestion at the side streets, as evidenced by the lower queue time in the Northbound and Southbound approaches;
- With respect to the total system queue time and total system throughput for oversaturated traffic conditions, the enhanced model can mitigate the congestion and blockage more effectively than with TRANSYT-7F due to the use of enhanced dynamic traffic flow equations. In addition, compared to TRANSYT-7F, the enhanced model does not incur excessive waiting time or queues on the side streets.

6.4. Closure

This chapter has presented a set of enhanced network flow equations which can precisely capture the complex interrelations between the queue overflow in each lane group and its impacts on the neighboring lanes. This critical model feature is essential for realistically accounting for the volume surge at local intersections and off-ramps due to the impact of detoured traffic. Through proper integration with the signal optimization model, the enhanced set of formulations has demonstrated its effectiveness in preventing the formation of intersection bottlenecks, and consequently improving the overall arterial network performance.

Chapter 7: Conclusions and Future Research

7.1. Research Summary and Contributions

This dissertation has addressed several critical issues on design of traffic control strategies for urban freeway corridors under non-recurrent congestion. Grounded on real-world operational constraints, this study has developed an integrated traffic control system that enables transportation agencies to exert effective control strategies, including diversion control, ramp metering, and arterial signal timings at all critical control points to best the corridor operational performance under incident conditions. The key features and capabilities of such a system are presented in Chapter 1.

Chapter 2 summarizes major studies by transportation researchers over the past several decades on various aspects of traffic corridor management during non-recurrent traffic congestion. It highlights both the critical issues and potential research directions identified in the existing literature on this vital subject. Some imperative areas which have not been adequately addressed in the literature have also been identified in the comprehensive review.

In responses to the identified research needs, Chapter 3 has illustrated the framework of the proposed integrated corridor control system for contending with non-recurrent congestion with its principle components. The proposed framework applies a hierarchical development structure that consists of a freeway and its

neighboring arterials. The focus of the integrated-level control is on maximizing the capacity utilization of the entire corridor under incident conditions, with several control strategies concurrently implemented over different time windows, including dynamic diversion rates at critical off-ramps, on-ramp metering rates, and arterial signal timing plans. Serving as a supplemental component, the strategy for local-level bottleneck management centers on enhancing the signal control plans generated from the integrated-level models so as to prevent the queue spillback or blockages at segments of off-ramps and intersections due to the demands of detoured traffic.

The key mathematical models for integrated control operations are detailed in Chapter 4, which starts with the development of innovative formulations using the lane-group-based concept for modeling arterial links and ramps. It offers a reliable representation of the relationships between the arriving and departing flows under various types of lane channelization (e.g. shared lanes) at each intersection approach. This unique modeling feature, when integrated with the freeway model, can accurately and efficiently capture the operational characteristics of traffic flows in the entire corridor optimization process. With this proposed formulation methodology for network flows, Chapter 4 has illustrated its applications with the following two categories of integrated control:

- The Base Model for single-segment corridor which involves one detour route, including the incident upstream on-ramp and off-ramp, the incident downstream on-ramp, and the connected parallel arterial; and

- The Extended Model for integrated control of a multi-segment corridor, in which multiple detour routes, comprising several on-ramps, off-ramps, and several segments of parallel arterials, are employed to coordinately divert traffic under incident conditions.

A multi-objective control framework is applied for both control models to allow the system user to efficiently explore the control effectiveness under different policy priorities between the target freeway and available detour routes. Due to the nonlinear nature of the proposed formulations and the concerns of computing efficiency, Chapter 4 has also developed a compromised GA-based heuristic that can yield sufficiently reliable solutions for applying the proposed models in practice with a multi-objective control function. The solution algorithm is then integrated with a successive optimization framework for real-time application of the proposed control model, in which the model input and control strategy are constantly updated to improve the computing efficiency and effectiveness under time-varying traffic conditions and potential system disturbances.

To explore the potential issues of the developed integrated control models for real-world operations, this study has conducted case studies with a segment along the I-95 northbound corridor and a hypothetical corridor network. The results of those case studies have demonstrated that with the information generated from the proposed models, the responsible agency can effectively implement control strategies in a timely manner at all control points to substantially improve the efficiency of the corridor control operations under incident conditions. The case study results also

reveal that the developed models and solution algorithms are sufficiently reliable for use in practice.

Chapter 6 has enhanced the lane-group-based model for arterial network flows to capture the complex interrelations between the overflow in each lane group and its impact on neighboring lanes, such as left-turn lane blockage due to a long through-traffic queue. This critical model feature is essential for realistically accounting for bottlenecks incurred by the detoured traffic at local traffic intersections. The enhanced formulations have further been integrated into an optimization model to fine-tune the arterial signal timings generated from the integrated control models. The results of extensive numerical experiments have shown that the enhanced signal model is effective in producing local control strategies to prevent the formation of bottlenecks, and thus consequently improve the overall arterial network performance.

In summary, this research has made the following key contributions:

- Propose an innovative lane-group-based model, which offers a reliable representation of queue evolution under various types of lane channelization (e.g. shared lanes) at each intersection approach. However, most previous studies model dynamic queue evolution either at a link-based level or at an individual-movement-based level, which could result in either difficulty in integrating with multiple signal phases or inaccuracy in modeling the queue discharging rates in a shared lane;
- Develop a set of formulations that can model the evolution of diversion traffic along the detour route and its impacts on intersection turning

movement patterns in a dynamic control environment. Most previous studies address this issue either by projecting the turning proportions at arterial intersections, based on assumed dynamic OD and travel time information, or by applying a fixed additional amount of flows to the impacted movement, which often does not reflect changes in the time-dependent pattern;

- Construct an overall corridor network flow model, and formulate a set of mathematical models for design of integrated corridor control strategies, which allow the system user to efficiently explore the control effectiveness under different policy priorities between the target freeway and available detour routes;
- Design an efficient solution algorithm that can yield sufficiently reliable solutions for applying the proposed models in practice with a multi-objective control function;
- Construct a new set of equations to capture the complex interrelations between the queue overflow in each lane group and its impacts on the neighboring lanes for realistically accounting for bottlenecks due to the impact of detoured traffic on local traffic conditions. These critical operational constraints often exist in real-world operations but have not yet been addressed in the literature; and
- Develop an arterial signal control model to produce control strategies that can effectively prevent the formation of local bottlenecks and further improve the operational efficiency of the entire corridor.

7.2. Future Research

Despite the effectiveness of this study in overcoming several critical issues for the real-time corridor control under incident conditions, a more efficient and reliable solution for implementing such a system in network-wide applications remains essential. Further studies along this line are listed below:

Development of efficient solution algorithms for integrated network-wide control

This study has employed a GA-based heuristic to solve the integrated corridor control formulations. For a large-scale network-wide application, the chromosome length will increase, and the GA-based heuristic will need a larger size of population and/or more generations of evolution to converge to a reliable solution, which may limit its efficiency in real-time applications. One potential solution to tackle this critical issue is to intelligently decompose the large corridor network into a series of sub-networks such that the search directions of the problem can be significantly narrowed down, and the parallel computing technique can also be employed for more efficient multi-tasking system operations and communications. Alternately, one may investigate other heuristics that are less sensitive to the dimensionality of the solution space size. For example, by employing the Simultaneous Perturbation Stochastic Approximation (SPSA) approach, it may yield the efficient solution for large-scale corridor networks. However, depending on the corridor network structure and traffic conditions, some key searching parameters of the SPSA need to be calibrated in advance to ensure its performance.

Development of robust solution algorithms for the proposed models when available control inputs are missing or contain some errors

The performance of the proposed integrated corridor control model is conditioned on the quality and availability of input data from the surveillance system. However, the availability and accuracy of the existing surveillance system always suffer from the hardware quality deficiency. Neglecting the impact of the data quality in the model formulations may degrade both operational efficiency and reliability in real-world applications. To contend with such deficiencies embedded in the existing models, one needs to develop a robust algorithm to account for measurement errors in system inputs so that it can yield control strategies less sensitive to the data measurement errors.

Development of an intelligent interface with advanced surveillance systems

For real-time implementation of the proposed control models, it requires real-time realization of the control input data from various sources of the surveillance system. This research has presented an on-line estimation module for control parameters used in the proposed control system. Many advanced detection technologies developed in recent years in the traffic control field have featured their capabilities in capturing the evolution of traffic flows at each individual movement or vehicle level, which offers the promise for a real-time control system to significantly reduce the cost in data processing and parameter estimation. Hence, to effectively operate an integrated real-time corridor control system, one should certainly develop

an intelligent interface to take advantage of those features embedded in the emerging advanced detection technologies.

Bibliography

- Abu-Lebdeh, G., Chen, H., Benekohal, R.F., “Modeling Traffic Output for Design of Dynamic Multi-Cycle Control in Congested Conditions,” *Journal of Intelligent Transportation Systems* 11(1), 25-40, 2007.
- Ben-Akiva, M., “Development of a deployable real-time dynamic traffic assignment system,” Task D Interim report: analytical developments for DTA system, MIT, Cambridge, MA, 1996.
- Ben-Akiva, M., M. Bierlaire, J. Bottom, H. Koutsopoulos, and R. Mishalani, “Development of a route guidance generation system for real-time application,” in 8th IFAC/IFIP/IFORS Symposium of Transportation Systems, pp. 433–439, 1997.
- Binning, J.C., Burtenshaw, G., and Crabtree, M., *TRANSYT 13 User Guide*. Transport Research Laboratory, UK, 2008.
- Blinkin, M., “Problem of optimal control of traffic flow on highways,” *Automatic Remote Control*, vol. 37, pp. 662–667, 1976.
- Bhourri, N., H. Hadj-Salem, M. Papageorgiou, J. M. Blosseville, “Estimation of traffic density on motorways,” *Traffic Engineering and Control*, v29, n11, 1988.
- Bhourri, N., M. Papageorgiou, and J. M. Blosseville, “Optimal control of traffic flow on Periurban ringways with application to the Boulevard Périphérique in Paris,” the 11th IFAC World Congress, vol. 10, pp. 236–243, 1990.
- Bhourri, N., and M. Papageorgiou, “Application of control theory to regulate traffic flow on Periurban ringways,” in Proceedings of the 2nd International

- Conference on Applications of Advanced Technology in Transportation, Minneapolis, Minnesota, 1991.
- Bogenberger, K., A.D. May, "Advanced coordinated traffic responsive ramp metering strategies," California PATH Paper UCB-ITS-PWP-99-19, 1999.
- Boillot, F., "Optimal signal control of urban traffic networks," in Proceedings of the 6th International Conference on Road Traffic Monitoring and Control, IEE, London, 1992.
- Chang, G. L., P. K. Ho, C. H. Wei, "A dynamic system-optimum control model for commuting traffic corridors," *Transportation Research* 1C, 3-22, 1993.
- Chang, G. L., J. Wu, S. L. Cohen, "Integrated real-time ramp metering modeling for non-recurrent congestion: framework and preliminary results," *Transportation Research Record*, 1446, 56-65, 1994.
- Chang, T.H., Z.Y. Li, "Optimization of mainline traffic via an adaptive coordinated ramp metering control model with dynamic OD estimation," *Transportation Research* 10C, 99-120, 2002.
- Charbonnier, C., J. L. Farges, and J.-J. Henry, "Models and strategies for dynamic route guidance-Part C: Optimal control approach," In Proceedings of DRIVE Conference, pp. 106–112, 1991.
- Chaudhary, N. A., Messer, C. J., "PASSER-IV: A program for optimizing signal timing in grid networks," presented at 72nd annual meeting of the Transportation Research Board, Washington, DC, 1993.
- Chen, L., A. D. May, D. M. Auslander, "Freeway ramp control using fuzzy set theory for inexact reasoning," *Transportation Research* 24A, 15-25, 1990.

- Chen, O. J., A. F. Hotz, and M. E. Ben-Akiva, "Development and evaluation of a dynamic ramp metering control model," in 8th IFAC/IFIP/IFORS Symposium of Transportation Systems, pp.1162–1168, 1997.
- Cheng, I. C., J. B. Cruz, and J. G. Paquet, "Entrance ramp control for travel rate maximization in expressways," *Transportation Research*, vol. 8, pp. 503–508, 1974.
- Cheng, R., and M. Gen, "Compromise approach-based genetic algorithm for bi-criterion shortest path problems," Technical Report, Ashikaga Institute of Technology, 1998.
- Cohen, S. L., Liu, C. C., "The bandwidth-constrained TRANSYT signal optimization program," *Transportation Research Record* 1057, 1-7, 1986.
- Cremer, M., and A. D. May, "An extended traffic flow model for inner urban freeways," Preprints 5th IFAC/IFIP/IFORS International Conference on Control in Transportation Systems, Vienna, Austria, pp. 383-388.
- Cremer, M., S. Schoof, "On control strategies for urban traffic corridors," In Proceedings of IFAC Control, Computers, Communications in Transportation, Paris, 1989.
- Daganzo, C., "The Cell Transmission Model: a dynamic representation of highway traffic consistent with hydrodynamic theory," *Transportation Research* 28B, 4, pp. 269-287, 1994.
- D'Ans, G. C., and D. C. Gazis, "Optimal control of oversaturated store-and-forward transportation networks," *Transportation Science* 10, 1-19, 1976.

- Davis, G. A., C. J. Lan, "Estimating intersection turning movement proportions from less-than-complete sets of traffic counts," *Transportation Research Record*, 1510, 53-59, 1995.
- Diakaki, C. and M. Papageorgiou, "Design and simulation test of coordinated ramp metering control (METALINE) for A10-west in Amsterdam," Technical Report 1994-2, Dynamic System Simulation Lab, Technical University of Crete, Chania, Greece, 1994.
- Dörge, L., C. Vithen, P. Lund-Srensen, "Results and effects of VMS control in Aalborg," In Proceedings of 8th International Conference on Road Traffic Monitoring and Control, 150–152, 1996.
- Elloumi, N., H. Haj-Salem, and M. Papageorgiou, "Integrated control of traffic corridors-application of an LP-methodology," The 4th Meeting EURO Working Group on Transportation Systems, Landshut, Germany, 1996.
- Eschenauer, H., Koski, J., Osyczka, A., *Multicriteria Design Optimization – Procedures and Applications*, Springer-Verlag, 1990.
- Gartner, N. H., Little, J. D. C., Gabbay, H., "Optimization of traffic signal settings by mixed integer linear programming, Part I: the network coordination problem," *Transportation Science* 9, 321-343, 1975a.
- Gartner, N. H., Little, J. D. C., Gabbay, H., "Optimization of traffic signal settings by mixed integer linear programming, Part II: the network synchronization problem," *Transportation Science* 9, 321-343, 1975b.

- Gartner, N. H., Assmann, S. F., Lasaga, F. L., Hou, D. L., “A multi-band approach to arterial traffic signal optimization,” *Transportation Research* 25B, 55-74, 1991.
- Gazis, D. C., and R. B. Potts, “The oversaturated intersection,” in Proceedings of the 2nd International Symposium on Traffic Theory, London, pp. 221-237, 1963.
- Goldstein, N. B., and K. S. P. Kumar, “A decentralized control strategy for freeway regulation,” *Transportation Research* 16B, 279-290, 1982.
- Gray, J., P. Lavallee, and A. D. May, “Segment-wide online control of freeways to relieve congestion and improve public safety,” Final Report, FHWA/CA/UCB-ITS-RR-90-11, Institute for Transportation Studies, UC Berkeley.
- Hawas, Y., H.S. Mahmassani, “A decentralized scheme for real-time route guidance in vehicular traffic networks,” In Proceedings of 2nd World Congress on Intelligent Transport Systems, pp. 1956–1963, 1995.
- Hourdakis, J., P.G. Michalopoulos, “Evaluation of ramp control effectiveness in two twin cities freeways,” *Transportation Research Record* 1811, 21–30, 2003.
- Iftar, A., “A decentralized routing controller for congested highways,” In Proceedings of 34th Conference on Decision and Control. New Orleans, LA, USA, pp. 4089-4094, 1995.
- Jacobson, L. N., K. C. Henry, and O. Mehvar, “Real-time ramp metering algorithm for centralized control,” *Transportation Research Record* 1232, 17-26, 1989.

- Kahng, S. J., C.-Y. Jeng, J. F. Campbell, and A. D. May, "Developing segment-wide traffic-responsive freeway entry control," *Transportation Research Record* 957, 5-13, 1984.
- Kashani, H.R., and Saridis, G.N., "Intelligent control for urban traffic systems," *Automatica* 19, 191-197, 1983.
- Kaya, A., "Computer and optimization techniques for efficient utilization of urban freeway systems," presented at the 5th IFAC World Congress, Paris, France, 1972.
- Koble, H. M., T. A. Adams, V. S. Samant, "Control strategies in response to freeway incidents," Vol. 2, Report FHWA/RD-80/005, ORINCON, Inc., 1980.
- Kotsialos, A., M. Papageorgiou, M. Mangeas, H. Haj-salem, "Coordinated and integrated control of motorway networks via non-linear optimal control," *Transportation Research* 10C, 65-84, 2002.
- Kotsialos, A., M. Papageorgiou, "Nonlinear optimal control applied to coordinated ramp metering," *IEEE Transactions on Control Systems Technology* 12, 920-933, 2004.
- Kwon, E., "Comparative analysis of operational algorithms for coordinated ramp metering," Center for Transportation Studies, University of Minnesota, 2000.
- Lafortune, S., R. Sengupta, D. E. Kaufman, and R. L. Smith, "Dynamic system-optimal traffic assignment using a state space model," *Transportation Research* 27B, 451-473, 1993.

- Levinson, D., Zhang, L., Das, S., Sheikh, A., “Evaluating ramp meters: evidence from the Twin Cities ramp meter shut-off,” Presented at the 81st TRB Annual meeting, Washington, DC, 2002.
- Li, M.-T., Gan, A.C., “Signal timing optimization for oversaturated networks using TRANSYT-7F,” *Transportation Research Record* 1683, 118–126, 1999.
- Little, J. D. C., Kelson, M. D., Gartner, N. H., “MAXBAND: a program for setting signals on arterials and triangular networks,” *Transportation Research Record* 795, 40-46, 1981.
- Lo, H., Chang, E., Chan Y., “Dynamic network traffic control,” *Transportation Research Part A* 35, 721-744, 2001.
- Looze, D. P., P. K. Houpt, N. R. Sandell, and M. Athans, “On decentralized estimation and control with application to freeway ramp metering,” *IEEE Transactions on Automatic Control*, 23, 268-275, 1978.
- Lovell, D., “Traffic control on metered networks without route choice,” Ph.D. Dissertation, University of California at Berkeley, 1997.
- Lovell, D., C.F. Daganzo, “Access control on networks with unique origin–destination paths,” *Transportation Research* 34B, 185-202, 2000.
- Mahmassani, H. S., S. Peeta, “Network performance under system optimal and user equilibrium dynamic assignments: implications for advanced traveler information systems,” *Transportation Research Record* 1408, 83-93, 1993.
- Mammar, S., A. Messmer, P. Jensen, M. Papageorgiou, H. Haj-Salem, and L. Jensen, “Automatic control of variable message signs in Aalborg,” *Transportation Research* 4C, 131–150, 1996.

- Masher, D. P., D.W. Ross, P. J. Wong, P. L. Tuan, H. M., Zeidler, and S. Peracek, "Guidelines for design and operating of ramp control systems," Stanford Research Institute, Report NCHRP 3-22, SRI Project 3340, 1975.
- Messmer, A., and Papageorgiou, M., "METANET: A macroscopic simulation program for motorway networks," *Traffic Engineering and Control* 31, 466-470, 1990.
- Messmer, A., M. Papageorgiou, "Automatic control methods applied to freeway network traffic," *Automatica*, 30, 691-702, 1994.
- Messmer, A., M. Papageorgiou, "Route diversion control in motorway networks via nonlinear optimization," *IEEE Transaction on Control System Technology*, 3, 144-154, 1995.
- Messmer, A., M. Papageorgiou, and N. Mackenzie, "Automatic control of variable message signs in the interurban Scottish highway network," *Transportation Research C*, 6, 173-187, 1998.
- Mirchandani, P. B., Nobe, S. A., Wu, W., "Online turning proportion estimation in real-time traffic-adaptive signal control," *Transportation Research Record* 1748, 80-86, 2001.
- Moreno-Banos, J. C., M. Papageorgiou, and C. Schöffner, "Integrated optimal flow control in traffic networks," *European Journal of Operations Research*, 71, 317-323, 1993.
- Morin, J.-M., "Aid-to-decision for variable message sign control in motorway networks during incident condition," In Proceedings of the 4th ASCE

- International Conference on Applications of Advanced Technologies in Transportation Engineering, pp. 378–382, 1995.
- Nihan, N. L., and D. B. Berg, “Predictive algorithm improvements for a real-time ramp control system,” Final Report, GC8286, WA-RD 213.1, Washington DOT, 1991.
- Nsour, S. A., S. L. Cohen, J. E. Clark, A. J. Santiago, “Investigation of the impacts of ramp metering on traffic flow with and without diversion,” *Transportation Research Record* 1365, 116-124, 1992.
- Papageorgiou, M., “A new approach to time-of-day control based on a dynamic freeway traffic model,” *Transportation Research* 14B, 349–360, 1980.
- Papageorgiou, M., and R. Mayr, “Optimal decomposition methods applied to motorway traffic control,” *International Journal of Control*, 35, 269–280, 1982.
- Papageorgiou, M., “A hierarchical control system for freeway traffic,” *Transportation Research* 17B, 251-261, 1983.
- Papageorgiou, M., “Multilayer control system design applied to freeway traffic,” *IEEE Transactions on Automatic Control*, 29(6), 482-490, 1984.
- Papageorgiou, M., and J.-M. Blosseville, “Macroscopic modeling of traffic flow on the Boulevard Périphérique in Paris,” *Transportation Research* 23B, 29-47, 1989.
- Papageorgiou, M., “Modeling and real-time control of traffic flow on the Southern Part of Boulevard Périphérique in Paris - Part I: Modeling,” *Transportation Research* 24A, 5, 345-359, 1990a.

- Papageorgiou, M., J.-M. Blosseville, H. Hadj-Salem, "Modeling and real-time control of traffic flow on the southern part of Boulevard Périphérique in Paris - Part II: Coordinated on-ramp metering," *Transportation Research* 24A, 5, 361-370, 1990b.
- Papageorgiou, M., "Dynamic modeling, assignment, and route guidance in traffic networks," *Transportation Research* 24B, 471-495, 1990c.
- Papageorgiou, M., H. Hadj-Salem, and J.-M. Blosseville, "ALINEA: A local feedback control law for on-ramp metering," *Transportation Research Record* 1320, 58-64, 1991.
- Papageorgiou, M., "An integrated control approach for traffic corridors," *Transportation Research* 3C, 19-30, 1995.
- Papageorgiou, M., A. Messmer, J. Azema, and D. Drewanz, "A neural network approach to freeway network traffic control," *Control Engineering Practice* 3(12), 1719-1726, 1995.
- Papageorgiou, M., C. Diakaki, V. Dinopoulou, A. Kotsialos, and Y. Wang, "Review of road traffic control strategies," *Proceedings of the IEEE* 91(12), 2043-2067, 2003.
- Park, B., Messer, C. J., Urbanik, T., "Traffic signal optimization program for oversaturated conditions: genetic algorithm approach," *Transportation Research Record* 1683, 133-142, 1999.
- Pavlis, Y., M. Papageorgiou, "Simple decentralized feedback strategies for route guidance in traffic networks," *Transportation Science* 33, 264-278, 1999.

- Payne, H. J., "Models of freeway traffic and control," *Simulation Conference Proceedings* 1, 51-61, 1971.
- Payne, H. J., W. A. Thompson, "Allocation of freeway ramp metering volumes to optimize corridor performance," *IEEE Transactions on Automatic Control* 19, 177-186, 1974.
- Payne, H. J., "FREFLO: A macroscopic simulation model of freeway traffic," *Transportation Research Record* 722, 68-77, 1979.
- Payne, H. J., D. Brown, J. Todd, "Demand responsive strategies for interconnected freeway ramp control systems, Vol. 1: Metering strategies," Verac Inc., 1985.
- Payne, H. J., D. Brown, S. L. Cohen, "Improved techniques for freeway surveillance," *Transportation Research Record* 1112, 52-60, 1987.
- Rathi, A., E. Lieberman, and M. Yedlin, "Enhanced FREFLO: Modeling of congested environments," *Transportation Research Record* 1112, 61-71, 1987.
- Reiss, R. A., "Algorithm development for corridor traffic control," in *Traffic, Transportation, and Urban Planning* Vol. 2, George Goodwin, London, 1981.
- Robertson, D.I., *TRANSYT: A traffic network study tool. RRL Report LR 253*, Road Research Laboratory, England, 1969.
- Ross, P., "Traffic Dynamics," *Transportation Research* 22B, 421-435, 1988.
- Sanwal, K. K., K. Petty, J. Walrand, and Y. Fawaz, "An extended macroscopic model for traffic flow," *Transportation Research* 30B, 1, 1-9, 1996.
- Sasaki, T., and Akiyama, T., "Development of fuzzy traffic control system on urban expressway," in *Proceedings of IFAC Control in Transportation Systems*, Vienna, Austria, 1986.

- Schwartz, S. C., H. H. Tan, "Integrated control of freeway entrance ramps by threshold regulation," in Proceedings of IEEE Conference on Decision and Control, pp. 984–986, 1977.
- Smadi, A., Baker, J., Birst, S., "Advantages of using innovative traffic data collection technologies," Proceedings of the 9th International Conference on Applications of Advanced Technology in Transportation, p 641-646, 2006.
- Stephanedes, Y., and K. K. Chang, "Optimal ramp metering control for freeway corridors," in Proceedings of the 2nd International Conference on Applications of Advanced Technology in Transportation, Minneapolis, Minnesota, 1991.
- Stephanedes, Y., E. Kwon, and K. K. Chang, "Control emulation method for evaluating and improving traffic-responsive ramp metering strategies," *Transportation Research Record* 1360, 42-45, 1992.
- Stephanedes, Y., and K. K. Chang, "Optimal control of freeway corridors," *ASCE Journal of Transportation Engineering* 119, 504-514, 1993.
- Stephanedes, Y., and X. Liu, "Neural networks in freeway control," in Proceedings of Pacific Rim TransTech Conference, Seattle, July, 1993.
- Stevanovic, A., Martin, P. T., Stevanovic, J., "VisSim-based genetic algorithm optimization of signal timings," *Transportation Research Record* 2035, 59-68, 2007.
- Tabac, D., "A linear programming model of highway traffic control," in Proceedings of 6th Annual Princeton Conference on Information Science and Systems, pp. 568–570, 1972.

- Taylor, C., D. Meldrum, L. Jacobson, "Fuzzy ramp metering-design overview and simulation results," *Transportation Research Record* 1634, 10-18, 1998.
- Van Aerde M., and S. Yagar, "Dynamic integrated freeway/traffic signal networks problems and proposed solutions," *Transportation Research* 22A, 6, 435-443, 1988.
- Van den Berg, De Schutter, A. Hegyi, B. and J. Hellendoorn, "Model predictive control for mixed urban and freeway networks," *Transportation Research Record*, 1748, 55-65, 2001.
- Van den Berg, A., Hegyi, B., De Schutter, Hellendoorn, J., "A macroscopic traffic flow model for integrated control of freeway and urban traffic networks," 42nd IEEE International Conference on Decision and Control, Hawaii, 2774-2779, 2003.
- Wall, M., "GALib, a C++ library of genetic algorithm components," Massachusetts Institute of Technology, 1999. <http://lancet.mit.edu/ga/>, Retrieved 04.16.2008.
- Wallace, C. E., Courage, K. G., Reaves, D. P., Shoene, G. W., Euler, G. W., Wilbur, A., TRANSYT-7F User's Manual: Technical Report. University of Florida, Gainesville, FL, 1988.
- Wang, J. J. and A. D. May, "Computer model for optimal freeway on-ramp control," *Highway Research Record* 469, 16-25, 1973.
- Wang, Y., M. Papageorgiou, "Feedback routing control strategies for freeway networks: A comparative study," In Proceedings of the 2nd International Conference on Traffic and Transportation Studies, pp. 642-649, 2000.

- Wang, Y., A. Messmer, and M. Papageorgiou, "Freeway network simulation and dynamic traffic assignment using METANET tools," *Transportation Research Record* 1776, 178-188, 2001.
- Wang, Y., M. Papageorgiou, and A. Messmer, "A predictive feedback routing control strategy for freeway network traffic," In Proceedings of American Control Conference, pp. 3606–3611, 2002.
- Wattleworth, J.A., Peak-period control of a freeway system—some theoretical considerations. Ph.D. Dissertation, Northwestern University, 1963.
- Wattleworth, J.A., "Peak-period analysis and control of a freeway system," *Highway Research Record*, 157, 1967.
- Wie, B., R. Tobin, D. Bernstein, and T. Friesz, "Comparison of system optimum and user equilibrium dynamic traffic assignment with schedule delays," *Transportation Research* 3C, 389–411, 1995.
- Wisten, M. B., M. J. Smith, "Distributed computation of dynamic traffic equilibria," *Transportation Research* 5C, 77–93, 1997.
- Wu, J., and G.L. Chang, "Heuristic method for optimal diversion control in freeway corridors," *Transportation Research Record* 1667, 8-15, 1999a.
- Wu, J., and G.L. Chang, "An integrated optimal control and algorithm for commuting corridors," *International Transactions on Operations Research* 6, 39-55, 1999b.
- Wu, J., "Development of an integrated real-time corridor control model and algorithm, University of Maryland at College Park, 1999c.
- Yagar, S., "Metering freeway access," *Transportation Quarterly*, 43, 215-224, 1989.

- Yu, X. H., Recker, W. W., “Stochastic adaptive control model for traffic signal systems,” *Transportation Research* 14C, 14, 263-282, 2006.
- Yuan, L. S., J. B. Kreer, “Adjustment of freeway ramp metering rates to balance entrance ramp queues,” *Transportation Research*, vol. 5, pp.127–133, 1971.
- Yun, I., Park, B., “Application of Stochastic Optimization Method for an Urban Corridor,” Proceedings of the Winter Simulation Conference, vol. 3-6, pp. 1493- 1499, 2006.
- Zhang, H., S. Ritchie, and Z. Lo, “A local neural network controller for freeway ramp metering,” in Proceedings of the 7th Symposium on Transportation Systems: Theory and Applications of Advanced Technologies, Tianjin, China, 1994.
- Zhang, H., and S. Ritchie, “An integrated traffic responsive ramp control strategy via non-linear state feedback,” presented at the 74th Annual Meeting of Transportation Research Board, Washington, DC, 1995.
- Zhang, H., S. Ritchie, W. Recker, “Some general results on the optimal ramp metering control problem,” *Transportation Research* 4C, 51-69, 1996.
- Zhang, H.M., “Freeway ramp metering using artificial neural network,” *Transportation Research* 5C, 273-286, 1997.
- Zhang, H.M., W. Recker, “On optimal freeway ramp control policies for congested traffic corridors,” *Transportation Research* 33B, 417-436, 1999.
- Zhang, L., D.M. Levinson, “Optimal freeway ramp control without origin–destination information,” *Transportation Research* 38B, 869-887, 2004.

Zhang, Y., A. Hobeika, "Diversion and signal re-timing for a corridor under incident conditions," presented at 77th Annual Meeting of Transportation Research Board, Washington, DC, 1997.